

**University of Alberta**

**The Synthesis of and Methodology for Archipelago Model Asphaltenes with  
a Benzo[b]anthraquinoline Core**

**by**

**Terry Heidt**

A thesis submitted to the Faculty of Graduate Studies and Research in partial  
fulfillment of the requirements for the degree of

Master of Science

Department of Chemistry

©Terry Heidt  
Fall 2013  
Edmonton, Alberta

Permission is hereby granted to the University of Alberta Libraries to reproduce single copies of this thesis and to lend or sell such copies for private, scholarly or scientific research purposes only. Where the thesis is converted to, or otherwise made available in digital form, the University of Alberta will advise potential users of the thesis of these terms.

The author reserves all other publication and other rights in association with the copyright in the thesis and, except as herein before provided, neither the thesis nor any substantial portion thereof may be printed or otherwise reproduced in any material form whatsoever without the author's prior written permission.

*To My Parents*

For encouraging me to work hard, set high standards, and to complete every task, I dedicate this work to you.

## Abstract

The efficient synthesis of model asphaltenes as polyaromatic, nitrogenous compounds is reported. These model asphaltenes are to be used for supramolecular investigation for developing enhanced bitumen processing methodology.

Our synthesis of benzo[f]quinoline and benzo[b]anthraquinoline derivatives linked to polyaromatic hydrocarbons by alkane and alkene tethers, including structures with complex steroidal fusions, make-up an `archipelago` motif and represent current models of asphaltene structure. With an optimized acid catalyzed multicomponent reaction and an improved preparation of 1-vinylpyrene, we developed efficient syntheses of model asphaltene fragments and developed methodology for expanding our library of asphaltene compounds.

## **Acknowledgements**

Thank you to Alisha Luther. You were there when I started and whenever I felt like giving up, you always brought me back on track. You encouraged me throughout this long process and brought balance to my life when things seem overwhelming.

Thank you Stryker group (Colin Diner, Devin Rough, Kirstin Tomlin, Robin Hamilton, Dominique Hebert, Wang Xi, Ting Zhao, Jeffrey Bunquin, Jeremy Gauthier) for your helpful input and informal insights. While our work was independent, without your support this research would not have succeeded. Special thanks to Verner Lofstand for selflessly providing peer-mentorship during research difficulty.

Thank you Dr. Jeff Stryker, my research supervisor, for your patience and expert guidance throughout this journey.

Thank you to the staff of the Spectral Services and MSPEC labs for all your assistance.

## Table of Contents

|  |    |
|--|----|
| Chapter 1 - Introduction.....  | 1  |
| 1.1 – Asphaltenes in Organic Chemistry.....  | 1  |
| 1.1.1 - Importance of Asphaltenes: An Overview.....  | 1  |
| 1.1.2 – Chemical Characteristics of Asphaltenes.....   | 2  |
| 1.2 – Structural Theories of Asphaltenes .....   | 4  |
| 1.2.1 - Continental Model Theory .....   | 4  |
| 1.2.2 – Problems with the Continental Model Theory .....   | 6  |
| 1.2.3 - Archipelago (Supramolecular Assembly) Model .....  | 8  |
| 1.3 – Application of the Archipelago Model.....  | 9  |
| 1.4 – References for Chapter 1.....  | 11 |
| Chapter 2 - Three-Component Reaction Catalyzed by Acid for the Synthesis of Benzo[f]quinoline and Benzo[b]anthraquinoline Derivatives: Improvements on Kozlov and Wang Cyclization Reactions ..... | 13 |
| 2.0 - Overview .....   | 13 |
| 2.1 – Discrepancy in Wang’s Cyclization .....  | 14 |
| 2.1.1 - Origin of benzo[f]quinolines from Three Component Coupling (Kozlov Reaction) ...   | 14 |
| 2.1.2 –Wang’s ‘Improved’ Three-Component Coupling Reaction: Issues with the Published Procedures.....  | 16 |
| 2.2 – Correction of Wang’s Three-Component Coupling Procedure and its Relation to The Kozlov Reaction .....  | 17 |
| 2.2.1 – Acid Catalysis Proposal of Wang’s Three Component Coupling.....  | 17 |
| 2.2.2 – Experimental Support for Acid Catalysis .....  | 18 |
| 2.2.3 – Development of an Optimized Acid Catalyst.....   | 21 |
| 2.2.4 – Mechanistic Analysis of Three Component Reaction .....   | 23 |
| 2.3 – Summary of Improved Methodology for the synthesis of Benzo[f]quinolines and Benzo[b]anthraquinolines.....  | 25 |
| 2.4 – References for Chapter 2.....  | 25 |
| Chapter 3 - Multi-Component Reaction Modifications.....  | 28 |
| 3.0 – Introduction.....  | 28 |
| 3.1 – Convenient procedures for large scale synthesis of 2-aminonaphthalene (1) and 2-aminoanthracene (10).....  | 29 |

|   |    |
|---|----|
| 3.1.1 – Synthesis of 2-aminoanthracene (10).....  | 29 |
| 3.1.2 – Synthesis of 2-aminonaphthalene (1).....  | 32 |
| 3.2 – Bromination of 2-amino-anthracene/naphthalene.....  | 32 |
| 3.2.1 – Desired use of 2-aminonaphthalene and 2-aminoanthracene brominated derivatives<br>.....                     | 32 |
| 3.2.2 – Bromination 2-aminonaphthalene (1).....   | 33 |
| 3.2.2 - Bromination of 2-aminoanthracene (10) .....   | 35 |
| 3.3 – Post Acid Catalysis Cyclization Modifications.....  | 36 |
| 3.3.1 – Bromination of Cyclization Product (12) to yield dibromo (26) .....   | 38 |
| 3.3.2 – Ethylation/Bromination of Cyclization Product (11) to yield 27 and 28.....                                  | 39 |
| 3.4 - References for Chapter 3 .....  | 39 |
| Chapter 4 – Synthesis of Model Asphaltenes.....   | 41 |
| 4.0 – Introduction.....   | 41 |
| 4.1 – Synthesis of Asymmetric Three Island Asphaltene Model (30).....   | 42 |
| 4.1.1 – Theoretical Model Asphaltene from Wang’s Three-Component Acid Catalyzed<br>Cyclocondensation Reaction. .... | 42 |
| 4.1.2 – Synthesis of 1-Pyrenebutanal (32).....  | 43 |
| 4.1.3 – Synthesis of Model Asphaltene 30 .....  | 43 |
| 4.1.3 – Characterization of Unsymmetric Model Asphaltene (30).....  | 44 |
| 4.2 –Synthesis of 32 – Coupling of Acid Catalysis Product .....   | 49 |
| 4.2.1 – Overview of Synthesis of 31 .....   | 49 |
| 4.2.2 – Synthesis of 1-Vinylpyrene (36).....  | 49 |
| 4.2.3 – Coupling of Dibromo Island 28 to 1-Vinylpyrene (34): Synthesis of Unsaturated<br>Asphaltene Model .....     | 51 |
| 4.2.4 – Characterization of Unsaturated Asphaltene Model (31) .....   | 52 |
| 4.2.5 – Attempted Hydrogenation to Obtain Saturated Model Asphaltene (38) .....                                     | 54 |
| 4.3 – Summary of Model Asphaltene Synthesis.....  | 56 |
| 4.4 - References for Chapter 4 .....  | 56 |
| Chapter 5 – Research Highlights and Future Considerations.....  | 58 |
| 5.1 – Research Highlights .....   | 58 |
| 5.2 - Future Considerations .....   | 59 |
| 5.2.1 – Possible Substrates for Model Asphaltene Synthesis.....   | 59 |

|  |    |
|--|----|
| 5.2.2 – Variations in Unsymmetric Model Asphaltene 30.....   | 60 |
| 5.2.3 – Advancement of 1-Vinylpyrene Procedure .....   | 61 |
| 5.2.4 - Hydrogenation of Unsaturated Model Asphaltene (30) .....   | 61 |
| 5.3 – References for Chapter 5.....  | 62 |
| Chapter 6 – Experimental Section .....   | 63 |
| 6.1 –General Experimental Details.....   | 63 |
| 6.1.1 - Methods .....  | 63 |
| 6.1.2 - Equipment .....  | 63 |
| 6.1.3 – Reagents and Literature Compounds .....  | 64 |
| 6.1.4 – Instrumentation.....   | 66 |
| 6.2 – Reaction Procedures.....   | 66 |
| 6.2.1 - 6-Bromo-2-naphthol (22) .....  | 66 |
| 6.2.2 - 2-Aminonaphthalene (1) .....   | 68 |
| 6.2.3 - 6-Bromo-2-aminonaphthalene (21) .....  | 69 |
| 6.2.4 - 2-Aminoanthracene (10) .....   | 70 |
| 6.2.5 - 1-Bromo-2-aminoanthracene (23) .....   | 71 |
| 6.2.6 - 1,10-Dibromo-2-aminoanthracene (24).....   | 72 |
| 6.2.7 - 5-(3-Bromophenyl)-1,2,3,4-tetrahydrobenzo[b]anthraquinoline (12) .....                             | 72 |
| 5-(3-Bromophenyl)-1,2,3,4-tetrahydrobenzo[b]anthraquinoline (12) .....                                     | 74 |
| 6.2.8 - 5-(3-Bromophenyl)-1,2,3,4-tetrahydrobenzo[b]anthraquinoline hydroiodide (15) ..                    | 75 |
| 6.2.9 - 5-(3-Bromophenyl)-2,3,4,5,21,N-hexahydrobenzo[b]anthraquinoline (13) .....                         | 76 |
| 6.2.10 - N-(3-Bromobenzyl)anthracen-2-amine (14).....  | 78 |
| 6.2.11 - 13-Bromo-5-(3-bromophenyl)-1,2,3,4-tetrahydrobenzo[b]anthraquinoline (26) ...                     | 79 |
| 6.2.12 - 5-(16-Ethylphenyl)-1,2,3,4-tetrahydrobenzo[b]anthraquinoline (27) .....                           | 81 |
| 6.2.13 - 13-Bromo-5-(3-ethylphenyl)-1,2,3,4-tetrahydrobenzo[b]anthraquinoline (28) .....                   | 83 |
| 6.2.14 - 1-Pyrenebutanol (34) .....  | 85 |
| 6.2.15 - 1-Pyrenebutanal (32).....   | 86 |
| 6.2.16 - 2-(1-Ethylpyrene)-3-(1-propylpyrene)-benzo[b]anthraquinoline (30):.....                           | 87 |
| 6.2.17 - 1-Vinylpyrene (36):.....  | 89 |
| 6.2.18 - 13-(1-Vinylpyrene)-5-(3-(1-vinylpyrene)phenyl)-1,2,3,4-tetrahydrobenzo[b]<br>anthraquinoline (31) |    |

|   |     |
|---|-----|
| 6.3 - References for Experimentals .....  | 92  |
| Appendix.....   | 94  |
| 1 – Selected spectra for 6-bromo-2-naphthol (20) .....  | 94  |
| 2 – Selected spectra for 2-aminonaphthalene (1).....  | 96  |
| 3 – Selected spectra for 6-Bromo-2-aminonaphthalene (21) .....  | 97  |
| 4 – Selected spectra for 2-aminoanthracene (10).....  | 99  |
| 5 – Selected spectra for 1-bromo-2-aminoanthracene (23) .....   | 101 |
| 5 – Selected spectra for 1,10-dibromo-2-aminoanthracene (24) .....  | 103 |
| 6 – Selected spectra for 5-(3-bromophenyl)-1,2,3,4-tetrahydrobenzo[b]<br>anthraquinoline(12).....                               | 105 |
| 7 – Selected spectra for 5-(3-bromophenyl)-1,2,3,4-tetrahydrobenzo[b]<br>anthraquinoline hydroiodide (15).....                  | 109 |
| 8 – Selected spectra for 5-(3-bromophenyl)-2,3,4,5,21,N-<br>hexahydrobenzo[b]anthraquinoline (13) .....                         | 111 |
| 9 – Selected spectra for N-(3-bromobenzyl)anthracen-2-amine (14).....   | 113 |
| 10 – Selected spectra for 13-bromo-5-(3-bromophenyl)-1,2,3,4-<br>tetrahydrobenzo[b]anthraquinoline (26).....                    | 115 |
| 11 –Selected spectra for 5-(16-Ethylphenyl)-1,2,3,4-tetrahydrobenzo[b]<br>anthraquinoline (27).....                             | 117 |
| 11 –Selected spectra for 13-Bromo-5-(3-ethylphenyl)-1,2,3,4-tetrahydrobenzo[b]<br>anthraquinoline (28).....                     | 119 |
| 12 –Selected spectra for 1-pyrenebutanol (34) .....   | 121 |
| 13 –Selected spectra for 1-pyrenebutanal (32).....  | 123 |
| 14 –Selected spectra for 2-(1-Ethylpyrene)-3-(1-propylpyrene)-benzo[b] .....  | 125 |
| anthraquinoline (32).....   | 125 |
| 15 –Selected spectra for 1-vinylpyrene (36) .....   | 128 |
| 15 –Selected spectra for 13-(1-vinylpyrene)-5-(3-(1-vinylpyrene)phenyl)-1,2,3,4-<br>tetrahydrobenzo[b]anthraquinoline (31)..... | 130 |



## List of Tables

|   |    |
|---|----|
| Chapter 1   |    |
| 1.1. Macro properties of asphaltenes <sup>13</sup> .....  | 3  |
| 1.2. Average properties of Athabasca asphaltenes <sup>1</sup> .....                               | 4  |
| Chapter 2   |    |
| 2.1. <sup>1</sup> H NMR selected chemical shifts ( $\delta$ ) for <b>15</b> and <b>12</b> . ..... | 21 |
| 2.2. Synthetic results of amine, ketone, and m-bromobenzaldehyde .....                            | 21 |
| Chapter 4   |    |
| 4.1. Structural features of two aliphatic chains of <b>30</b> based on 1H NMR and COSY data.....  | 45 |
| 4.2. Evidence for pyrene connections to chains A and B in <b>30</b> .....                         | 46 |
| 4.3. Selected TROSEY and HMBC correlations for <b>30</b> . .....                                  | 47 |

## List of Figures

|   |    |
|---|----|
| Chapter 1   |    |
| 1.1. Basic components of crude oil.....   | 2  |
| 1.2. Aggregation of substituted HBC .....   | 6  |
| 1.3. Archipelago (Supramolecular Assembly) model of asphaltenes. ....                                   | 9  |
| Chapter 2   |    |
| 2.1. <sup>1</sup> H NMR spectra (aromatic region) of intermediate <b>14</b> and product <b>11</b> ..... | 20 |

## List of Schemes

|  |    |
|--|----|
| Chapter 1  |    |
| 1.1. Continental model of asphaltene. ....   | 5  |
| 1.2. Desired structural motif of model asphaltene and its interaction with water.....      | 10 |
| Chapter 2  |    |
| 2.1. Benzo[f]quinoline core. ....  | 13 |
| 2.2. Kozlov et al. two step procedure for the synthesis of benzo[f]quinolines.....         | 15 |
| 2.3. Three-component Kozlov reaction. ....   | 15 |
| 2.4. `Improved` three-component coupling Kozlov reaction reported by Wang.....             | 16 |
| 2.5. Three-component coupling using Wang's procedure and with the addition of water..      | 17 |
| 2.6. Iodine-catalyzed three-component reaction using Wang's procedure.....                 | 18 |
| 2.7. Pyridinium salt <b>15</b> as an intermediate to Wang's three-component coupling. .... | 19 |
| 2.8. Updated mechanism for Wang's three-component coupling reaction.....                   | 23 |
| Chapter 3  |    |
| 3.1. Acid catalysis product <b>12</b> in which further modifications are made. ....        | 28 |
| 3.2. Resonance structures of 2-aminoanthraquinone ( <b>17</b> ) .....                      | 29 |
| 3.3. Partial reduction of 1,8-diaminoanthraquinone ( <b>18</b> ). .....                    | 30 |
| 3.4. Synthesis of 2-aminoanthracene ( <b>10</b> ).....                                     | 31 |
| 3.5. Suspected impurity in 2-aminoanthracene ( <b>10</b> ). .....                          | 31 |

|   |    |
|---|----|
| 3.6. Synthesis of 2-aminonaphthalene ( <b>1</b> ).....                                | 32 |
| 3.7. Retrosynthetic installation of bromine into the asphaltene island model.....     | 33 |
| 3.8. Synthesis of 6-bromo-2-aminonaphthalene ( <b>21</b> ) .....                      | 34 |
| 3.9. Model asphaltene island ( <b>22</b> ) .....                                      | 34 |
| 3.10. Direct bromination of 2-aminoanthracene. ....                                   | 35 |
| 3.11. Possible route to 10-bromo-2-aminoanthracene ( <b>25</b> ) .....                | 36 |
| 3.12. Model asphaltene 'island' derivatives, <b>26-28</b> .....                       | 37 |
| 3.13. Numbering system for benzo[b]anthraquinoline derivatives. ....                  | 37 |
| 3.14. Intermediate <b>29</b> during direct bromination of MCR product <b>12</b> ..... | 38 |

#### Chapter 4

|   |    |
|---|----|
| 4.1. Model asphaltene product <b>30</b> as well as product <b>31</b> , from attempted model asphaltene synthesis. ....  | 41 |
| 4.2. Theoretical reaction of 1-pyrenebutanal ( <b>32</b> ), 2-aminoanthracene ( <b>10</b> ), and cyclohexanone based on previous three component acid catalysis results. .... | 42 |
| 4.3. Synthesis of 1-pyrenebutanal ( <b>32</b> ).....  | 43 |
| 4.4. Synthesis of asymmetric model asphaltene <b>30</b> .....   | 44 |
| 4.5. Postulated mechanism for formation of compound <b>30</b> .....   | 48 |
| 4.6. Retrosynthetic analysis of model asphaltene <b>31</b> .....  | 49 |
| 4.7. Two-step synthesis of 1-vinylpyrene ( <b>36</b> ).....   | 50 |
| 4.8. Synthesis of compound <b>31</b> .....  | 51 |
| 4.9. HMBC correlations linking benzene ring to pyridine ring in <b>31</b> .....   | 53 |
| 4.10. Comparison of apparent singlet in <b>31</b> and 1-vinylpyrene. ....   | 53 |
| 4.11. HMBC correlations of a bridging alkene to the substituted benzene ring in <b>31</b> . ....  | 54 |
| 4.12. Target model asphaltene <b>38</b> .....   | 55 |

#### Chapter 5

|   |    |
|---|----|
| 5.1. Possible substrates for future model asphaltenes. .... | 60 |
| 5.2. Possible future model asphaltene targets.....          | 61 |

## Abbreviations

DCM – dichloromethane  
DMF - dimethylformamide  
DMSO – dimethyl sulfoxide  
EtOAc - ethyl acetate  
RBF – round bottom flask  
HBC - hexabenzocoronene  
Hex - hexanes  
m-BBA - m-bromobenzaldehyde  
MCR – multicomponent reaction  
POC - proof of concept  
Py - pyrene  
RBF – round bottom flask  
THF – tetrahydrofuran  
TLC – thin layer chromatography

### *NMR symbols:*

(+) - quaternary or methylene carbon  
(-) - methine or methyl carbon.  
 $\delta$  - NMR chemical shift in ppm  
ABq - AB quartet  
abs - absorbance  
app - apparent  
br - broad  
d – doublet  
dt - doublet of triplets. *J* values are given as the doublet first, then the triplet.  
p - pentet  
s - singlet  
t - triplet

## Chapter 1 - Introduction

A study of the synthesis of compounds to model aspects of asphaltene structure is presented within. The following introductory chapter defines what asphaltenes are and explains their significance in oil extraction and refining. The importance of modelling asphaltene compounds is discussed and structural motifs that directed our research are presented.

### 1.1 – Asphaltenes in Organic Chemistry

#### 1.1.1 - Importance of Asphaltenes: An Overview

Nondistillable, high molecular weight materials from heavy oils and bitumen create technological difficulties in their production and upgrading.<sup>1</sup> The heaviest fraction, the one with the greatest molecular weight, from these materials and other oil deposits are known as asphaltenes (Figure 1.1).<sup>1</sup>**Error! Bookmark not defined.**

Their propensity to precipitate and deposit within extraction pipes and process plants is a problem in the petroleum industry.**Error! Bookmark not defined.** This causes a significant reduction in productivity which stems from flow assurance problems, injectivity (the rate and pressure at which oil can be pumped), and blockage of piping equipment such as wellbores. As well, the blending of different crude oils may lead to precipitation of asphaltenes, further increasing maintenance costs and reducing productivity.<sup>2,3,4,5,6</sup> Asphaltene deposition has profound economic consequences on oil production.<sup>7</sup>

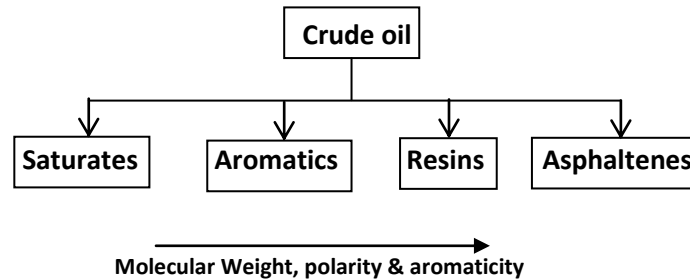


**Figure 1.1.** Basic components of crude oil.<sup>8</sup>

---

### 1.1.2 – Chemical Characteristics of Asphaltenes

Asphaltene deposition currently remains an unsolved challenge. Experimental techniques and theoretical models attempting to predict asphaltene behaviour hope to address the potential problem of asphaltene deposition during oil production. **Error! Bookmark not defined.** Overcoming deposition problems may require a deeper understanding at the molecular level of the mechanisms by which asphaltenes precipitate.<sup>1</sup> **Error! Bookmark not defined.** Specifically, model compounds that mimic the structure and behaviour of asphaltenes may lead to understanding their nature of self-aggregation. Insights into the degree and type of intermolecular forces and functional groups involved may reveal methods to facilitate the petroleum industry's battle on asphaltene deposition. Gray, et al.,<sup>9</sup> list eight experimentally determined characteristics of asphaltenes that must be inherent in an asphaltene model (Table 1.1). These characteristics indicate that asphaltenes cannot be defined by a few molecular

motifs. Rather, a panel of motifs is required and any molecular asphaltene theory must account for these properties.

**Table 1.1.** Macro properties of asphaltenes<sup>9</sup>

| Characteristic                                     | Description   |
|--|---|
| Molecular Complexity                               | Multiple functional groups interact in liquid phase.  |
| Heterogeneous aggregation and coagulation behavior | Precipitation due to coagulation, colloidal aggregates and insolubility range in sizes in a polydisperse distribution.  |
| Occlusion in asphaltene aggregates                 | Asphaltene precipitation results in the entrapment of n-alkane soluble material.  |
| Porosity of asphaltene aggregates                  | Aggregates are porous enough to enable exchange with surrounding solvents.  |
| Adhesion to surfaces                               | Asphaltenes adhere avidly to a range of surfaces particularly to oxides.  |
| Formation of films at oil-water interfaces         | Asphaltenes combine with crude oil colloidal mineral particles to form viscoelastic films at interfaces, playing a role in the stabilization of water- in-oil emulsions.  |
| Mechanical properties                              | The elastic extension of the aggregates is consistent with a long-chain polymer under pulling by an external force. Aggregates on silica in solvent behave like polymers, with properties that depended on the solvent composition. |
| Interactions with resins and surfactants           | The apparent molecular weight depends on both concentration of asphaltene and concentration of resin components in solution.  |

By definition, asphaltenes are the fraction in petroleum oils that is soluble in aromatic solvents, such as benzene or toluene, and insoluble in saturated hydrocarbons, such as n-pentane or n-heptane.<sup>10</sup> However this definition poses little insight into what specific structures are present. Molecular diffusion techniques estimates petroleum asphaltenes to have an

average molecular weight of ~750 g/mol but the spectrum of molecular weights varies widely and it is not uncommon to observe average weights of over double that amount.<sup>11</sup>

Elemental analysis and <sup>1</sup>H and <sup>13</sup>C NMR spectroscopy of Athabasca asphaltenes (Table 1.2) reveal material that is made of predominantly carbon (80%) with far lesser amounts of heteronuclei. Although asphaltene composition is a nearly infinite set of biogeological decomposition products, global structural patterns do exist. The majority of carbon is saturated and the aromatic carbons are largely quaternary. The low percentage of aromatic methines infers an aromatic cluster motif. Thus, structural theories include polyaromatic organic compounds with a wide range of functionality.

**Table 1.2.** Average properties of Athabasca asphaltenes<sup>1</sup>

| Elemental Analysis, wt % |      | <sup>1</sup> H and <sup>13</sup> C NMR       |      |
|--------------------------|------|--|------|
| C                        | 79.9 | aromatic C per 100C                          | 37   |
| H                        | 8.3  | saturated C per 100C                         | 63   |
| N                        | 1.2  | aromatic H per 100 C                         | 8    |
| S                        | 7.8  | saturated H per 100C                         | 116  |
| O                        | 2.8  | H <sub>aromatic</sub> /C <sub>aromatic</sub> | 0.23 |

Two main theories on the composite structure of asphaltenes exist: the continental (colloidal particle) model and the archipelago (supramolecular assembly) model. Continental model compounds are, in general, highly alkylated condensed polycyclic aromatic compounds. This model has persisted for almost 90 years but has now been largely replaced with the archipelago model, which depicts asphaltenes as smaller aromatic and cycloalkyl clusters linked together with alkyl carbon bridges.

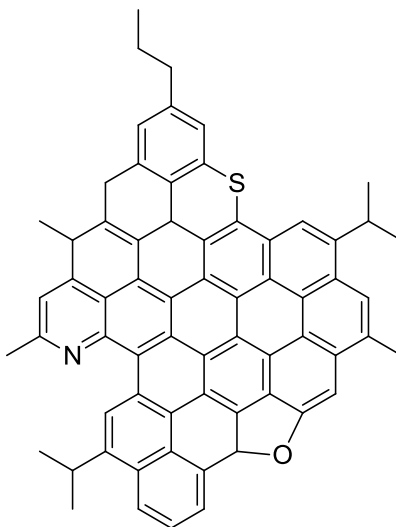
## 1.2 – Structural Theories of Asphaltenes

### 1.2.1 - Continental Model Theory

The idea of asphaltenes as colloidal particles stabilized by resins was popularized by Pfeiffer and Saal.<sup>12</sup> This model yields a structure shaped “like your hand”, with a single fused aromatic core and peripheral alicyclic and alkane substituents (Scheme 1.1).<sup>13</sup> A large number of condensed benzene rings were assumed to form the aromatic system of asphaltenes with the majority of the heteroatoms residing in the aromatic interior.<sup>14</sup>

---

**Scheme 1.1.** Continental model of asphaltene.



---

Proponents of this model explain aggregation in terms of van der Waal interactions between regions of aromatic clusters.<sup>15</sup> The aromatic clusters physically stack on top of each



other forming supramolecular aggregates (Figure 1.2). These aggregates are thought to form a colloid in solution.

A highly studied class of compounds exhibiting a tendency to aggregate are the hexabenzocoronenes (HBC). Hexasubstituted derivatives of HBCs have been shown to aggregate under specific concentration and temperature-dependent conditions.<sup>16</sup> Lateral packing of HBC has been characterized in lattices of 2D intercolumnar hexagonal arrangements.<sup>17</sup> This 'π-π' stacking is the presumed driving force behind aggregation from the continental model.

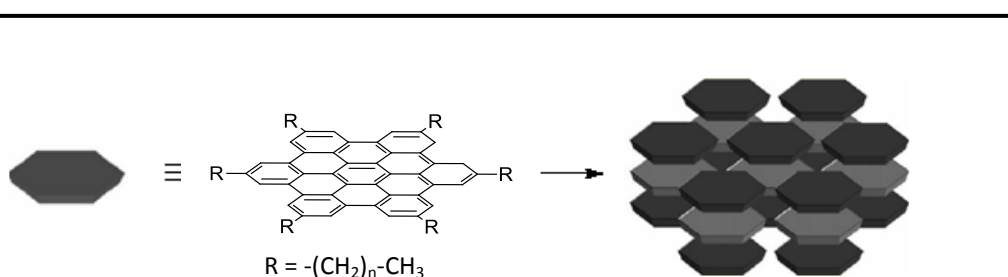


**Figure 1.2.** Aggregation of substituted HBC. Reprinted with permission from Rakotondradany et al.<sup>15</sup> Copyright 2013 American Chemical Society.

---

### 1.2.2 – Problems with the Continental Model Theory

However, this model does not mimic real asphaltene behaviour.<sup>9-18,19</sup> For example, toluene competes successfully for adsorption to the planar aromatic ring of HBCs so that stacking in solution is weak and equilibrating at room temperature. In contrast, asphaltene aggregation in toluene occurs even in highly dilute solutions.<sup>9</sup> These results show that the π-π stacking of large aromatics is too weak in toluene solutions to account for aggregation of asphaltenes in highly dilute solution or at elevated temperature.<sup>9</sup> As well, model HBC

aggregates do not adhere to glass surfaces as asphaltenes do and they completely dissolve at 42°C. At 70°C, measurement of the apparent molecular weight of a C6-HBC analogue in toluene by vapor-pressure osmometry revealed the presence of only dimers in toluene solution, whereas asphaltenes aggregate in temperatures exceeding 120 °C.<sup>14</sup>

A compound with a large polyfused aromatic core does not give strong adsorption on silica. The alkyl side chain motif of this model also fails to exhibit absorption onto oxide surfaces as required by property 5 from Table 1.19

Asphaltenes aggregate randomly without repetition of assembly.<sup>9</sup> The 'π-π' stacking requirement of all continental models create long repetitive structures (i.e. fibres) and this type of pattern is not observed in real asphaltenes.<sup>9</sup> Thus, an appropriate model must account for randomized supramolecular aggregation, resulting in a very limited length scale of repetitive structures.<sup>9</sup>

Incidentally, the same geochemical processes that generate the light components of petroleum, such as n-alkanes, simultaneously produce some of the most complex heavy components in asphaltenes.<sup>1</sup> This creates difficulty in fitting asphaltenes into the continental model as large polyaromatic clusters differ markedly in structure and property compared to n-alkanes.

According to Sirota,<sup>14</sup> asphaltenes' colloid-like appearance is due to the fact that its phase is often below its glass transition. Aggregates therefore appear solid, exhibiting a fractal-like morphology only because of the kinetic inability for the 'droplets' to coalesce.<sup>19</sup> Current theory now places asphaltenes in a liquid state.<sup>9</sup>

Some Asphaltene substructures have been identified and it was found that pericondensed aromatic units play a very minor role in the molecular structure of petroleum asphaltene.<sup>20</sup> For example, the oxidative degradation by ruthenium ions of the asphaltene core

unveils that the bulk of the chemical constituents of petroleum asphaltenes consists of normal alkanolic-derived hydrocarbons and heterocycles, with minor amounts of pigments, terpenoids, and other biotic material.<sup>21</sup> Alkylpyridines, quinolines, *n*-alkanoic/alkenoic acids, *n*-alkylamides, and some *n*-alcohols were all identified in asphaltenes.<sup>12</sup>

Extending beyond the continental model, specific intermolecular interactions of asphaltenes were further demonstrated to include all major intermolecular forces: acid-base interactions, hydrogen bonding, hydrophobic interactions driven by van der Waals interactions, and  $\pi$ - $\pi$  stacking.<sup>9</sup> Deeper chemical and supramolecular analysis of asphaltenes has led to the newer and more complex supramolecular assembly model (Figure 1.3).

### 1.2.3 - Archipelago (Supramolecular Assembly) Model

Figure 1.3 depicts the currently accepted model of asphaltenes as a supramolecular assembly. In this model, all intermolecular forces are at play. Acid-base interactions and hydrogen bonding in the upper middle portion of the diagram link the smaller benzo[f]quinoline and benzoic acid derivatives to the larger central molecule. Hydrophobic interactions are depicted between aliphatic rings in the middle left region.  $\pi$ - $\pi$  stacking is shown between the pyrene, naphthalene, phenanthrene, and dibenzofuran moieties. Notably, aromatic regions are covalently linked by 1-4 methylene carbon tethers. The toluene molecule in the middle left region imbedded in the pyrene derivative represents the inclusion of small molecules into the asphaltene framework and depict the porosity nature of asphaltenes. This model lends support for strong intermolecular adhesions between asphaltene molecules as well as the thousands of representative molecules observed in real asphaltenes.

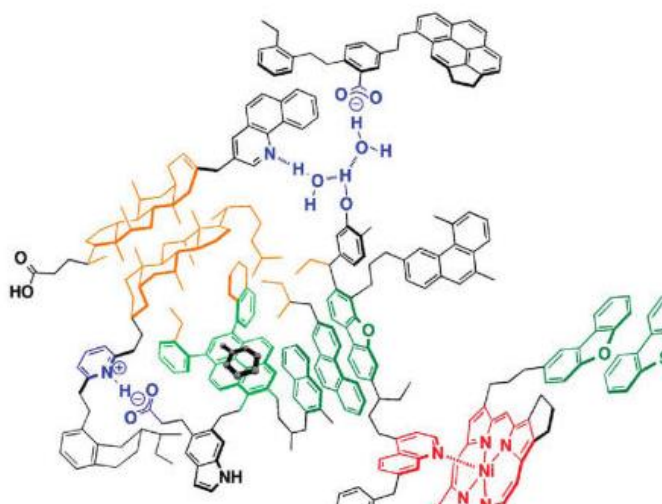


**Figure 1.3.** Archipelago (Supramolecular Assembly) model of asphaltenes. Reprinted with permission from Gray et al.<sup>9</sup> Copyright 2013 American Chemical Society.

---

### 1.3 – Application of the Archipelago Model

The archipelago model has directed the research described herein. The goal of this research is to build model asphaltene compounds, adding to an array of possible molecular asphaltene candidates. These model asphaltenes will be, both individually and as mixtures, scrutinized in terms of their supramolecular aggregation, adhesion, and precipitation properties as described in Table 1.1. Just as the continental/colloidal particle model has been abandoned

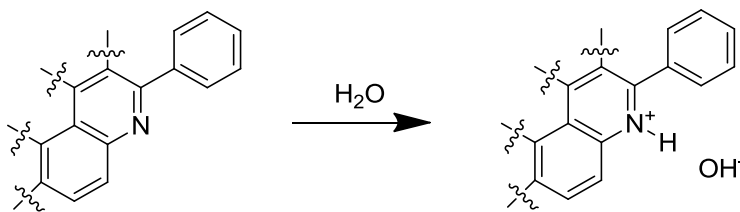
due to experimental testing of asphaltenes and model compounds, the supramolecular assembly model will be tested and compared to asphaltenes as well as future model candidates.

Previously in the Tykwinski and Stryker groups, aromatic carbo- and heterocycles with bridging aliphatic regions were synthesized.<sup>22</sup> The purpose of this study was to add to this library and to produce model compounds that may show some adhesion to water, preferably in a clathrate structure.

Our attention turned to aromatic nitrogenous bases as possible candidates. A model with basic nitrogen imbedded in a 'bay region' that accommodates water was desired. Scheme 1.1 illustrates the structural motif investigated and depicts how a water molecule may complex to the aromatic system.

---

**Scheme 1.2.** Desired structural motif of model asphaltene and its interaction with water.



As well, we envisioned incorporating steroidal motifs into our models. Steroidal compounds are ubiquitous in petroleum.

In the following chapter, the synthesis of several benzo[f]quinolines and benzo[b]anthraquinolines, which incorporate the motif from Scheme 1.2, is described. Improvements from literature procedures were required in order for the syntheses to proceed. Chapter 3 describes modifications to the benzo[b]anthraquinoline periphery, adding new functionality to the series. Chapter 4 describes in preliminary form the full syntheses of a few

archipelago model asphaltenes. Lastly, Chapter 5 summarizes the models synthesized and describes prospective research.

#### 1.4 – References for Chapter 1

- 
1. Payzant, J. D.; Lown, E. M.; Strausz, O. P. Structural units of Athabasca asphaltene: The aromatics with a linear carbon framework. *Energy Fuels* **1991**, *5*, 445–453.
  2. Wiehe, I.; Kennedy, R. J. The Oil Compatibility Model and Crude Oil Incompatibility. *Energy Fuels* **2000a**, *14*, 56-59.
  3. Wiehe, I., and Kennedy, R. J. Application of the Oil Compatibility Model to Refinery Streams. *Energy Fuels* **2000b**, *14*, 60-63.
  4. van den Berg, F. G. A.; Kapusta, S. D.; Ooms, A. C.; Smith, A. J. Fouling and compatibility of crudes as basis for a new crude selection strategy. *Pet. Sci. Technol.* **2003**, *21*, 557–568.
  5. Schermer, W. E. M.; Melein, P. M. J.; van den Berg, F. G. A. Simple techniques for evaluation of crude oil compatibility. *Petrol. Sci. Tech.* **2004**, *22*, 1045–1054.
  6. Carbognani, L.; Orea, M.; Fonseca, M. Complex Nature of Separated Solid Phases from Crude Oils. *Energy Fuels* **1999**, *13*, 351-358.
  7. Creek, J.L. Freedom of Action in the State of Asphaltenes: Escape from Conventional Wisdom. *Energy Fuels* **2005**, *19*, 1212-1224.
  8. Wang, J. *Asphaltene: A General Introduction*, Petroleum Recovery Research Center, New Mexico Tech, Presented October 18, 2000.
  9. Gray, M. R.; Tykwinski, R. R.; Stryker, J.M.; Tan, X. Supramolecular Assembly Model for Aggregation of Petroleum Asphaltenes, *Energy Fuels* **2011**, *25*, 3125-3134.
  10. Liao, Z. W.; Zhao, J.; Creux, P.; Yang, C. P. Discussion on the Structural Features of Asphaltene Molecules. *Energy Fuels* **2009**, *23*, 6272-6274.
  11. Betancourt, S. S.; Ventura, G. T.; Pomerantz, A. E.; Vilorio, O.; Dubost, F. X.; Zuo, J.; Monson, G.; Bustamante, D.; Purcell, J. M.; Nelson, R. K.; Rodgers, R. P.; Reddy, C. M.; Marshall, A. G.; Mullins, O. Nanoaggregates of Asphaltenes in a Reservoir Crude Oil and Reservoir Connectivity. *Energy Fuels* **2003**, *23*, 1178-1188.
  12. Pfeiffer, J. P.; Saal, R. N. J. Asphaltic Bitumen as Colloid System. *J. Phys. Chem.* **1940**, *44*, 139-149.
  13. Andreatta, G.; Goncalves, C. C.; Buffin, G.; Bostrom, N.; Quintella, C. M.; Arteaga-Larios, F.; Perez, E.; Mullins, O. C. Nanoaggregates and Structure-Function Relations in Asphaltenes. *Energy Fuels* **2005**, *19*, 1282-1289.
  14. Sirota, E. B.; Physical Structures of Asphaltenes. *Energy Fuels* **2005**, *19*, 1290-1296.
  15. Rakotondradany, F.; Fenniri, H.; Rahimi, P.; Gawrys, K. L.; Kilpatrick, P. K.; Gray, M. R. Hexabenzocoronene Model Compounds for Asphaltene Fractions: Synthesis & Characterization. *Energy Fuels* **2006**, *20*, 2439-2447.
  16. Wu, J. S.; Fechtenkotter, A.; Gauss, J.; Watson, M. D.; Kastler, M.; Fechtenkotter, C.; Wagner, M.; Mullen, K. Controlled Self-Assembly of Hexa-peri-hexabenzocoronenes in Solution. *J. Am. Chem. Soc.* **2004**, *126*, 11311-11321.
  17. Pisula, W.; Tomovic, Z.; Simpson, C.; Kastler, M.; Pakula, T.; Mullen, K. Relationship between Core Size, Side Chain Length, and the Supramolecular Organization of Polycyclic Aromatic Hydrocarbons. *Chem. Mater.* **2005**, *17*, 4296-4303.

- 
18. Murgich, J. Intermolecular Forces in Aggregates of Asphaltenes and Resins. *Pet. Sci. Technol.* **2002**, *20*, 983–997.
  19. Bagheri, S. R.; Bazyleva, A.; Gray, M. R.; McCaffrey, W.C.; Shaw, J. M. Observation of Liquid Crystals in Heavy Petroleum Fractions. *Energy Fuels* **2010**, *24*, 4327-4332.
  20. Strausz, O. P.; Mojelsky, T. W.; Faraji, F.; Lown, E. M. Additional Structural Details on Athabasca Asphaltene and Their Ramifications. *Energy Fuels* **1999**, *13*, 207-227.
  21. Strausz, O. P.; Lown, E.M.; *The Chemistry of Alberta Oil Sands, Bitumen and Heavy Oils*. Alberta Energy Research Institute: Calgary, 2003.
  22. Alshareef, A. H.; Scherer, A.; Tan, X.; Azyat, K.; Stryker, J. M.; Tykwinski, R.; Gray, M. R. Formation of archipelago structures during thermal cracking implicates a chemical mechanism for the formation of petroleum asphaltenes. *Energy Fuels* **2011**, *25*, 2130–2136.

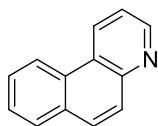
## Chapter 2 - Three-Component Reaction Catalyzed by Acid for the Synthesis of Benzo[f]quinoline and Benzo[b]anthraquinoline Derivatives: Improvements on Kozlov and Wang Cyclization Reactions

### 2.0 - Overview

As discussed in Chapter One, benzo[f]quinolines and benzo[b]anthraquinolines were of interest to us due to their potential as model asphaltene compounds. To recap, asphaltenes, the heaviest and nondistillable fraction in bitumen and crude oil, are mainly represented as one of two models: continental (colloidal particle) model<sup>23</sup> and the archipelago (supramolecular assembly) model.<sup>24</sup> Experimental and theoretical research has largely invalidated the older continental model in favour of the newer archipelago model.<sup>25,26</sup> Adhering to the archipelago model, we envisioned preparing a benzo[f]quinoline core (Scheme 2.1) with halogen functionalization to act as sites for future coupling of additional tethered polyaromatic islands and short-chain peripheral alkyl segments, as found in authentic asphaltenes.

---

**Scheme 2.1.** Benzo[f]quinoline core.





The aromatic nitrogen may complex with water, forming the basis of supramolecular interactions that nucleate a complex aggregate structure (Scheme 1.1, Chapter 1).<sup>27</sup> Experimental support validated the benzo[f]quinoline core as a potential structural model as our collaborators have found this motif during thermal cracking of petroleum asphaltenes.<sup>28</sup> As well, steroidal fragments have been isolated from the thermal cracking of asphaltenes.<sup>28</sup> Included in this chapter is a description of how we synthesized complex compounds with benzo[f]quinoline and steroidal motifs from simple precursors.

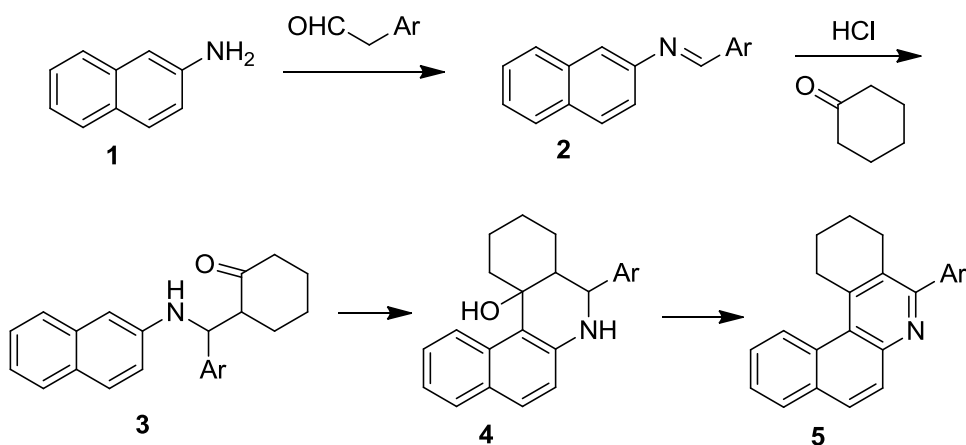
In addition to their potential as model asphaltenes, benzo[f]quinolines exhibit a range of biological activity, including antibacterial properties,<sup>29</sup> inhibition of 5- $\alpha$ -reductase<sup>30</sup> and HIV reverse transcriptase (HIV-1 RT),<sup>31</sup> as well as blocking dopamine receptors.<sup>32</sup> Certain derivatives are carcinogenic in mice and rats, produce mutagenic products along metabolic pathways, and are detected in vehicle exhaust.<sup>33</sup> Thus, synthetic pathways to benzo[f]quinolines have long been of interest.<sup>34</sup>

## **2.1 – Discrepancy in Wang’s Cyclization**

### **2.1.1 - Origin of benzo[f]quinolines from Three Component Coupling (Kozlov Reaction)**

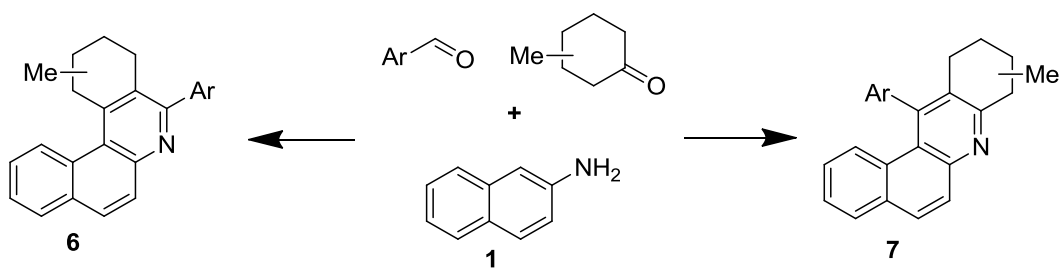
The synthesis of quinoline derivatives via acid-catalyzed Kozlov reaction conditions has been extensively investigated and Kozlov and coworkers discovered a synthesis of benzo[f]quinolines by using a two step procedure (Scheme 2.2).<sup>35</sup> The imine **2** formed in the first step was isolated and then subjected to an acid-catalyzed cyclocondensation to form **5**.

**Scheme 2.2.** Kozlov et al. two step procedure for the synthesis of benzo[f]quinolines.<sup>36</sup>



Most pertinent to us, Kozlov and colleagues furthered this reaction for certain substrates by developing a three-component, one pot, acid-catalyzed analog from simple starting materials (Scheme 2.3) to afford **6** and **7**.<sup>36,37</sup> However, these MCRs suffered from poor yields.

**Scheme 2.3.** Three-component Kozlov reaction.<sup>36,37</sup>

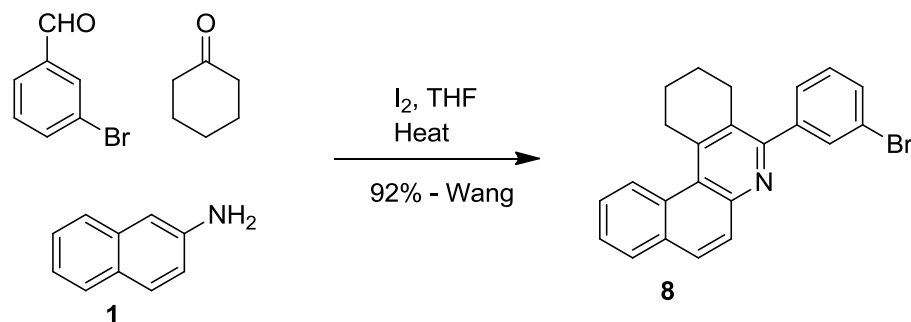


### 2.1.2 –Wang’s ‘Improved’ Three-Component Coupling Reaction: Issues with the Published Procedures.

Wang and coworkers developed an improvement to Kozlov’s methodology, claiming high yields by the use of iodine as a catalyst under anhydrous conditions.<sup>38</sup> However, we were unable to reproduce Wang’s results (reported 92% yield) when using 2-aminonaphthalene, cyclohexanone, and 3-bromobenzaldehyde, a reaction that should have afforded compound **8** (Scheme 2.4). At best, 3% yield of the desired product was obtained.

---

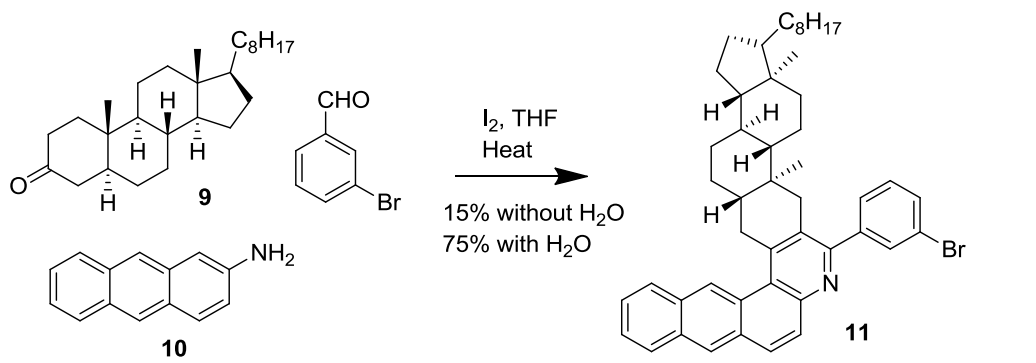
**Scheme 2.4.** ‘Improved’ three-component coupling Kozlov reaction reported by Wang.<sup>38</sup>



---

Similarly, our trial reaction, the iodine-catalyzed cyclocondensation of 5 $\alpha$ -cholestan-3-one (**9**), *m*-bromobenzaldehyde, and 2-aminoanthracene (**10**) in THF gave at best 15% yield of **11** under dry and anaerobic conditions (Scheme 2.5). The regiochemical orientation of the steroid component was determined by comparing our spectroscopic data with those of our collaborator, who obtained an X-ray crystal structure.<sup>39</sup>

**Scheme 2.5.** Three-component coupling using Wang's procedure and with the addition of water.



Previous work in the Tykwinski group in Erlangen, Germany, collaborators with the Stryker group, have found similarly poor yields and resorted instead to the synthesis of benzo[f]quinoline derivatives using Kozlov's two-step method.<sup>40</sup>

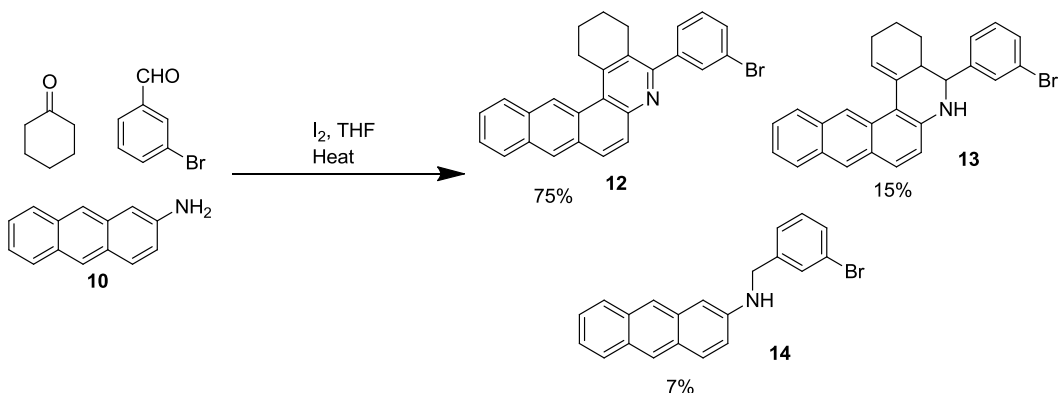
## 2.2 – Correction of Wang's Three-Component Coupling Procedure and its Relation to The Kozlov Reaction

### 2.2.1 – Acid Catalysis Proposal of Wang's Three Component Coupling

Wang and coworkers demonstrated the iodine-catalyzed three-component reaction using 2-aminoanthracene, *m*-bromobenzaldehyde, and 2,3-dihydrofuran.<sup>41</sup> We substituted cyclohexanone for 2,3-dihydrofuran (Scheme 2.6) and, using Wang's conditions, obtained compound **12** in good yield (75%). By-products **13** and **14** are discussed later in the chapter.

---

**Scheme 2.6.** Iodine-catalyzed three-component reaction using Wang's procedure.



The success of this reaction prompted us to investigate why the reaction worked with 2-aminoanthracene (**10**) and not 2-aminonaphthalene (**1**). After many trials, it appears that the active catalyst is not the mild Lewis acid iodine, as published by Wang and coworkers, but is instead a Brønsted acid derived from iodine under the reaction conditions and is thus similar to the Kozlov three-component coupling procedure.

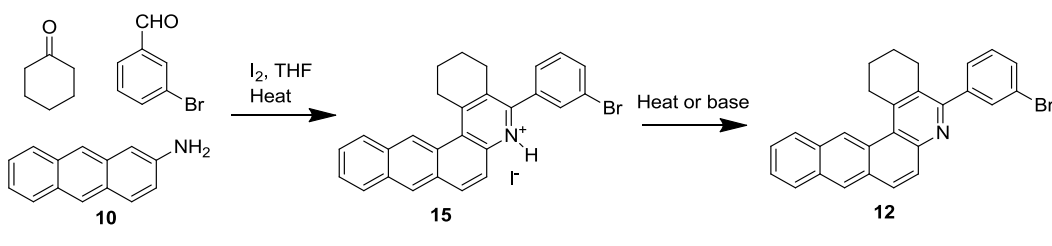
Taken together, our experiments suggest that the large difference in yields observed among us, Kozlov, and Wang, may be attributed to differences in the molar ratio of water and protic acid compared to the starting materials. Wang's MCR procedure with iodine "in anhydrous THF" is convenient but proceeds only upon the addition of water, while the low yields reported by Kozlov et al., may be due to water in excess of optimal.<sup>42</sup>

### 2.2.2 – Experimental Support for Acid Catalysis

Under reaction conditions presented by Wang and coworkers, a yellow precipitate forms when 2-aminoanthracene, cyclohexanone, and 3-bromobenzaldehyde are heated to reflux with 5% iodine in THF (Scheme 2.7). Upon filtration, this insoluble precipitate **15** was characterized as a hydriodic salt of the desired product **12** by spectroscopic and elemental analysis. Moreover, the filtrate from the reaction contained the expected neutral compound **12**. The percent yield of acidified **15** was either comparable to or less than the mole percent of iodine catalyst added to the reaction (5-15%). Although iodine is known to ring-open, as well as polymerize THF catalytically,<sup>43</sup> the observation of the intermediate salt suggests a protic acid-catalyzed, Kozlov-like mechanism.

---

**Scheme 2.7.** Pyridinium salt **15** as an intermediate to Wang's three-component coupling.



More evidence of the protic acid catalyzed nature of this reaction was revealed in the <sup>1</sup>H NMR spectrum of purified **14** by the presence of a 'wandering' broad doublet (Figure 2.1). This doublet has a chemical shift of δ 9.20 upon immediate collection of the spectrum of isolated **14**. When dissolved in solvents including CHCl<sub>3</sub>, DCM, or THF, the broad doublet moves upfield over time until the signal becomes half of an AB quartet, along with another doublet, matching the

spectrum of **15** (Figure 2.1). This transformation is complete in 24 hours at room temperature and accelerated with added heat. The conversion occurs immediately during an aqueous base wash.

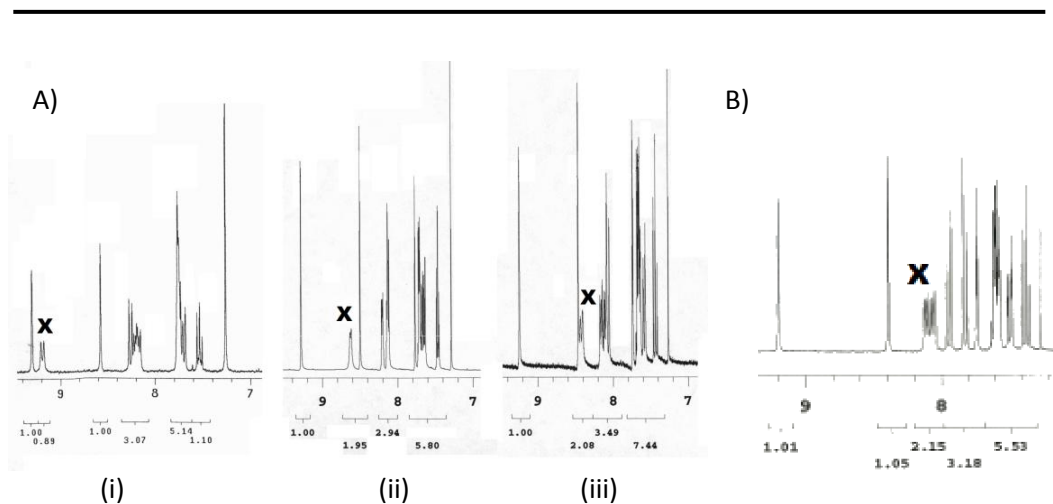


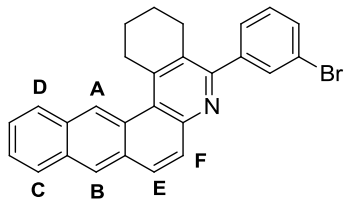
**Figure 2.1.** <sup>1</sup>H NMR spectra (aromatic region) of intermediate **14** and product **11**. (A) Doublet X in moves up field as freshly synthesized **14** remains in CDCl<sub>3</sub> for (i) 0 hrs; (ii) 12 hrs; (iii) 24 hrs. (B) Aromatic region for **11**.

---

Comparing <sup>1</sup>H NMR chemical shifts of HI adduct **15** and expected MCR product **12** lends support to the hypothesis that the aromatic region of **15** is more electron-poor, as what would be expected from an electron withdrawing quaternary nitrogen. <sup>1</sup>H NMR chemical shifts of H<sub>a</sub> to H<sub>e</sub> for **15** are shifted significantly more down field compared to **12** (Table 2.1, Scheme 2.8). Further discussions on the spectroscopic characterizations of three-component coupling products and the hydriodic salt **15** are included in Chapter 3.

**Table 2.1.**  $^1\text{H}$  NMR selected chemical shifts ( $\delta$ ) for **15** and **12**.

| $\text{H}_x$ | Compound  |           |
|--------------|-----------|-----------|
|              | <b>15</b> | <b>12</b> |
| A            | 9.3       | 9.2       |
| B            | 8.49      | 8.4       |
| C,D          | 8.22-8.06 | 8.18-8.01 |
| E            | 8.23      | 7.97      |
| F            | 9.2       | 7.91      |



### 2.2.3 – Development of an Optimized Acid Catalyst

We were perplexed as to how a Brønsted acid catalyst could form in situ under Wang's reactions conditions until one of us<sup>44</sup> added water to the reaction shown in Scheme 2.5, which successfully afforded the desired MCR product **12**. The use of commercial aqueous hydroiodic acid as catalyst instead of iodine and water also gave the desired product, as originally postulated (Table 2.2). Different Brønsted and Lewis acids were evaluated (Table 2.2); aqueous Brønsted acids consistently gave the desired product. Trialkylboron reagents and boric acid do not catalyze the reaction, further suggesting that the active catalyst involves a protic acid.

**Table 2.2.** Synthetic results of amine, ketone, and m-bromobenzaldehyde

| Entry | Ar-NH <sub>2</sub> * | Cyclic ketone | Catalysis                      | Solvent     | Water (%) | Product   | Yield <sup>†</sup> (%) |
|-------|----------------------|---------------|--------------------------------|-------------|-----------|-----------|------------------------|
| 1     | naph-NH <sub>2</sub> | cyclohexanone | I <sub>2</sub>                 | THF         | 0         | <b>8</b>  | 3                      |
| 2     | naph-NH <sub>2</sub> | cyclohexanone | I <sub>2</sub>                 | THF         | 1.0       | <b>8</b>  | 60                     |
| 3     | anth-NH <sub>2</sub> | cyclohexanone | I <sub>2</sub>                 | THF         | 0         | <b>12</b> | 74                     |
| 4     | anth-NH <sub>2</sub> | cyclohexanone | I <sub>2</sub>                 | THF         | 1.3       | <b>12</b> | 86                     |
| 5     | anth-NH <sub>2</sub> | cyclohexanone | I <sub>2</sub>                 | 1,4-dioxane | 0         | /         | 0                      |
| 6     | anth-NH <sub>2</sub> | cyclohexanone | HI                             | THF         | N/A       | <b>12</b> | POC                    |
| 7     | anth-NH <sub>2</sub> | cyclohexanone | HBr                            | THF         | N/A       | <b>12</b> | POC                    |
| 8     | anth-NH <sub>2</sub> | cyclohexanone | HCl                            | THF         | N/A       | <b>12</b> | POC                    |
| 9     | anth-NH <sub>2</sub> | cyclohexanone | H <sub>2</sub> SO <sub>4</sub> | THF         | N/A       | <b>12</b> | POC                    |
| 11    | anth-NH <sub>2</sub> | cyclohexanone | BPh <sub>3</sub>               | THF         | 0         | /         | 0                      |
| 12    | anth-NH <sub>2</sub> | cyclohexanone | BEt <sub>3</sub>               | THF         | 0         | /         | 0                      |



|    |                      |                             |                |     |     |           |    |
|----|----------------------|-----------------------------|----------------|-----|-----|-----------|----|
| 13 | anth-NH <sub>2</sub> | 5 $\alpha$ -cholestan-3-one | I <sub>2</sub> | THF | 0   | <b>11</b> | 15 |
| 14 | anth-NH <sub>2</sub> | 5 $\alpha$ -cholestan-3-one | I <sub>2</sub> | THF | 1.3 | <b>11</b> | 84 |

\* naph-NH<sub>2</sub> is 2-aminonaphthalene; anth-NH<sub>2</sub> is 2-aminoanthracene

† POF = proof of concept

The large differences in product yields obtained using HI, HBr, HCl, and H<sub>2</sub>SO<sub>4</sub> may have been attributed to differences in the water content for each experiment. Although water is clearly required for catalysis, too much water seems to hamper the reaction. To test this hypothesis, water optimization experiments were performed to determine the amount of water that delivers the greatest yield (Table 2.2).<sup>45</sup> Applying the optimized water and iodine concentration to the MCR in Scheme 2.5 afforded **12** in 86% yield, now comparable to Wang's reported yield. Higher reaction temperatures obtained by the use of 1,4-dioxane or prolonged reaction times do not increase yield.

These experiments established that 1.3 mol% of water in THF with 5 mol% iodine produces an 84% yield of **11** from 2-aminoanthracene and 5 $\alpha$ -cholestan-3-one. Under optimal conditions, the previously failed 2-aminonaphthalene/cyclohexanone case gave a 60% yield, demonstrating the sensitivity of the multicomponent cyclocondensation reaction to experimental conditions.

Iodine and water form equilibria (1) and (2) and this is presumably the protic acid that is required for the MCR.<sup>46</sup>



As such, iodine acts as a precatalyst. In theory adding hydroiodo acid directly ought to produce better yields than adding iodine since iodine must first hydrolyze to become effective.

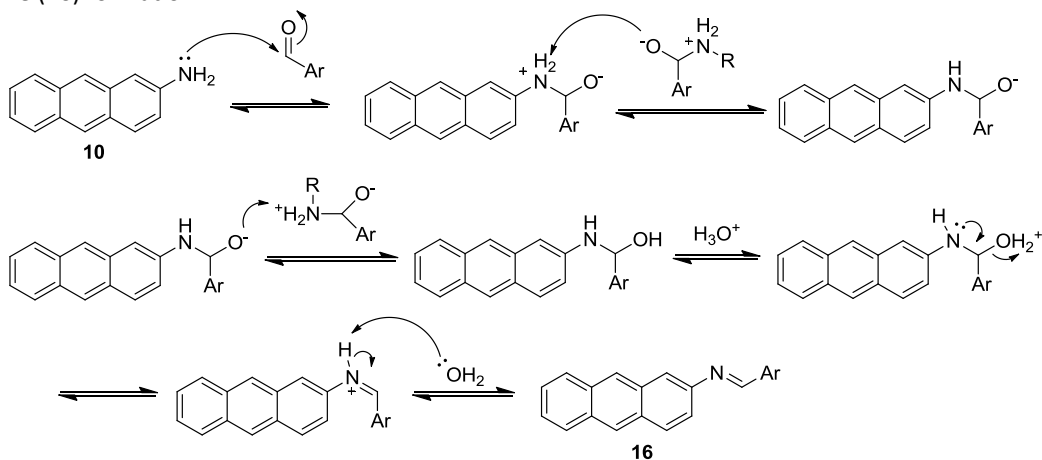
Good yields were not obtained from concentrated hydroiodo acid possibly due to the high water content. As well, hydroiodo acid may be too strong of an acid to produce good yields.

## 2.2.4 – Mechanistic Analysis of Three Component Reaction

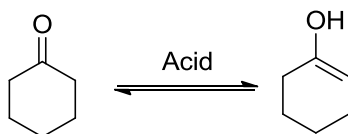
From the above evidence, a protic acid-catalyzed mechanism (Scheme 2.8) is reasonable. This mechanism is consistent with Kozlov's original acid catalysis proposal and corrects Wang's assumption that molecular iodine itself acts as catalyst. Initially, the imine **16** is formed from **10** and arylaldehyde. From our observations and others<sup>47</sup> acid is not necessary to catalyze the imine formation.

**Scheme 2.8.** Updated mechanism for Wang's three-component coupling reaction.

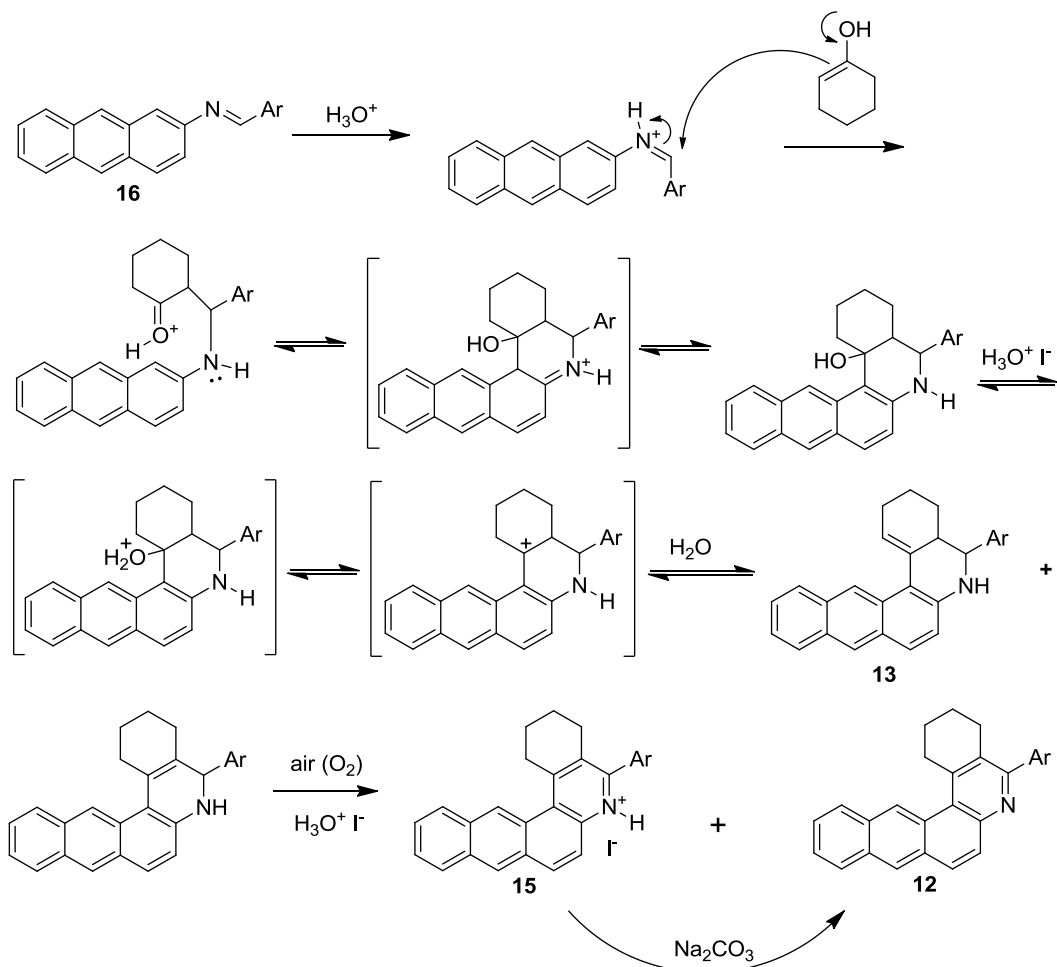
i) Imine (**16**) formation



ii) Keto-enol tautomerization of cyclohexanone



iii) Acid catalyzed mechanism



Ar = *m*-bromobenzaldehyde

Interestingly, two by-products, nonaromatized **13** and reductive amination product **14**, not reported by Wang, were isolated and characterized in this work (Scheme 2.6). The major by-product **13** likely forms by elimination outside of the pyridine ring during the ring closing

condensation. The mechanism leading to the reduction of **16** to the give minor by-product **14** remains unclear. Aside from the addition of water, further improvement in product yield is obtained by adding an aqueous base wash to the workup.

### **2.3 – Summary of Improved Methodology for the synthesis of Benzo[f]quinolines and Benzo[b]anthraquinolines**

In summary, the synthesis of a new class of potential model asphaltene compounds was assembled from simple starting materials using a three-component cyclocondensation reaction reported in the literature. In practise, the reaction did not proceed as claimed and exploration into the cause of this failure was undertaken. Collaboration with fellow group members<sup>48</sup> led to the discovery of why the reaction failed in our hands and ultimately resulted in an improved procedure. We now have a comprehensive, reproducible procedure for the synthesis of substituted benzo[f]quinolines and benzo[b]anthraquinolines bearing aliphatic appendages, including complex steroidal fusions. The latter mimics sterane biomarkers present in all asphaltenes to serve as building blocks to build our model asphaltene library.

### **2.4 – References for Chapter 2**

- 
23. Continental model examples: (a) Groenzin, H.; Mullins, O. C. Molecular Size and Structure of Asphaltenes from Various Sources. *Energy Fuels* **2000**, *14*, 677-684. (b) Zhao, S.; Kotlyar, L. S.; Woods, J. R.; Sparks, B. D.; Hardacre, K.; Chung, K. H. Molecular transformation of Athabasca bitumen end-cuts during coking and hydrocracking. *Fuel* **2001**, *80*, 1155-1163.
24. Archipelago model examples: (a) Murgich, J.; Abanero, J. A.; Strausz, O. P. Molecular Recognition in Aggregates Formed by Asphaltene and Resin Molecules from the Athabasca Oil Sand. *Energy Fuels* **1999**,

- 
- 13, 278-286. (b) Sheremata, J. M.; Gray, M. R.; Dettman, H. D.; McCaffrey, W. C. Quantitative Molecular Representation and Sequential Optimization of Athabasca Asphaltenes. *Energy Fuels* **2004**, *18*, 1377-1384.
25. Gray, M. R.; Tykwinski, R. R.; Stryker, J.M.; Tan, X. Supramolecular Assembly Model for Aggregation of Petroleum Asphaltenes. *Energy Fuels* **2011**, *25*, 3125-3134.
26. Shedid, A. Influence of Asphaltene Precipitation on Capillary Pressure and Pore Size Distribution of Carbonate Reservoirs, *Petroleum Science and Technology* **2001**, *19*, 503-519.
27. Maris, A.; Melandri, S.; Miazzi, M.; Zerbetto, F. Interactions of Aromatic Heterocycles with Water: The driving Force from Free-Jet Rotational Spectroscopy and Model Electrostatic Calculations. *Chem Phys Chem* **2008**, *9*, 1303-1308.
28. Alshareef, A. H.; Scherer, A.; Tan, X.; Azyat, K.; Stryker, J. M.; Tykwinski, R.; Gray, M. R. Formation of archipelago structures during thermal cracking implicates a chemical mechanism for the formation of petroleum asphaltenes. *Energy Fuels* **2011**, *25*, 2130-2136.
29. Albert, A.; Rubbo, S.; Burlrill, M. The Influence of Chemical Constitution on Antibacterial Activity. Part IV: A Survey of Heterocyclic Bases, with Special Reference to Benzquinolines, Phenanthridines, Benzacridines, Quinolines and Pyridines. *British Journal of Experimental Pathology* **1949**, *30*, 159-175.
30. Smith, E.C.; McQuaid, L.A.; Goode, R.L.; McNulty, A.M.; Neubauer, B.L.; Rocco, V.P.; and Audia, J.E. Synthesis and 5 $\alpha$ -reductase inhibitory activity of 8-substituted benzo[f]quinolinones derived from palladium mediated coupling reactions. *Bioorg. Med. Chem. Lett.* **1998**, *8*, 395-398.
31. Monge, A.; Alvarez, E.; San Martin, C.; Nadal, E.; Ruiz, I.; Font, M.; Martinez-lrujo, J.J.; Santiago, E.; Prieto, I.; Lasarte, J.J.; Sarobe, P.; Borrás, F. Synthesis and evaluation of new Reissert analogs as HIV-1 RT inhibitors. 2. Benzo[f]quinoline and pyridine derivatives *Drug Des. Discovery* **1997**, *14*, 291-303.
32. Cymerman, C.J.; Torkelson, S.M.; Findell, P.R.; Weiner, R.I. Synthesis and Dopaminergic Activity of 2-Substituted Octahydrobenzo[f]quinolines. *J. Med. Chem.* **1989**, *32*, 961-968.
33. Dubey, S.K.; Kumar, S. Synthesis of Dihydro Diol Epoxides of Benzo[f]quinoline. *J. Org. Chem.* **1986**, *51*, 3407-3412.
34. Bejan, V.; Mangalagiu, I.I. Benzo[f]quinoline: Synthesis and Structural Analysis. *Rev Chim.* **2011**, *62*, 199-200.
35. Kozlov, N.G.; Gusak, K.N.; Kadutskii, A.P.; Development of the Catalytic Synthesis of Compounds of the Quinoline Series (The N.S. Kozlov Reaction) (Review). *Chem. Heterocycl. Compd.* **2010**, *46*, 505-528.
36. Kozlov, N.G.; Basalaeva, L.I.; Firgang, S. I.; Shashkov A. S.; Reaction of Methylcyclohexanones with Substituted Benzaldehydes and 2-Naphthylamine. *Russ, J. Org. Chem.* **2004**, *40*, 518-524.
37. Kozlov N.G.; Basalaeva L.I. Synthesis of 5-aryl-1-methyl-1,2,3,4-tetrahydrobenzo[a]phenanthridines. *Russ, J. Org. Chem.* **2009**, *45*, 587-590.
38. Wang, X.S.; Li, Q.; Yao, C.S.; Tu, S.J. An Efficient Method for the Synthesis of Benzo[f]quinoline and Benzo[a]phenanthridine derivatives Catalyzed by Iodine by a Three-Component Reaction of Arenecarbaldehyde, Naphthalen-2-amine, and Cyclic Ketone. *Eur. J. Org. Chem.* **2008**, *20*, 3513-3518.
39. Scherer, A. Postdoctorate fellow in the Tykwinski group at the University of Erlangen-Nuremberg, Erlangen, Germany.
40. Alshareef, A. H.; Scherer, A.; Tan, X.; Azyat, K.; Stryker, J. M.; Tykwinski, R.; Gray, M. R. Formation of archipelago structures during thermal cracking implicates a chemical mechanism for the formation of petroleum asphaltenes. *Energy Fuels* **2011**, *25*, 2130-2136.
41. Wang, X.S.; Zhou, J.; Yin, M.Y.; Yang, K.; Tu, S.J. Efficient and Highly Selective Method for the Synthesis of Benzo(naphtho)quinoline Derivatives Catalyzed by Iodine. *J. Comb. Chem.* **2010**, *12*, 266-269.
42. Wang, X., B.Sc. Honours candidate in the Stryker group at the University of Alberta, worked in tandem with the author.
43. Cataldo, F. Iodine: A Ring opening Polymerization Catalyst for Tetrahydrofuran, *Eur. Polym. J.* **1996**, *32*, 1297-1302.
44. Wang, X., B.Sc. Honours candidate in the Stryker group at the University of Alberta, made this discovery.

- 
45. Wang, X., B.Sc. Honours candidate in the Stryker group at the University of Alberta, conducted these experiments.
46. Nagy, K.; Kortvelyesi, T.; Nagypal, I. Iodine Hydrolysis Equilibrium. *J. Solution Chem.* **2003**, *32*, 385-393.
47. Formation of archipelago structures during thermal cracking implicates a chemical mechanism for the formation of petroleum asphaltenes.
48. Stryker, J. M., primary researcher and supervisor in the Stryker group at the University of Alberta; Wang, X., B.Sc. Honours candidate in the Stryker group at the University of Alberta.

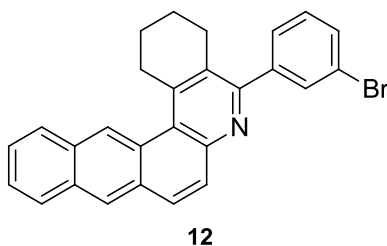
## Chapter 3 - Multi-Component Reaction Modifications

### 3.0 – Introduction

In the last chapter, the development of an improved three-component cyclocondensation reaction was described for the ultimate purpose of synthesizing potential model archipelago-like asphaltenes. In this chapter, variation in the starting materials and post MCR modifications of **12** (Scheme 3.1) are described. Meta-bromobenzaldehyde was chosen as the aromatic aldehyde to allow the partly aromatic benzoquinoline **12** to couple to another model asphaltene island (i.e. polycyclic aromatic) by a 2-4 carbon alkanone tether at the halogen position (Chapter 4).

---

**Scheme 3.1.** Acid catalysis product **12** in which further modifications are made.



---

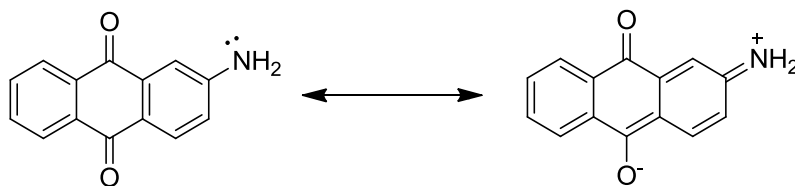
Bromination of either the product or starting materials generated different halogenated positions, which could serve as future points of attachment. As well, ethylated versions of the

island may be useful model candidates according to the asphaltene supramolecular assembly theory since short chain alkyl substituents on aromatic cores are ubiquitous in bitumen.

### 3.1 – Convenient procedures for large scale synthesis of 2-aminonaphthalene (**1**) and 2-aminoanthracene (**10**)

#### 3.1.1 – Synthesis of 2-aminoanthracene (**10**)

As a starting reagent, 2-aminoanthracene **10** is quite costly and we hoped to synthesize it from the reduction of 2-aminoanthraquinone **17** which costs much less. However, both the Clemmensen reduction and Wolff-Kishner reduction were fruitless in reducing 2-aminoanthraquinone. As well,  $\text{NaBH}_4$  in either  $\text{EtOH}$ <sup>49</sup> or  $i\text{PrOH}$ <sup>50</sup> solvent did not reduce the aminoquinone starting material. Possibly, reduction of both carbonyl groups is problematic due to conjugation of the amine with the carbonyl in the C<sub>10</sub> position, making it less electrophilic (Scheme 3.2) for an electron transfer.

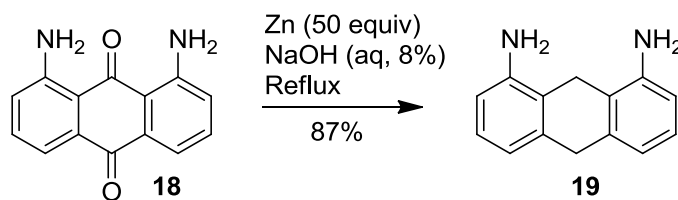




Success in reducing 2-aminoanthraquinone was found from methodology by Zhang and coworkers,<sup>51</sup> who used a zinc reduction under basic conditions. However, under these conditions they reduced 1,8-diaminoanthraquinone **18** to the dihydro species **19** (Scheme 3.3).

---

**Scheme 3.3.** Partial reduction of 1,8-diaminoanthraquinone (**18**).

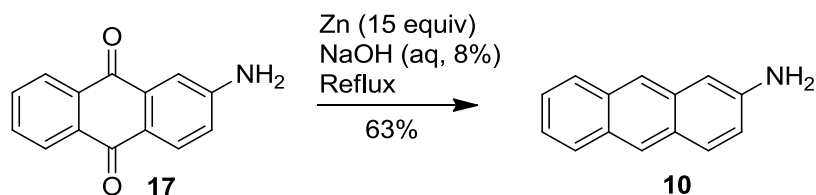


---

Zhang and coworkers<sup>51</sup> mentioned that “...the aryl ketones without a hydroxyl or amino group *ortho* or *para* to the carbonyl group tend to be reduced to a secondary alcohol or an alkene derivative” (p. 658). Their synthesis of anthracene from anthraquinone in 92% yield using the same conditions supported their argument. We therefore explore this methodology in hopes of using it as a viable route to 2-aminoanthracene and indeed it worked (Scheme 3.4). The reaction conditions were then modified such that the number of equivalents of zinc was decreased from 50 to 22, the volume of aqueous NaOH was decreased and the solvent was deoxygenated before use (not mentioned by Zhang and coworkers but was crucial for the reaction to proceed) since oxygen may affect the electron transfer during the reaction.

---

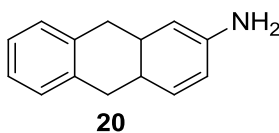
**Scheme 3.4.** Synthesis of 2-aminoanthracene (**10**).



The moderate yield we obtained (63%) may be due to the presence of the dihydro reduced species **20** (Scheme 3.5). Even after sequential recrystallization, small impurities (<5%) of what is postulated to be 2-amino-9,10-dihydroanthracene were present. This impurity was not characterized and the reaction solvent and mother liquor after successive recrystallizations were not analyzed for the presence of a dihydroanthracene species. TLC gave two spots separated by a large R<sub>f</sub> value (R<sub>f</sub> [10:1 Hex/EtOAc]: 0.03 [**5**], 0.60 [impurity]) but further purification was not performed as the impurity was minor and easily removed following recrystallization of the three-component reaction products.

---

**Scheme 3.5.** Suspected impurity in 2-aminoanthracene (**10**).

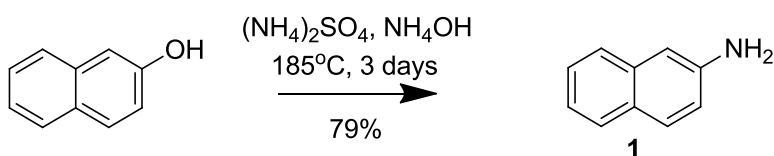


### 3.1.2 – Synthesis of 2-aminonaphthalene (1)

2-Aminonaphthalene (**1**) was made in 79% yield from standard literature procedures with a slight variation in reaction temperature and reaction time (Scheme 3.6).

---

**Scheme 3.6.** Synthesis of 2-aminonaphthalene (**1**)



The 2-aminonaphthalene (**1**) was accompanied by a minor impurity. No noticeable by-products were observed via <sup>1</sup>H or <sup>13</sup>C NMR spectroscopy but the carbon content of the product material was 1.5% higher than the expected percentage according to elemental analysis. Since no observable by-products were observed in the NMR spectra, **1** was used without further purification.

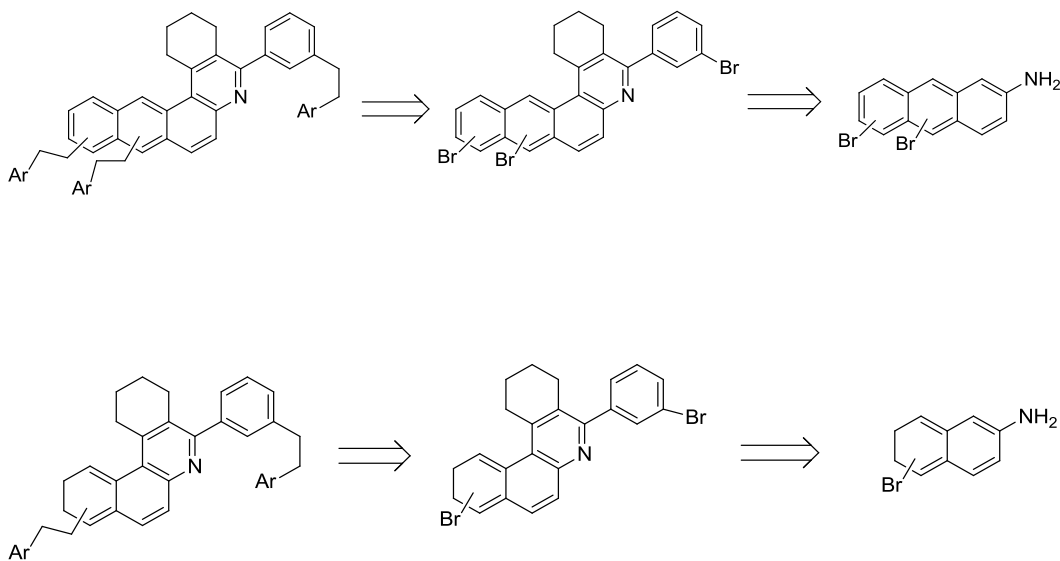
## 3.2 – Bromination of 2-amino-anthracene/naphthalene

### 3.2.1 – Desired use of 2-aminonaphthalene and 2-aminoanthracene brominated derivatives

Bromination of 2-aminonaphthalene (**1**) and 2-aminoanthracene (**10**) was desired since the three-component acid catalyzed cyclization product would give a model asphaltene island with two points of attachment for other polyaromatic heterocycles (Scheme 3.7).

---

**Scheme 3.7.** Retrosynthetic installation of bromine into the asphaltene island model



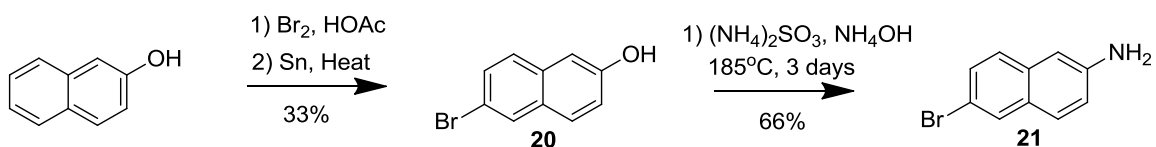
### 3.2.2 – Bromination 2-aminonaphthalene (**1**)

6-Bromo-2-aminonaphthalene (**21**) was synthesized in two steps from 1-naphthol using literature procedures (Scheme 3.8). Firstly, 6-bromo-naphthol (**20**) was made using literature methodology,<sup>52</sup> albeit in low yield (33%). Koelsch reported 96-100% yield for this reaction and at least two factors may have contributed to the low yield obtained. 30 mesh tin

used was used instead of mossy tin which may have had some affect. However, this reaction was my first in a graduate laboratory and my laboratory skills were in their infancy. For the second step, the Bucherer reaction afforded **21** (66%).

---

**Scheme 3.8.** Synthesis of 6-bromo-2-aminonaphthalene (**21**)

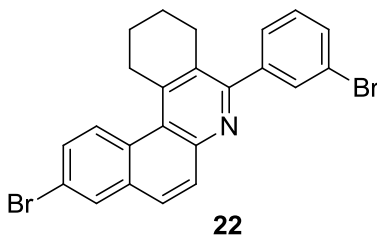


---

6-bromo-2-aminonaphthalene (**21**) was subjected Wang's three-component reaction but failed using his published conditions, similarly to what was seen with 2-aminonaphthalene (discussed in Chapter 2). The three-component acid catalysis problem was not solved when this reaction was undertaken and **21** was not subjected to our corrected three component coupling conditions. However, the methodology for synthesis of model asphaltene island **22** is now in place.

---

**Scheme 3.9.** Model asphaltene island (**22**)

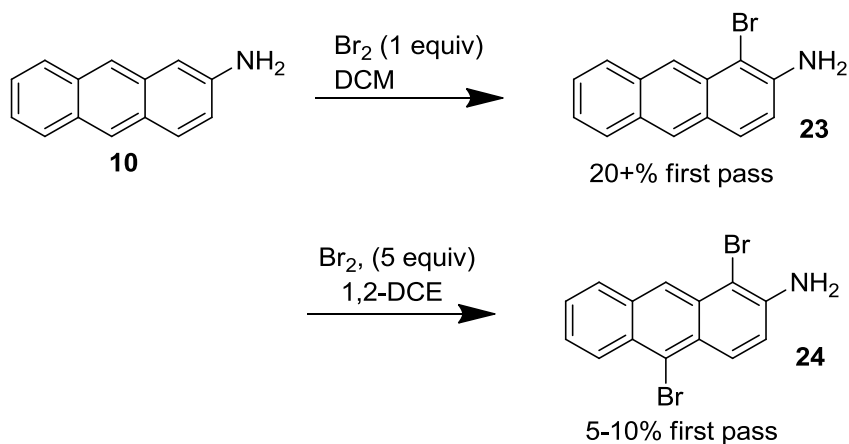


### 3.2.2 - Bromination of 2-aminoanthracene (**10**)

Since 2-aminoanthracene was found to work under Wang's published conditions, bromination of this starting material was hoped to lead to other points of attachment to the archipelago island (Scheme 3.7). Direct bromination of 2-aminoanthracene occurred first at the C<sub>1</sub> position to yield **23**, followed by C<sub>10</sub> to yield **24** (Scheme 3.10).

---

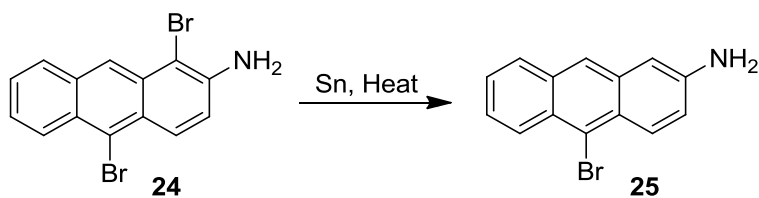
**Scheme 3.10.** Direct bromination of 2-aminoanthracene.



1-Bromo-2-aminoanthracene (**23**) was not subjected to the three-component cyclization as the C<sub>1</sub> position was needed for nucleophilic attack onto the carbonyl carbon of cyclohexanone (Chapter 2: Scheme 2.8). However, 1,10-dibromoaminoanthracene (**24**) may be selectively debrominated at C<sub>1</sub> using Koelsch's methodology<sup>52</sup> to give 10-bromoaminoanthracene (**25**) (Scheme 3.11).

---

**Scheme 3.11.** Possible route to 10-bromo-2-aminoanthracene (**25**)



---

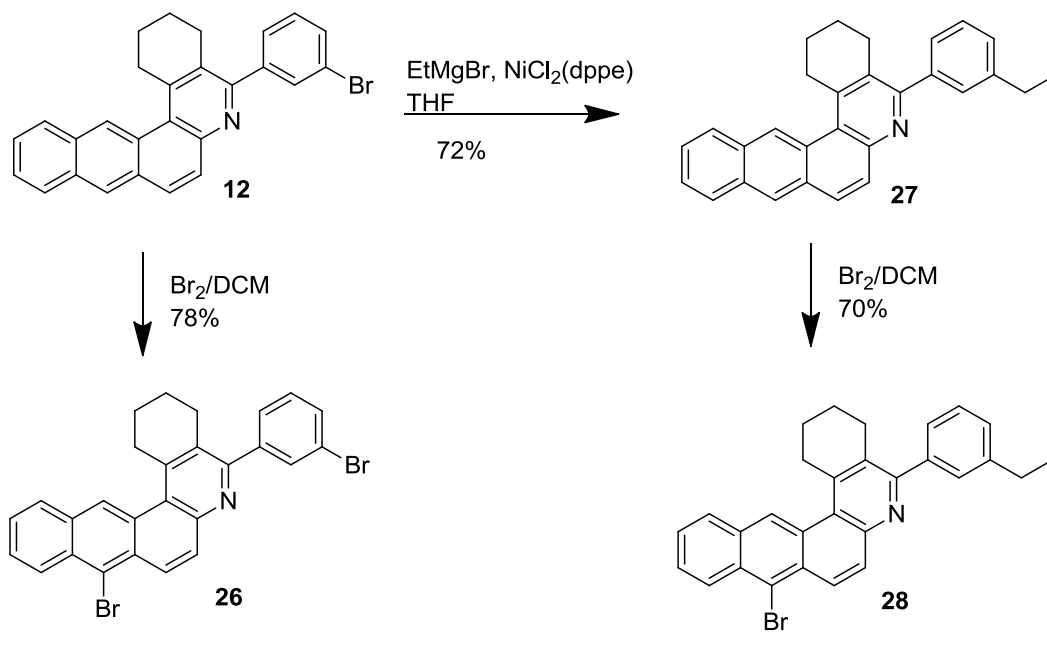
Compound **25** could be subjected to acid catalysis conditions described in Chapter 2. However, this potential pathway was abandoned once it was discovered that direct bromination of the three-component cyclic condensation product **12** occurred selectively at the C<sub>13</sub> position to yield **26** (Scheme 3.12) in good yield without a debromination step.

### 3.3 – Post Acid Catalysis Cyclization Modifications

Sequential bromination/ethylation of MCR product **12** to afford three new derivatives of model asphaltene compounds (**26, 27, 28**) has been accomplished (Scheme 3.12).

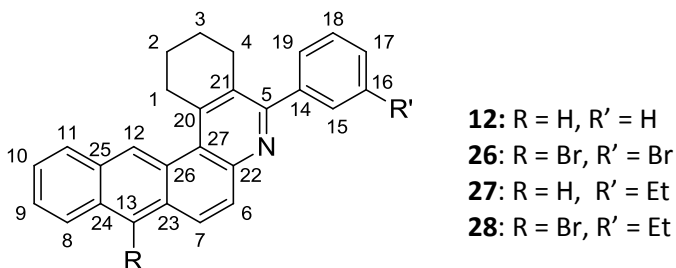
---

Scheme 3.12. Model asphaltene 'island' derivatives, **26-28**.



These derivatives add to our asphaltene island library and provide additional options for archipelago total synthesis. Scheme 3.13 depicts the numbering system denoted to these and related benzo[b]anthraquinolines.

Scheme 3.13. Numbering system for benzo[b]anthraquinoline derivatives.

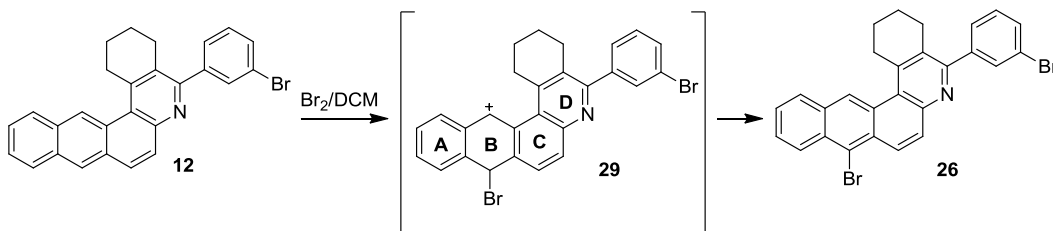




### 3.3.1 – Bromination of Cyclization Product (12) to yield dibromo (26)

Consistent with the archipelago model of asphaltenes, **12** was further brominated to allow for two points of attachment to other polycyclic aromatic islands (Scheme 3.12). Interestingly, bromination occurred highly selectively at C<sub>13</sub> to afford dibromo derivative **26** with no observed over bromination products. This may be explained by electronic effects where bromination at C<sub>13</sub> leads to a carbocation intermediate with resonance form **29** (Scheme 3.14), which is stabilized by two quaternary sp<sup>2</sup> carbons and leads to loss of aromaticity in the B ring only.

**Scheme 3.14.** Intermediate **29** during direct bromination of MCR product **12**



The greatest impediment to the utility of the reaction was incomplete conversion of starting material to product. Increasing the reaction time did increase product conversion but after multiple days at reflux, by-products eventually formed. Maximum conversion to **26** with no regioisomeric dibrominated by-products and no detectable over bromination was obtained in good yield (78%) after 48 hours at reflux. An advantage of this reaction is that it is performed

open to the atmosphere using reagent grade DCM. The remaining starting material was easily recovered pure by chromatography.

### 3.3.2 – Ethylation/Bromination of Cyclization Product (11) to yield 27 and 28

Among the most desirable archipelago model asphaltene are those that contain polycyclic aromatic systems that are decorated with short alkyl side chains (Chapter 1, Figure 1.4). Therefore, **12** was ethylated at the aryl bromide position by Kumada coupling to yield compound **27** in 72% yield (Scheme 3.12). To further its potential as an asphaltene candidate, **27** must be coupled to other aromatic islands. To that end, direct bromination was performed under the same conditions used to afford dibromo compound **28**. This reaction selectively brominated at the C<sub>13</sub> position in 70% yield with minor impurities (Scheme 3.12). The major by-product was recovered starting material (**27**), similar to the bromination of **12**.

This ethylation/bromination methodology yields two additional targets for supramolecular study: dibromo derivative **26** as a ‘central’ island allowing for two points of attachment and **28** as a ‘terminal’ island. Incorporation of these compounds into archipelago models remains under current investigation.

## 3.4 - References for Chapter 3

---

49. Dahan, A.; Ashkenazi, T.; Kuznetsov, V.; Makievski, S.; Drug, E.; Fadeev, L.; Bramson, M.; Schokoroy, S.; Rozenshine-Kemelmaker, E.; Gozin, M. Synthesis and Evaluation of a Pseudocyclic Tristhiourea-Based Anion Host. *J. Org. Chem.* **2007**, 72, 2289-2296.

- 
50. Miao, R.; Zheng, Q. Y.; Chen, C.F; Huang, Z. T. A novel calyx[4]arene fluorescent receptor for selective recognition of acetate anion. *Tetrahedron Lett.* **2005**, *46*, 2155-2158.
51. Zhang, C. Z.; Yang, H.; Wu, D.L.; Lu, G.Y. A Convenient and Environmentally Benign Method of Reducing Aryl Ketones or Aldehydes by Zinc Powder in an Aqueous Alkaline Solution. *Chin. J. Chem.* **2007**, *25*, 653-660.
52. Koelsch, F. C.; 6-Bromo-2-naphthol. *Org. Synth.* **1955**, *3*, 132.

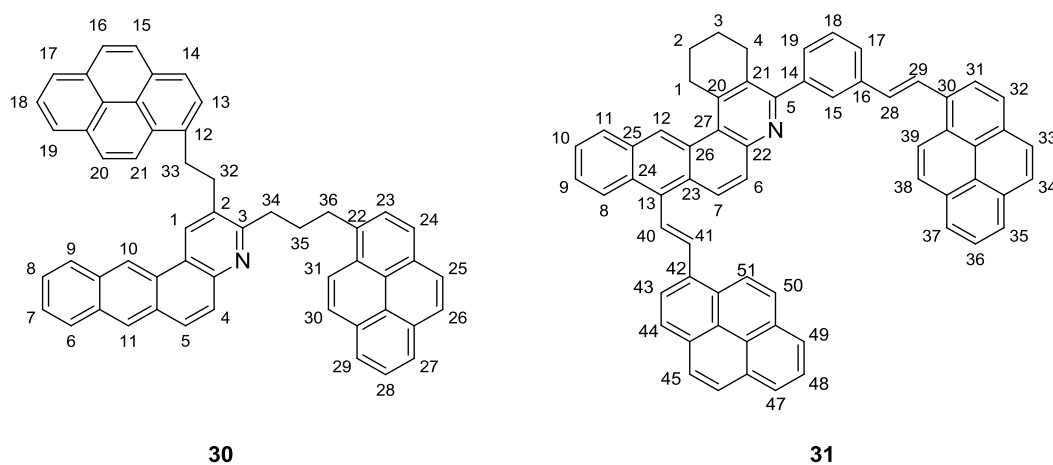
## Chapter 4 – Synthesis of Model Asphaltenes

### 4.0 – Introduction

In this chapter is discussed the synthesis of model asphaltene **30** as well as **31**, the latter of which was an attempted model asphaltene synthesis (Scheme 4.1). Both compounds contain the benzo[b]anthraquinoline core as seen in previous chapters and were constructed according to acid catalysis procedures discussed in Chapter 2. In contrast, compound **30** does not contain the tetrahydro or pendant phenyl rings as seen in **12**. Another striking difference is that the aliphatic chains in **30** are two- and three-carbon lengths whereas the tethers in **31** are two carbons in length. Pyrene was chosen as terminal islands since they have been observed in the thermal cracking of asphaltenes.<sup>53</sup>

---

**Scheme 4.1.** Model asphaltene product **30** as well as product **31**, from attempted model asphaltene synthesis.



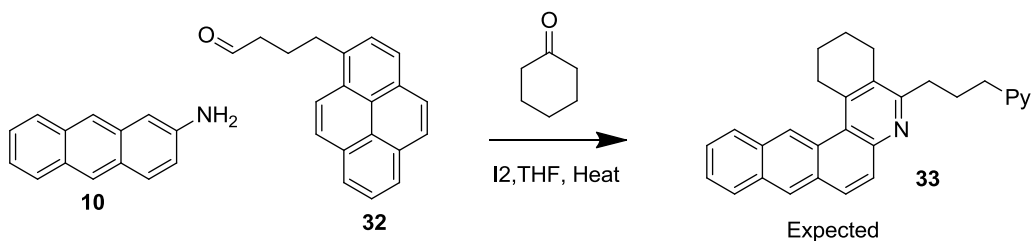
## 4.1 – Synthesis of Asymmetric Three Island Asphaltene Model (30)

### 4.1.1 – Theoretical Model Asphaltene from Wang’s Three-Component Acid Catalyzed Cyclocondensation Reaction.

In extending the scope of the three-component acid catalyzed reaction, we were interested in knowing if aliphatic aldehydes were suitable substrates. 1-Pyrenebutanal (**32**) was chosen since, if the MCR was successful, a two ‘island’ model asphaltene could be synthesized. According to the acid catalyzed MCR’s mechanism, 1-pyrenebutanal, cyclohexanone, and 2-aminoanthracene are expected to cyclize and afford **33** (Scheme 4.2).

---

**Scheme 4.2.** Theoretical reaction of 1-pyrenebutanal (**32**), 2-aminoanthracene (**10**), and cyclohexanone based on previous three component acid catalysis results.



Note: Py =pyrene

---

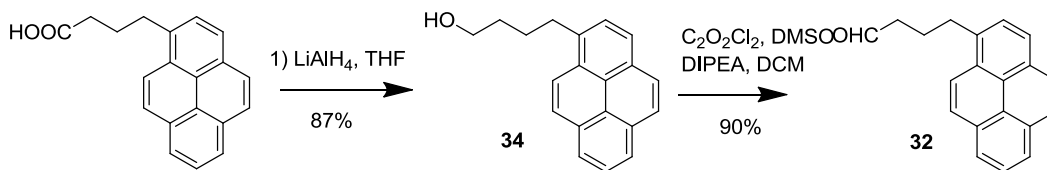
Theoretical compound **33** has two aromatic islands tethered by a saturated three carbon bridge and thus displays an archipelago motif. Extending beyond **33** may include direct bromination(s) and sequential ethylation via Kumada coupling.

#### 4.1.2 – Synthesis of 1-Pyrenebutanal (**32**)

1-Pyrenebutanal (**32**) was synthesized in two steps from 1-pyrenebutyric acid in 79% overall yield (Scheme 4.3).<sup>54</sup> Firstly, the 1-pyrenebutyric acid (purchased from Aldrich) was reduced to the alcohol **34** with  $\text{LiAlH}_4$  and then oxidized to the aldehyde **32** using a Swern oxidation.

---

**Scheme 4.3.** Synthesis of 1-pyrenebutanal (**32**)



---

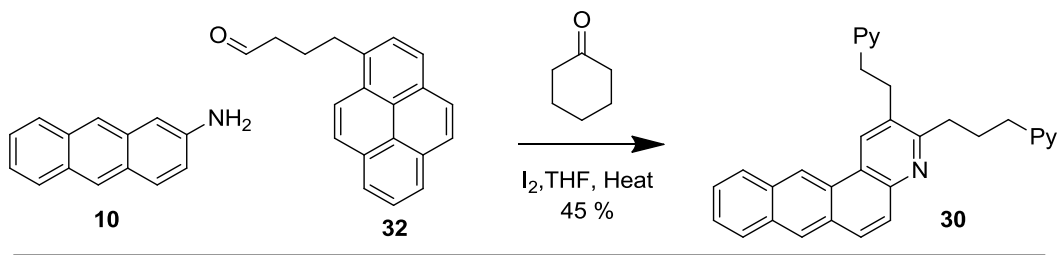
The alcohol and aldehyde products (**34** and **32**, respectively) were brown oils that resisted recrystallization and were not pure by elemental analysis. However, these products were clean by  $^1\text{H}$  NMR spectroscopy and were thus used for the next step.

#### 4.1.3 – Synthesis of Model Asphaltene **30**

Subjecting 2-aminoanthracene (**10**), 1-pyrenebutanal (**32**), and cyclohexanone to our modified Wang's conditions did not produce **33** as expected but instead produced **30** (Scheme 4.4). This product contains no cyclic tetrahydro component. In fact, the formation of product was observed even before the addition of cyclohexanone or heating above room temperature. Two equivalence of 1-pyrenebutanal reacted for every 1 equivalent of 2-aminoanthracene.

---

**Scheme 4.4.** Synthesis of asymmetric model asphaltene **30**.



With this reaction, a complex archipelago asphaltene model was synthesized in one step from starting materials that can be purchased or easily made. Product formation was observed even at room temperature. Most model asphaltenes synthesized in the Stryker group tend to be symmetric and **30** adds another depth for supramolecular analysis as it is unsymmetric in two ways: (1) the pyrene islands are connected at adjacent positions on the compound and (2) the carbon bridges differ in length.

#### 4.1.3 – Characterization of Unsymmetric Model Asphaltene (**30**)

Spectroscopic characterization of **30** was sufficient to elucidate its structure although not every hydrogen and carbon was assigned. ESI-MS confirmed a molecular formula of C<sub>54</sub>H<sub>37</sub>N. This presents an index of hydrogen deficiency of 37: thirteen on the Benzo[b]anthraquinoline core and twelve on each pyrene unit.

<sup>1</sup>H NMR and COSY analysis revealed five methylenes divided into two aliphatic chains: one being two carbons in length and the other one three carbons in length (Table 4.1). The absence of COSY correlations outside the chains suggests that each end is connected to a quaternary carbon.

**Table 4.1.** Structural features of two aliphatic chains of **30** based on <sup>1</sup>H NMR and COSY data.

| Chain A         |          |                            | Chain B         |          |                                |
|-----------------|----------|----------------------------|-----------------|----------|--------------------------------|
|                 | $\delta$ |                            |                 | $\delta$ |                                |
| H <sub>33</sub> | 3.68     | (t, <i>J</i> = 8.4 Hz, 2H) | H <sub>36</sub> | 3.49     | (t, <i>J</i> = 7.2 Hz, 2H)     |
| H <sub>32</sub> | 3.32     | (t, <i>J</i> = 8.4 Hz, 2H) | H <sub>34</sub> | 3.21     | (t, <i>J</i> = 7.0 Hz, 2H)     |
|                 |          |                            | H <sub>35</sub> | 2.47     | (app p, <i>J</i> = 7.8 Hz, 2H) |

Spectroscopic data of starting material 1-pyrenebutanal (**32**) was compared to the expected dipyrene product **30** because 1-pyrenebutanal was a starting reagent in the reaction. Thus, one end of each chain may contain a pyrene moiety. NMR spectroscopic data lends evidence to suggest that one pyrene moiety is attached to H<sub>33</sub> in chain A and another pyrene is attached to H<sub>36</sub> in chain B (Figure 4.1 A and B). H<sub>33</sub> displays HMBC correlations to quaternary carbon C<sub>12</sub> ( $\delta$  134.9). This carbon closely matches quaternary C<sub>14</sub> ( $\delta$  135.5) in 1-pyrenebutanal



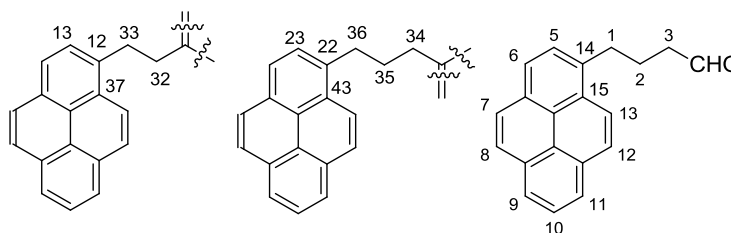
(Figure 4.2 C). H<sub>33</sub> also shows HMBC correlation to aromatic quaternary carbon ( $\delta$  130.1) and aromatic methine carbon ( $\delta$  127.2) and these correlations match closely to observed correlations in 1-pyrenebutanal:  $\delta$  131.4 (quaternary) and  $\delta$  127.5 (methine). H<sub>36</sub> shows similar correlations.

**Table 4.2.** Evidence for pyrene connections to chains A and B in **30**.

A) HMBC correlations

Chain A  $\delta$  3.68 (H<sub>33</sub>)  $\leftrightarrow$   $\delta$  134.9 (+), 130.1 (+), 127.2(-)

Chain B  $\delta$  3.68 (H<sub>36</sub>)  $\leftrightarrow$   $\delta$  136.5 (+), 130.9 (+), 127.2 (-)



|                                | Chain A pyrene              | Chain B pyrene              | 1-Pyrenebutanal           |
|--------------------------------|-----------------------------|-----------------------------|---------------------------|
| B) <sup>13</sup> C NMR signals | $\Delta$                    | $\delta$                    | $\delta$                  |
|                                | 134.9 (+, C <sub>12</sub> ) | 136.5 (+, C <sub>22</sub> ) | 135 (+, C <sub>14</sub> ) |
|                                | 130.1 (+, C <sub>37</sub> ) | 130.9 (+, C <sub>43</sub> ) | 131 (+, C <sub>15</sub> ) |
|                                | 127.2 (-, C <sub>13</sub> ) | 127.2 (-, C <sub>23</sub> ) | 128 (-, C <sub>5</sub> )  |

With H<sub>33</sub> and H<sub>36</sub> each adjacent to a pyrene ring, H<sub>32</sub> and H<sub>34</sub> must be bonded to the central island. H<sub>32</sub> had only a single HMBC correlation ( $\delta$  3.31  $\leftrightarrow$   $\delta$  133.1), linking to a quaternary carbon but H<sub>34</sub> displays TROESY correlations to all aliphatic carbons (Table 4.3). This suggests that the two aliphatic chains are in close proximity to each other. Additionally, H<sub>32</sub> and H<sub>35</sub> are in close proximity due to their TROESY correlation. In addition, The TROESY correlation between H<sub>34</sub> and H<sub>32</sub> is much stronger than H<sub>34</sub> and H<sub>33</sub> and there is an absence of correlation between H<sub>35</sub> and H<sub>33</sub>. This evidence strongly supports a structure in which H<sub>32</sub> and H<sub>34</sub> are attached to adjacent carbons. HMBC correlations also help deduce the position of H<sub>36</sub> and H<sub>32</sub>.

Both protons correlate to different quaternary carbons ( $\delta$  136.5, 130.9 for H<sub>36</sub>;  $\delta$  130.1, 127.2 for H<sub>32</sub>).

**Table 4.3.** Selected TROSEY and HMBC correlations for **30**.

TROSEY correlations

3.21 (H<sub>34</sub>)  $\leftrightarrow$   $\delta$  3.68 (weak, H<sub>33</sub>), 3.49 (weak, H<sub>36</sub>), 3.31 (strong, H<sub>32</sub>), 2.47 (strong, H<sub>35</sub>)

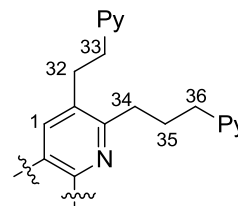
3.68 (H<sub>33</sub>)  $\leftrightarrow$   $\delta$  3.31 (strong, H<sub>32</sub>), 3.21 (strong, H<sub>34</sub>), 2.47 (weak, H<sub>35</sub>)

8.59 (H<sub>1</sub>)  $\leftrightarrow$  3.31 (H<sub>32</sub>)

HMBC correlations

$\delta$  3.31 (H<sub>32</sub>)  $\leftrightarrow$   $\delta$  130.1 (+, C<sub>7</sub>), 127.2 (-, C<sub>1</sub>)

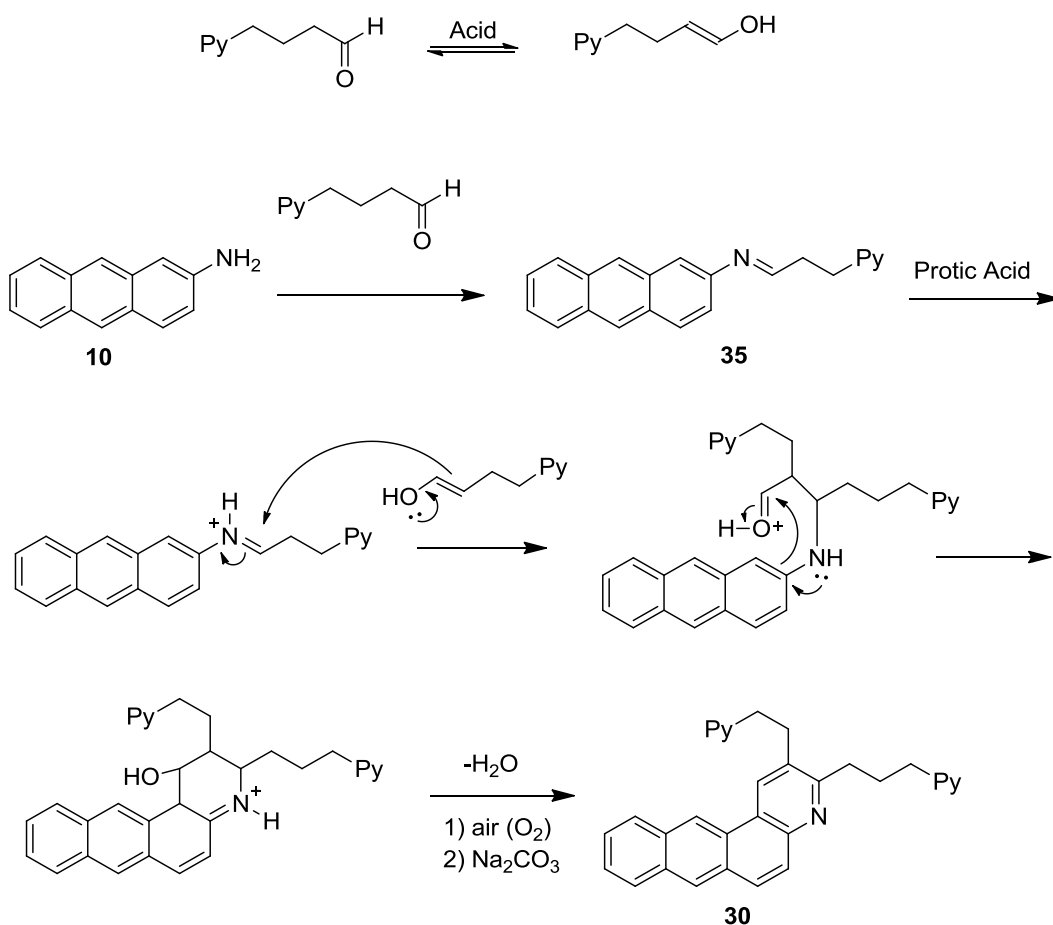
$\delta$  3.68 (H<sub>36</sub>)  $\leftrightarrow$   $\delta$  136.5 (C<sub>22</sub>), 130.9 (C<sub>43</sub>)



TROSEY correlation ( $\delta$  8.59 (H<sub>1</sub>)  $\leftrightarrow$   $\delta$  3.31 (H<sub>32</sub>)) and HMBC correlation ( $\delta$  3.31 (H<sub>32</sub>)  $\leftrightarrow$   $\delta$  127.2 (-, C<sub>1</sub>)) places H<sub>32</sub> in close proximity to the singlet at  $\delta$  8.59. This configuration suggests that C<sub>32</sub> and C<sub>34</sub> are attached to the pyridium ring in **31**. If C<sub>32</sub> and C<sub>34</sub> were attached to a ring in the starting material 2-aminoanthracene (**10**) then a multitude of spectroscopic inconsistencies would appear such as: the <sup>1</sup>H NMR would not exhibit three <sup>1</sup>H NMR singlets outside of the peaks that pertain to pyrene, FTIR would display a primary or secondary N-H stretch, the index of hydrogen deficiency would not match up, or the aliphatic chains would be of different length.

A second analysis that lends support for structure **30** comes from mechanistic analysis of the reaction (Scheme 4.5). Both Kozlov<sup>55</sup> and Wang's<sup>56</sup> studies predict that **10** and **32** will combine to form the imine **35**. Consistent with the MCR in Chapter 2, the acid catalyzed cyclization can occur but with the enol form of the aldehyde **32** instead of cyclohexanone.

**Scheme 4.5.** Postulated mechanism for formation of compound **30**.



Since cyclohexanone is not utilized, we suggest that the enol formation of 1-pyrenebutanal may be faster than the enol formation of cyclohexanone. The literature shows that the enolization of aldehydes typically occurs faster than for ketones.<sup>57</sup> This is because the keto form of cyclohexanone is stabilized by two alkyl groups whereas the keto form of the aldehyde is only stabilized by one. Additionally, formation of the enol of cyclohexanone would disrupt the 'chair' conformation, adding nearly 10 kcal/mol of angle strain.

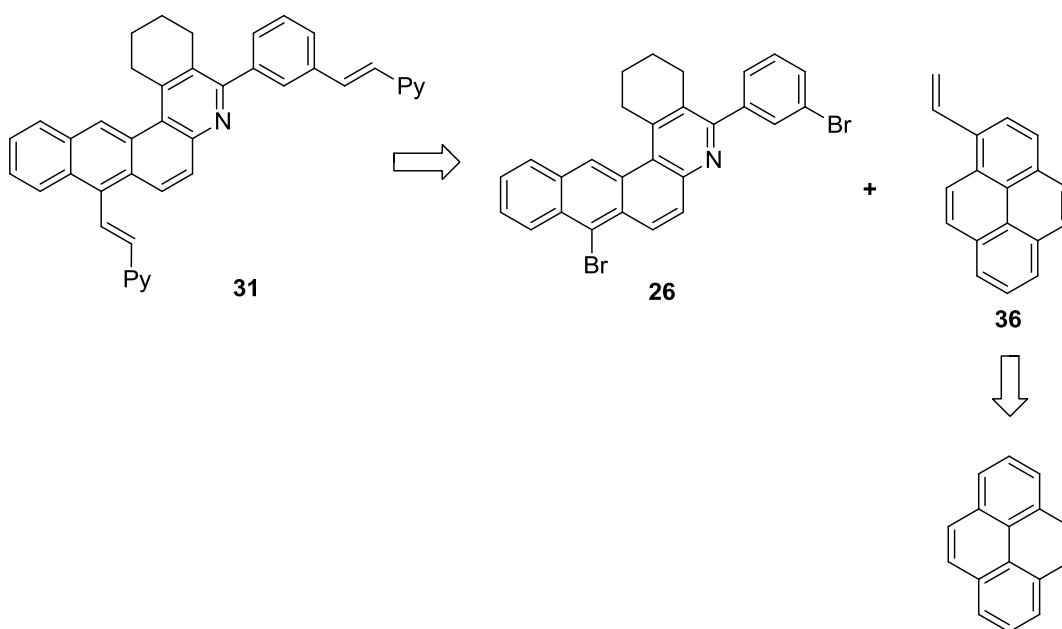
## 4.2 –Synthesis of 32 – Coupling of Acid Catalysis Product

Since other Stryker group members<sup>58</sup> were working on methodology that linked polyaromatic islands by three and four methylene carbon units, a two-carbon tether was targeted. Specifically, two 1-vinylpyrene (**36**) units were linked to dibromide **26** to yield model asphaltene **31** (Scheme 4.6). Synthesis of **36** started with commercial pyrene.

### 4.2.1 – Overview of Synthesis of 31

---

**Scheme 4.6.** Retrosynthetic analysis of model asphaltene **31**



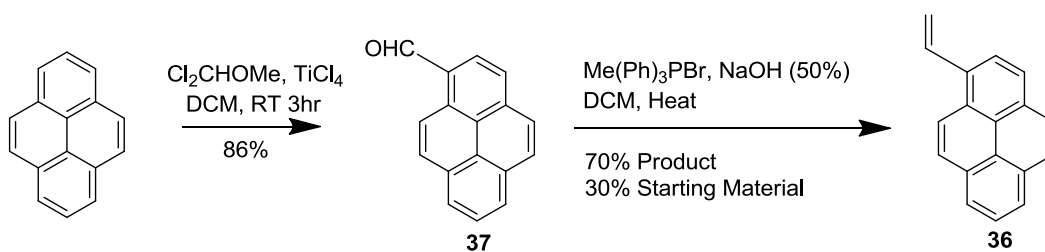
### 4.2.2 – Synthesis of 1-Vinylpyrene (**36**)

---

In a forward sense, the synthesis of 1-vinylpyrene (**36**) is presented in Scheme 4.7. Since pyrene is readily available at low cost and 1-formylpyrene (**37**) can be made in upwards of 90% yield, virtually all literature preparations of 1-vinylpyrene come from first synthesizing 1-formylpyrene. Therefore, pyrene was first converted to **37** in 86% yield using Yamato et al. methodology,<sup>59</sup> with Cl<sub>2</sub>CHOMe and TiCl<sub>4</sub> in THF.

---

**Scheme 4.7.** Two-step synthesis of 1-vinylpyrene (**36**).



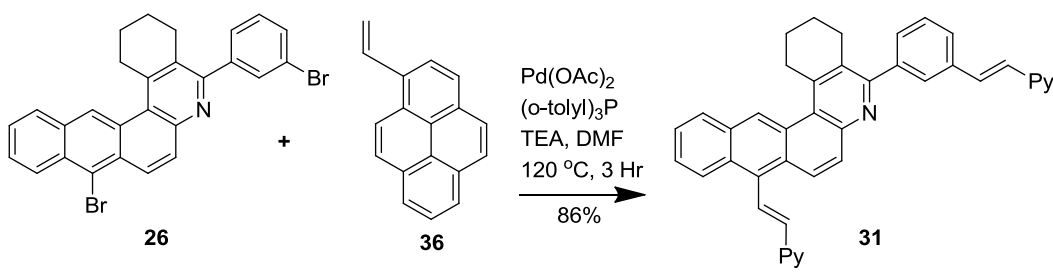
---

Literature methods for the conversion of 1-formylpyrene to 1-vinylpyrene are either low yielding, contain multiple steps, require dry materials in an inert atmosphere, or demand tedious purification methods.<sup>60</sup> A simple and good-yielding reaction was desired because our research sponsors require multigram quantities of these model asphaltene for supramolecular analysis. Exploring methodology from Silversmith<sup>61</sup> 1-vinylpyrene was prepared in a proof-of-concept low-yield two-phase reaction. This reaction involved rapidly stirring 1-formylpyrene (**37**) and methyltriphenylphosphonium bromide (MePh<sub>3</sub>PBr) in a combination of DCM and 50% NaOH at room temperature in an open Erlenmeyer flask. Adjusting the reaction conditions afforded **36** with 70% yield (Scheme 4.7). Heating the reaction mixture to reflux gave the greatest conversion. Changing solvents from DCM to CHCl<sub>3</sub> produced only 1-vinylpyrene polymer.

Since triphenylphosphine oxide was separated by an aqueous workup, the major impurity present in the crude product is starting material **37**. Addition of up to five equivalents of MePh<sub>3</sub>PBr increased conversion. 1-Formylpyrene is soluble in EtOAc whereas 1-vinylpyrene is insoluble and therefore, using EtOAc as a solvent was expected to assist in pushing the reaction to completion. Indeed, 1-vinylpyrene was formed (observed by <sup>1</sup>H NMR spectroscopy) but it polymerized as it precipitated out of solution. Purification consisted of running the DCM extract from the workup through a silica plug in hexanes to yield pure 1-vinylpyrene. The column was then washed with DCM to yield pure starting material **37** which was used for iterative syntheses of **36**. Extensive purification of 1-vinylpyrene increases the chances of polymerization but the methodology we adopted yields virtually no polymer.

#### 4.2.3 – Coupling of Dibromo Island **28** to 1-Vinylpyrene (**34**): Synthesis of Unsaturated Asphaltene Model

**Scheme 4.8.** Synthesis of compound **31**



The Heck reaction was used to couple two 1-vinylpyrene units onto dibromo **26**, which afforded the anticipated product **31** in 86% yield (Scheme 4.8).**Error! Bookmark not defined.** Care must be taken due to 1-vinylpyrene's propensity to polymerize. If the 1-vinylpyrene cannot be used immediately after synthesis, then it should be stored in a cool place away from light.<sup>60</sup>

Difficulties in coupling **26** and **36** stemmed not from incorrect conditions but from being unaware that a portion of 1-vinylpyrene had polymerized. While polymerization may sometimes be detected by a slight darkened yellow colour compared to the starting material, it can be readily observed via  $^1\text{H}$  NMR as a large broad bump from approximately 7-9 ppm.

#### 4.2.4 – Characterization of Unsaturated Asphaltene Model (**31**)

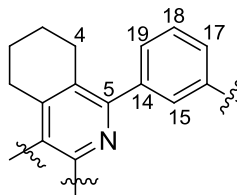
Characterization and reaction analysis of **31** was sufficient to determine the structure although not every atom was assigned. ESI-MS confirmed a molecular formula of  $\text{C}_{63}\text{H}_{41}\text{N}$ . This lends to an index hydrogen deficiency of 44: fourteen on the tetrahydrobenzo[b]anthraquinoline core, four on the disubstituted benzene ring, twelve on each pyrene unit, and 4 for each olefin chain. The FTIR shows an absence of N-H functionality.

The disubstituted benzene ring was deduced by COSY and HMBC analysis of **31** in comparison to **12** (Scheme 4.9).  $\text{H}_{15}$  and  $\text{H}_{17}$  -  $\text{H}_{19}$  in **31** show similar coupling patterns as **12**. HMBC correlations link the benzene and pyridine rings since both  $\text{H}_4$  and  $\text{H}_{19}$  correlate with  $\text{C}_5$ .

The observed  $^1\text{H}$  NMR singlet in **31** ( $\delta$  9.20,  $\text{H}_{12}$ ) compares well to the singlet in **26** ( $\delta$  9.17,  $\text{H}_{12}$ ). The  $^{13}\text{C}$  APT NMR spectrum of **31** shows no quaternary carbons in the  $\delta$  122-124 range indicating the absence of bromine. By comparing  $^1\text{H}$ ,  $^{13}\text{C}$ , HSQC, and HMBC NMR spectra between starting material **26** and **36**, we conclude that the benzo[f]anthraquinoline structure from **26** remains intact and that both bromines have been replaced by a substituent other than hydrogen.

---

**Scheme 4.9.** HMBC correlations linking benzene ring to pyridine ring in **31**.



HMBC correlations

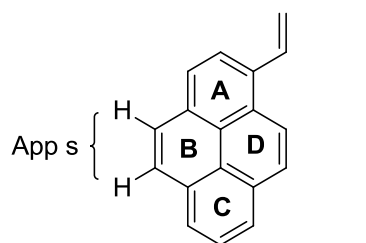
$\delta$  158.9 ( $C_5$ )  $\leftrightarrow$   $\delta$  7.95 ( $H_{15}$ ), 7.78 ( $H_{19}$ ), 7.58 ( $H_{17}$ ), 3.04 ( $H_4$ )

---

The presence of pyrene is revealed through the apparent singlet at  $\delta$  8.06 in  $^1\text{H}$  NMR. Pyrene substituted at the 1-position contains an apparent singlet from the two hydrogens at  $C_4$  and  $C_5$  of the B ring (Scheme 4.10). Two pyrenes have been coupled in this reaction and so two overlapping apparent singlets are observed. As a comparison, the  $^1\text{H}$  NMR chemical shift of the apparent singlet for 1-vinylpyrene **36** is  $\delta$  8.04 and for **31** it is  $\delta$  8.06.

---

**Scheme 4.10.** Comparison of apparent singlet in **31** and 1-vinylpyrene.



|                   |           | App s ( $\delta$ ) |
|-------------------|-----------|--------------------|
| Starting material | <b>36</b> | 8.04               |
| Product           | <b>31</b> | 8.06               |

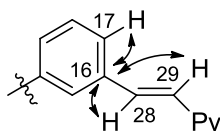
---



The final unknown segment is the presence of two bridging alkenes. For one alkene, adjacent to the substituted benzene ring, HMBC correlations were observed for H<sub>17</sub>, H<sub>28</sub>, and H<sub>29</sub> to C<sub>16</sub> (Figure 4.11). H<sub>28</sub> and H<sub>29</sub> exhibit a large coupling constant ( $J = 16.0$  Hz), indicative of trans-coupling across a double bond. Ortho-coupling in pyrene and the central island is typically 8.0 Hz.

---

**Scheme 4.11.** HMBC correlations of a bridging alkene to the substituted benzene ring in **31**.



HMBC correlations

$\delta$  138.1 (C<sub>16</sub>)  $\leftrightarrow$   $\delta$  8.28 (H<sub>28</sub>), 7.46 (H<sub>29</sub>), 7.61 (H<sub>18</sub>)

---

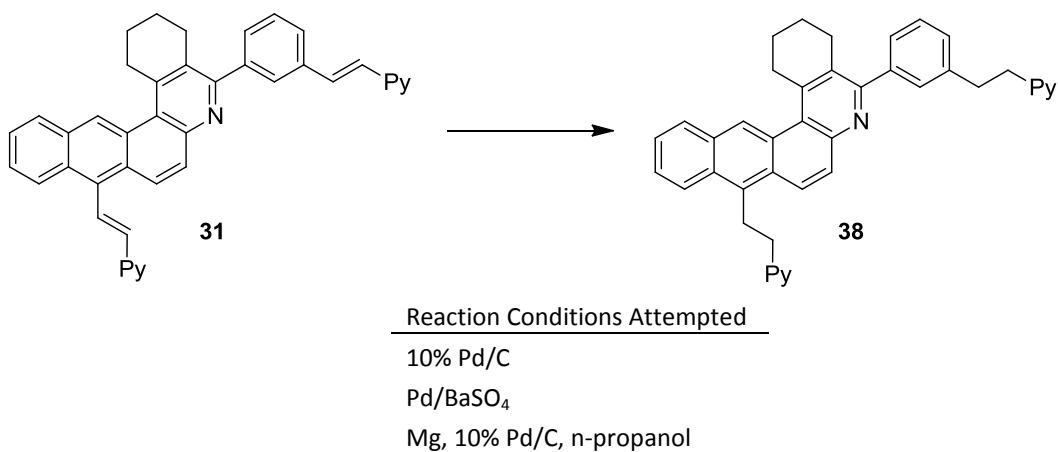
The alkene bridge attached to the anthracene core has proved difficult to assign spectroscopically. The multitude of isolated yet overlapping doublets in <sup>1</sup>H NMR spectra as well as overlaps in HMBC, HSQC, and TROESY spectra creates ambiguity in the assignments. However, the molecular formula and index of hydrogen deficiency requires a two-carbon alkenyl bridge between the pyrenes and the anthracene core. This assignment also fits well with the anticipated reaction product.

#### 4.2.5 – Attempted Hydrogenation to Obtain Saturated Model Asphaltene (**38**)

The hydrogenation of the alkene bridges in **31** to yield **38** (Scheme 4.12) was desired because only the saturated linkers in **38** adhere to the archipelago model of asphaltene. This target contains indeed polyaromatic islands attached together with aliphatic linkages.

---

**Scheme 4.12.** Target model asphaltene **38**.



---

The hydrogenation of **31** to **38**, proved difficult and remains unrealized. Interestingly, catalytic hydrogenation using Pd/C resulted in different results between our collaborator Alex Scherer and former Stryker group member Verner Lofstrand. Hydrogenation worked fine for Scherer<sup>1</sup> at 1200 psi but seemed to over hydrogenate at 1000 psi in Lofstrand's hands. One difference was that Scherer purged and evacuated the hydrogenation chamber three times with hydrogen whereas we simply added hydrogen to the autoclave but it is unclear how this could affect hydrogenation. The use of Pd/BaSO<sub>4</sub> was attempted as BaSO<sub>4</sub> provides a larger scaffold in terms of surface area and may weaken the hydrogenation reactivity compared to Pd/C. <sup>1</sup>H NMR

analysis of the crude product mixture suggested over-hydrogenation, due to the presence of multiple peaks in the 4-5 ppm range. This last step, while potentially yielding a desired archipelago compound, remains unsolved.

### 4.3 – Summary of Model Asphaltene Synthesis

In summary, two model asphaltenes were synthesized. Unsymmetric **30** was synthesized in one step from simple starting materials by three-component cyclocondensation. Unsaturated **31** was synthesized by linking 1-vinylpyrene to **26**. In this process, an efficient synthesis of 1-vinylpyrene was discovered. Hydrogenation of **31** to yield target **38** was unattained.

### 4.4 - References for Chapter 4

- 
53. Alshareef, A. H.; Scherer, A.; Tan, X.; Azyat, K.; Stryker, J. M.; Tykwinski, R.; Gray, M. R. Formation of archipelago structures during thermal cracking implicates a chemical mechanism for the formation of petroleum asphaltenes. *Energy Fuels* **2011**, *25*, 2130–2136.
54. Dondoni, A.; Perrone, D. Synthesis of 1,1-Dimethylethyl (S)-4-Formyl-2,2-Dimethyl-3-Oxazolidine Carboxylate by Oxidation of the Alcohol. *Org. Synth* **2000**, *77*, 64-71.
55. Kozlov, N. G.; Gusak, K. N.; Kadutskii, A. P.; Development of the Catalytic Synthesis of Compounds of the Quinoline Series (The N.S. Kozlov Reaction) (Review). *Chem. Heterocycl. Compd.* **2010**, *46*, 505-528.
56. Wang, X. S.; Li, Q.; Yao, C. S.; Tu, S. J. An Efficient Method for the Synthesis of Benzo[f]quinoline and Benzo[a]phenanthridine derivatives Catalyzed by Iodine by a Three-Component Reaction of Arenecarbaldehyde, Naphthalen-2-amine, and Cyclic Ketone. *Eur. J. Org. Chem.* **2008**, *20*, 3513-3518.
57. Keefe, J. R.; Kresgu, A. J.; Schepp, N. P. Keto-enol Equilibrium Constants of Simple Monofunctional Aldehydes and Ketones in Aqueous Solution. *J. Am. Chem. Soc.* **1990**, *112*, 4862-4868.
58. Diner, C.; Reaugh, D. PhD candidates in the Stryker group at the University of Alberta.
59. Yamato, T.; Fujimoto, M.; Nagano, Y.; Miyazawa, A.; Tashiro, M. Electrophilic Substitution of t-tert-Butyl-1-Substituted Pyrenes. A New Route for the Preparation of 1,2-Disubstituted Pyrenes. *Org. Prep. Proced. Int* **1997**, *29*, 321-330.
60. A) Rajakumar, P.; Visalakshi, K.; Ganesan, S.; Maruthamuthu, P.; Suthanthiraraj, S.A. Synthesis and Dye-sensitized Solar cell Application of Polyolefinic Aromatic Molecules with Pyrene as Surface Group. *Aust. J. Chem.* **2011**, *64*, 951-956. B) Chen, Wei.; Zuckerman, N. B.; Lewis, J. W.; Konopelski, J. P.; Chem, S.

---

Pyrene-Functionalized Ruthenium Nanoparticles: Novel Fluorescence Characteristics from Intraparticle Extended Conjugation. *J. Phys. Chem. C* **2009**, *113*, 16988-16995. C) Tanikawa, K.; Ishizuka, T.; Suzuki, K.; Kusabayashi, S.; Mikawa, H. Synthesis of 3-Vinylpyrene by Wittig's reaction, and Syntheses and Electrical Properties of Polyvinylpyrene and Its Charge Transfer Complexes. *Bull. Chem. Soc. Jpn.* **1968**, *41*, 2719-2722. D) O'Malley, J. J.; Yanus, J. F.; Pearson, J. M. Anionic Polymerization of 1-Vinylpyrene. *ACS Macro Letters* **1972**, *5*, 158-161.

61. Silversmith, E. D. A Wittig Reaction that Gives Only One Stereoisomer. *J. Chem. Ed.* **1986**, *63*, 645-646.

## Chapter 5 – Research Highlights and Future Considerations

### 5.1 – Research Highlights

A complex model asphaltene island (**12**) was synthesized from a three-component reaction. The reaction worked with 2-aminoanthracene but did not proceed using 2-aminonaphthalene. This problem was solved alongside other former Stryker group researchers.<sup>62</sup> We determined that what Wang claimed to be the catalyst (iodine) is actually an indirect, but simple extension of Kozlov's historic acid-catalyzed three-component cyclocondensation reaction. The presence of water created the necessary acidic conditions for the reaction to proceed, especially when using 2-aminonaphthalene as a substrate. That is, protic acids are required and aqueous HCl, HBr, HI, and H<sub>2</sub>SO<sub>4</sub> all produced the desired product.

The original three-component acid catalyzed cyclocondensation product **12** was brominated to yield dibromo **26** or ethylated to yield **27**, and sequentially ethylated then brominated to afford **28**.

The synthesis of unsymmetric model archipelago asphaltene **30** using the three-component acid catalysis reaction was discovered. A convenient large-scale preparatory procedure for 1-vinylpyrene was developed. This procedure is less time-consuming in terms of materials required and number of setup/purification steps and higher yielding than previously published procedures.

Two pyrene units were coupled to dibrominated central island **26** to yield unsaturated model asphaltene **31**, using a convergent double Heck reaction developed in conjunction with a co-worker.

## 5.2 - Future Considerations

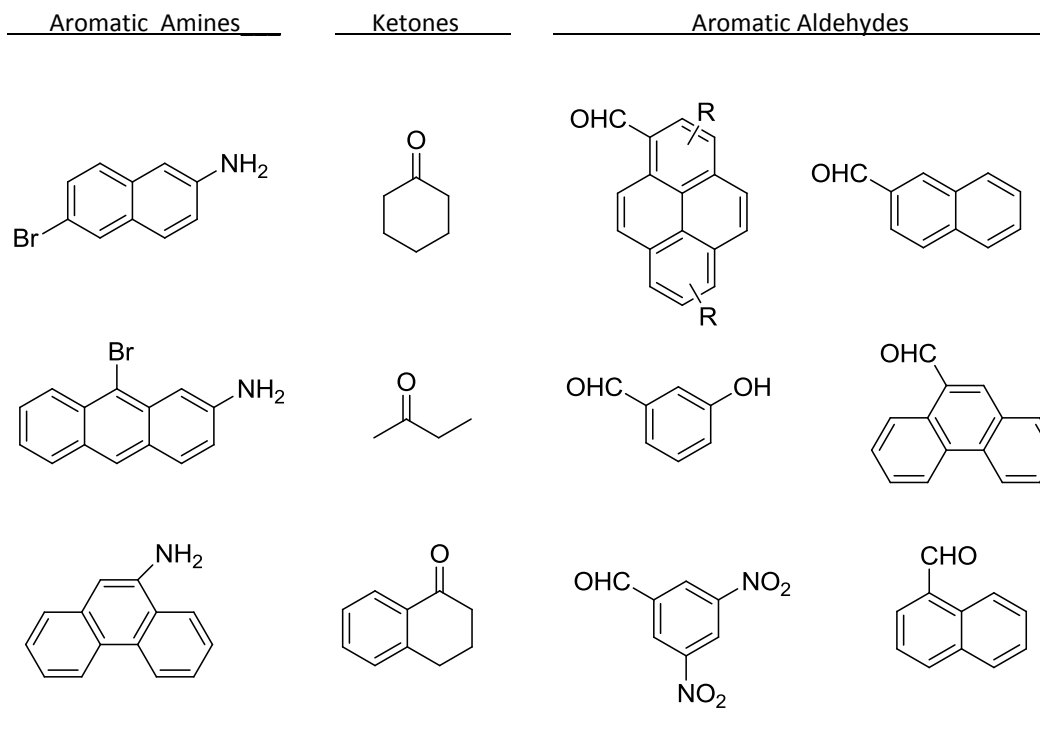
### 5.2.1 – Possible Substrates for Model Asphaltene Synthesis

Now that the three-component acid catalysis problem has been solved, multiple archipelago islands for the synthesis of model asphaltenes can be readily made in one pot from easily obtainable starting materials (Scheme 5.2). The aromatic amine can be varied broadly. The use of 6-Bromo-2-aminonaphthalene and 9-bromo-2-aminoanthracene would yield variations in the points of attachment. The use of 9-aminophenanthrene and brominated derivatives may produce additional model asphaltene islands.

Variations of the aromatic aldehyde may include using 1-formylpyrene, 1 or 2-formylnaphthalene, 9-formylphenanthrene and any corresponding brominated derivatives. The aliphatic ketone can either be cyclic or acyclic, as demonstrated by Kozlov.<sup>63</sup> Alpha-tetralone may provide a structural motif that adds an additional aromatic ring and gives semi-helical structures. The stage is now set to establish a large library of nitrogenous model asphaltene islands that may be linked to other aromatic islands or further functionalized, for example with a carboxylic acid, for supramolecular bonding.

---

**Scheme 5.1.** Possible substrates for future model asphaltenes.



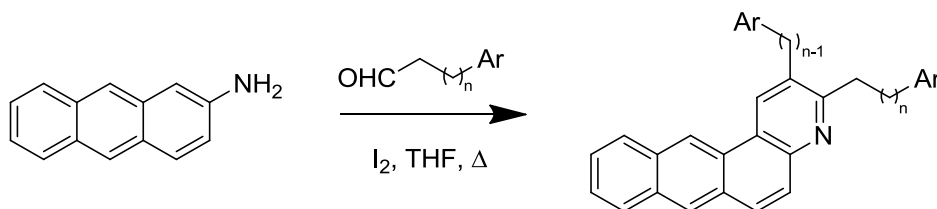
### 5.2.2 – Variations in Unsymmetric Model Asphaltene 30

Model asphaltenes consisting of linked archipelago islands can be directly synthesized using this three-component reaction (Scheme 5.2). Variations in the aliphatic aldehyde will produce islands with varying tethered carbons as well as variations in the type of polycyclic aromatic structure. First the amine can be treated with one reactive aldehyde to form the imine. Then adding the second aldehyde, containing a different aromatic region or tether, may

undergo acid catalyzed cyclization. Such diversity in the multicomponent reaction has not been explored.

---

**Scheme 5.2.** Possible future model asphaltene targets.



### 5.2.3 – Advancement of 1-Vinylpyrene Procedure

In addition to its potential to make model asphaltenes, 1-vinylpyrene is used in research and development for semiconductors.<sup>64</sup> The preparation described in this thesis offers a simple setup, sensitive to neither oxygen nor water, uses reagent-grade material, and requires only a single purification to yield pure 1-vinylpyrene. The yields easily match or surpass those of the most extensive and careful procedures. The recovered starting material, which is flushed pure from the silica plug can be heated to reflux under the reaction conditions again to obtain a total yield of 93%. If larger scale is required, an alternative to the silica plug is recrystallization (e.g., ETOAc in DCM: 1-formylpyrene remains in solution while 1-vinylpyrene precipitates out).

### 5.2.4 - Hydrogenation of Unsaturated Model Asphaltene (30)



Since much methodology in the Stryker group has been to link aromatic islands via palladium-catalyzed Heck coupling, selectively hydrogenating the bridging alkenes without affecting the pyrene units would be most useful. Gentler catalysis conditions may be necessary. Varying the hydrogen pressure, time, and molar ratio of Pd/C may result in conditions that yield the desired hydrogenated product. If over hydrogenation is inevitable, then reoxidation (i.e, refluxing while bubbling through O<sub>2</sub>) may return the aromaticity of the pyrene units.

### 5.3 – References for Chapter 5

---

62. Lofstrand, V., PhD candidate and former Stryker group member at the University of Alberta; Wang, Xi, B.Sc. Honours candidate in the Stryker group at the University of Alberta.
63. Kozlov, N.G.; Gusak, K.N.; Kadutskii, A.P. Development of the Catalytic Synthesis of Compounds of the Quinoline Series (The N.S. Kozlov Reaction) (Review). *Chem. Heterocycl. Compd.* **2010**, *46*, 505-528.
64. Rajakumar, P.; Visalakshi, K.; Ganesan, S.; Maruthamuthu, P.; Suthanthiraraj, S.A. Synthesis and Dye-sensitized Solar cell Application of Polyolefinic Aromatic Molecules with Pyrene as Surface Group. *Aust. J. Chem.* **2011**, *64*, 951-956.

## Chapter 6 – Experimental Section

### 6.1 –General Experimental Details

#### 6.1.1 - Methods

Laboratory work was performed in a ventilated fume hood equipped with argon, water, vacuum and air lines using standard Schlenk techniques or in a dry, nitrogen atmosphere glove-box. High vacuum traps were cooled by liquid nitrogen. Reactions requiring elevated temperatures were heated in a bath of oil (heavy mineral or silicon) using IKA heating/stir plates or in sand-filled heating mantles using Canlab® or Fischer Scientific magnetic stirrers. Reactions requiring temperatures lower than in the laboratory were cooled in an ice/water or a dry ice/acetone bath, unless indicated otherwise.

All reactions were performed by the author unless indicated otherwise. Instrumentation staff performed elemental analysis, FTIR spectroscopy, UV spectroscopy, and mass spectrometry. NMR spectroscopic experiments were performed by the author with occasional support from instrumentation staff.

#### 6.1.2 - Equipment

Thin layer chromatography was performed on silica gel coated plates back with glass, plastic, or aluminum. Flash column chromatography was performed in a ventilated fume hood using 40-63  $\mu\text{m}$  silica gel, sand, and a solvent system as mentioned in the specific procedure.

Vacuum filtration was performed using Whatman or Fisherbrand filter paper (P1-P5) and Buchner funnels or Fritz Filters under the laboratory equipped vacuum line. Evaporation of solvents under vacuum was performed using a Buchi Rotoevapor R-114 equipped with a dry ice condenser and a Vacuubrand electric vacuum pump or water aspirator. Further evaporation was performed under a Schlenk line vacuum or a high vacuum line equipped with a diffusion pump.

Stopcocks used (e.g. dropping funnels, separatory funnels and columns, stir bars) were Teflon coated. Plastic, calibrated sterile syringes with stainless steel needles were used to measure liquid reagents at room temperature.

Chemicals were handled in glass vessel made of Pyrex. Glassware used as part of a reaction apparatus was dried in an oven (100-120 $^{\circ}\text{C}$ ) for at least one hour or flame dried with a Bunsen burner and cooled under vacuum immediately before use.

All ground glass joints used in reactions were coated with Dow Corning<sup>®</sup> high vacuum grease and glassware was secured with plastic clips or copper wire.

NMR samples were placed in standard 5mm NMR tubes sealed with plastic caps.

### **6.1.3 – Reagents and Literature Compounds**

The following reagents were purchased from either Sigma Aldrich or Alfa Aesar and were used without further purification unless specified in the procedures below: 35% ammonium hydroxide, ammonium sulfate monohydrate, 1,2-bis(diphenylphosphino)ethane nickel(II) chloride, bromine, cyclohexanone, m-bromobenzaldehyde, N,N-diisopropylethylamine, ethylmagnesium bromide, glacial acetic acid, 38% hydrochloric acid, iodine, lithium aluminum hydride, 2-naphthol, magnesium sulfate, methyltriphenylphosphonium bromide, oxalyl chloride, palladium(II) acetate, potassium hydroxide, 1-pyrenebutanoic acid, sodium carbonate, sodium chloride, sodium hydroxide, 30 mesh tin, triethylamine, and tris(2-methoxyphenyl)phosphine. 1-Formylpyrene was made according to the referenced procedure.<sup>65</sup> All other reagents and intermediates were made by using modified procedures adapted from the literature and are included in the experimental section. Purified liquid reagents and solvents were stored in Schlenk flasks or if stored for extended periods of time under an argon or nitrogen atmosphere in glass containers sealed by Teflon coated screw caps fitted with a side arm to allow liquid extraction under a dry and inert atmosphere. All solid reagents and reaction products were stored in glass vials sealed with plastic caps, unless otherwise indicated. Solvents used on a daily basis (DCM, THF, EtOAc, Et<sub>2</sub>O, toluene, hexanes, acetone) that were not used in water sensitive reactions were stored in Pyrex containers and dispensed using glass Pasteur Pipettes. Argon, nitrogen, and hydrogen were taken from standard gas cylinders and used without further purification.

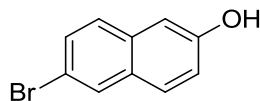
THF, benzene, diethyl ether, 1,4-dioxane were distilled over sodium/benzophenone in a nitrogen atmosphere. DCM was distilled over calcium hydride in a dry atmosphere. Isopropanol and methanol were heated to reflux over magnesium and distilled under an argon atmosphere. DMSO was distilled under argon.

#### 6.1.4 – Instrumentation

$^1\text{H}$  and  $^{13}\text{C}$  NMR experiments were performed using Varian Inova 300 MHz, Varian Inova 400 MHz, Varian Mercury 400 MHz, Varian Inova 500 MHz, Varian Inova 600 MHz at 27°C, or Varian Inova 500 MHz NMR spectrometer equipped with a  $^{13}\text{C}/^1\text{H}$  dual cold probe.  $^1\text{H}$  NMR and  $^{13}\text{C}$  NMR chemical shifts are reported in ppm ( $\delta$ ) which is measured using either tetramethylsilane or the protonated NMR solvent peak(s) that occurs as impurities. X-ray crystallographic analysis was performed by Robert McDonald and Michael J. Ferguson at the X-Ray Crystallography Laboratory at the University of Alberta using a Bruker DB diffractometer equipped with a SMART APEX II CCD area detector. FTIR spectroscopy was conducted using a Nicolet Magna 750 FTIR Spectrometer equipped with a Nic-Plan FTIR Microscope. Mass spectrometry was performed using a Kratos Analytical MS-50 -high resolution electron impact for high resolution electron impact, Agilent Technologies 6220 aoTOF mass spectrometer for high resolution electrospray ionization, or an Agilent Technologies 5975C MSD –GCMS for samples requiring GC-MS.

### 6.2 – Reaction Procedures

#### 6.2.1 - 6-Bromo-2-naphthol (22)

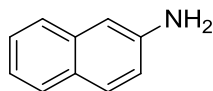


The procedure of Koelsch<sup>66</sup> was generally followed with one exception: 30 mesh tin was used instead of mossy tin. The yield was greatly diminished from the reported procedure.

A dry three neck round flask was equipped with a Teflon coated magnetic stir bar, reflux condenser, glass stopper, and a dropping funnel with an equalizing tube. The system was evacuated and purged under argon three times. 2-Naphthol (1.00 g, 6.9 mmol) and glacial AcOH (0.45 mL) was added to the round bottom flask under an argon purge. The dropping funnel was charged with a solution of Br<sub>2</sub> (0.46 mL, 8.9 mmol) in AcOH (0.45 mL). The bromine solution was added dropwise over 10 minutes and the solution was cooled to 0 °C near the end of the addition. Water was added (0.45 mL) under an argon purge and the system was heated to reflux and the cooled to 100 °C. 30 mesh tin (0.67 g, 5.6 mmol) was added at 100°C in three portions while between portions, the system was heated to reflux and then allowed to cool back down. After the final portion of tin was added, the mixture was heated to reflux for 3 hours. The mixture was filtered under vacuum and washed with cold AcOH. The filtrate was added to cold water (10 mL) and the precipitate collected under vacuum filtration to give the title compound as a light pink powder (0.51 g, 33 %). Spectroscopic data matched that of the literature.

Pink powder; IR (cast film, cm<sup>-1</sup>): 3566 (w), 3262 (br s), 3065 (w), 1629 (m) 1588 (m), 1503 (m), 1340 (w), 1204 (s), 907 (s), 858 (m), 810 (m), 750 (m); <sup>1</sup>H NMR (500 MHz, CDCl<sub>3</sub>): δ 7.95 (s, 1H), 7.68 (d, *J* = 8.3 Hz, 1H), 7.55 (d, *J* = 8.0 Hz, 1H), 7.52 (d, *J* = 8.0 Hz, 1H), 7.33 (br s, 2H, 2H), 5.20 (br s, 1H, -OH); <sup>13</sup>C NMR (125 MHz, CDCl<sub>3</sub>): δ 153.6, 133.1, 130.0, 129.9, 129.8, 129.0, 128.1, 118.8, 117.2, 109.8; EI-HRMS *m/z* calculated for: C<sub>10</sub>H<sub>7</sub>O (M<sup>+</sup>), 221.9680; Found: C<sub>10</sub>H<sub>7</sub>O (M<sup>+</sup>), 221.9680.

## 6.2.2 - 2-Aminonaphthalene (1)



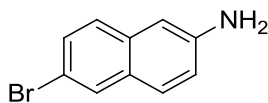
The procedure of Rasowsky<sup>67</sup> was generally followed with one exception: the steel bomb was heated to 170 °C for 72 h as opposed to 140 °C for 96 h as described in the literature.

2-Naphthol (6.62 g, 46 mmol), (NH<sub>4</sub>)<sub>2</sub>SO<sub>4</sub>H<sub>2</sub>O (15.29 g, 0.102 mol), and NH<sub>4</sub>OH (79.4 mL) were added to a steel bomb equipped with a Teflon coated magnetic stir bar. No glass liner was used. The bomb was sealed and the mixture was heated to 170 °C for 3 days under vigorous stirring. The contents were then filtered and washed with cold water. The filtered solid was dissolved in methylene chloride, washed with water three times, and dried with MgSO<sub>4</sub>. Evaporation of the solvent gave the title compound (5.17 g, 79 %). Spectroscopic data matched that of the literature. The compound is not quite pure according to elemental analysis but was used without further purification.

Slightly impure brown powder; **IR** (cast film, cm<sup>-1</sup>): 3397 (m), 3321 (m), 3208 (m), 3049 (m), 1630 (s), 1600 (m), 1513 (m), 1364 (w), 1184 (w), 959 (w), 869 (s), 843 (s), 813 (s), 743 (s); **<sup>1</sup>H NMR** (500 MHz, CDCl<sub>3</sub>): δ 7.73 (d, J = 8.0 Hz, 1H), 7.69 (d, J = 8.5 Hz, 1H), 7.63 (d, J = 8.0 Hz, 1H) 7.40 (app t, J = 7.5 Hz, 1H), 7.26 (app t, J = 8.0 Hz), 7.02 (br s, 1H), 6.98 (dd, J = 8.5 2.0 Hz, 1H), 3.92 (br s, 2H, -NH<sub>2</sub>) ; **<sup>13</sup>C NMR** (125 MHz, CDCl<sub>3</sub>): δ 144.1, 134.9, 129.2, 128.0, 127.7, 126.4, 125.8, 122.5, 118.3, 108.6; **ESI-HRMS** m/z calculated for: C<sub>10</sub>H<sub>10</sub>N (M+H)<sup>+</sup>, 144.0813;

Found: C<sub>10</sub>H<sub>10</sub>N (M+H)<sup>+</sup>, 144.0806. **Elemental Analysis** calculated for C<sub>10</sub>H<sub>9</sub>N: C, 83.87 %; H, 6.34 %; N, 9.54%; Found: C, 82.40 %; H, 6.63 %; N, 9.54 %.

### 6.2.3 - 6-Bromo-2-aminonaphthalene (**21**)

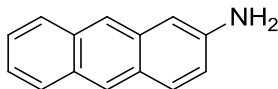


6-bromo-2-naphthol (**21**) (97.4 mg, 4.4 mmol), (NH<sub>4</sub>)<sub>2</sub>SO<sub>4</sub>·H<sub>2</sub>O (0.731 g, 4.87 mmol), and NH<sub>4</sub>OH (1.2 mL) were added to a steel bomb equipped with a Teflon coated magnetic stir bar. The bomb was sealed and the mixture was heated to 165 °C for 3 days. The contents were filtered under vacuum and washed with cold water to give the title compound as a red solid (63.7 mg, 66 %). Spectroscopic data matched that of the literature.

Red powder **IR** (neat film, cm<sup>-1</sup>): 3460 (w), 3372 (w), 3055 (w), 3021 (w), 2958 (w), 2925 (m), 2854 (w), 1631 (s), 1612 (s), 1506 (m), 1214 (m), 863 (m), 815 (m), 756 (s); **<sup>1</sup>H NMR** (500 MHz, CDCl<sub>3</sub>): δ 7.86 (d, *J* = 1.8 Hz, 1H), 7.59 (d, *J* = 8.4 Hz, 1H), 7.48 7.44 (AB quartet with 7.44 signals split into doublets, *J* = 8.9 1.9 Hz, 2H), 6.99 (d, *J* = 2.3 Hz, 1H), 6.68 – 6.50 (m, 1H), 3.90 (br s, 2H, -NH<sub>2</sub>); **<sup>13</sup>C NMR** (125 MHz, CDCl<sub>3</sub>): δ 144.5, 133.4, 129.7, 129.6, 129.0, 128.6, 127.5, 119.1, 115.7, 108.4; **EI-MS** *m/z* calculated for: C<sub>10</sub>H<sub>8</sub>BrN (M<sup>+</sup>), 220.9840; Found: C<sub>10</sub>H<sub>8</sub>BrN (M<sup>+</sup>), 220.9840.



#### 6.2.4 - 2-Aminoanthracene (10)

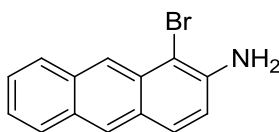


A modified procedure from Zhang et al.<sup>68</sup> was followed. 2-aminoanthraquinone (27.97 g, 0.12 mol) and zinc powder (176.4 g, 2.70 mol) were added to a 3L round bottom flask equipped with a large Teflon-coated magnetic stir bar. The flask was fitted with a condenser and the system was evacuated via vacuum and purged with argon three times. A solution of 8% aqueous NaOH (800mL) was added via cannula transfer under argon. The NaOH solution was deoxygenated before it was transferred by purging the solution with argon while stirring for 1 hr and venting through a mineral bubbler. The mixture was heated to reflux for 3 days and slowly turned from red to green (some red colour remained). The aqueous phase was removed by filtration under vacuum. The filtered solid was extracted with DCM in a soxhlet apparatus under reflux overnight. The solvent was removed via rotoevaporation and recrystallized with EtOAc. Vacuum filtration of the precipitate followed by rinsing with first cold EtOAc:Hexanes (1:1) and then hexanes gave the title compound (15.24 g, 63 %) accompanied by unidentified minor impurities. This material was not further purified.

Green powder **IR** (cast film,  $\text{cm}^{-1}$ ): 3399 (w), 3326 (w), 3208 (w), 3048 (w), 1637 (s), 1485 (m), 1460 (m), 1279 (w), 1217 (w), 955 (m), 886 (s), 805 (m), 737 (m);  **$^1\text{H NMR}$**  (500 MHz,  $\text{CDCl}_3$ ):  $\delta$  8.27 (s, 1H), 8.10 (s, 1H), 7.91 (d,  $J = 8.4$  Hz, 1H), 7.86 (d,  $J = 8.4$  Hz, 1H), 7.84 (d,  $J = 9.0$  Hz), 7.93 (app t,  $J = 6.9$  Hz, 1H), 7.33 (app t,  $J = 7.6$  Hz, 1H), 7.77 (d,  $J = 1.6$  Hz, 1H), 6.99 (dd,  $J = 8.9$

2.1 Hz, 1H), 3.92 (br d, 2H,  $-\text{NH}_2$ );  $^{13}\text{C}$  NMR (125 MHz,  $\text{CDCl}_3$ ):  $\delta$  143.3, 133.2, 132.4, 129.8, 129.7, 128.2, 127.6, 127.5, 126.2, 125.3, 123.8, 122.6, 120.0, 106.2; **ESI-HRMS**  $m/z$  calculated for:  $\text{C}_{14}\text{H}_{12}\text{N}$  ( $\text{M}+\text{H}$ ) $^+$ , 194.0970; Found: ( $\text{M}+\text{H}$ ) $^+$  194.0963; **Elemental Analysis** calculated for  $\text{C}_{14}\text{H}_{11}\text{N}$ : C, 87.01 %; H, 5.74 %; N, 7.25 %; Found: C, 80.92 %; H, 6.54 %; N, 5.44 %.

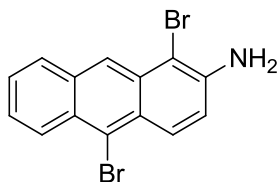
### 6.2.5 - 1-Bromo-2-aminoanthracene (**23**)



2-Aminoanthracene (**10**) (56.3 mg, 0.29 mmol) was added to a round bottom flask equipped with a magnetic stir bar followed by 2 mL of dry DCM. The round bottom flask was then connected to a reflux condenser and cooled in an ice bath. 0.92 mL of a 0.303 M solution of bromine (0.279 mmol) in DCM was added dropwise via syringe while stirring. The deep purple mixture was allowed to warm to room temperature and then stirred for 2 h. The mixture was filtered under vacuum, washed with water, aqueous  $\text{Na}_2\text{CO}_3$ , and allowed to dry under vacuum. Purification via flash chromatography (10:1, hexanes – EtOAc) afforded the title compound (15.3 mg, 19 %).

Dark green powder; **IR** (cast film,  $\text{cm}^{-1}$ ): 3357 (w), 3190 (w), 2958 (m), 2922 (s), 2851 (m), 1631 (w), 1464 (w), 1261 (w), 1029 (w), 802 (w);  $^1\text{H}$  NMR (300 MHz,  $\text{CDCl}_3$ ):  $\delta$  8.52 (s, 1H,  $\text{H}_{10}$ ), 8.27 (s, 1H,  $\text{H}_9$ ), 8.00 (d,  $J = 8.7$  Hz, 1H,  $\text{H}_8$ ), 7.94 (d,  $J = 8.4$  Hz,  $\text{H}_5$ ), 7.79 (d,  $J = 9.0$  Hz,  $\text{H}_3$ ), 7.47 (td,  $J = 6.6$  1.2 Hz, 1H,  $\text{H}_7$ ), 7.40 (td,  $J = 6.6$ , 1.2 Hz,  $\text{H}_6$ ), 7.01 (d,  $J = 8.7$  Hz,  $\text{H}_3$ ), 4.35 (br d, 2H,  $-\text{NH}_2$ ); **COSY** (400 MHz,  $\text{CHCl}_3$ ):  $\delta$  8.52  $\leftrightarrow$   $\delta$  8.27, 7.94, 7.80;  $\delta$  8.27  $\leftrightarrow$   $\delta$  8.00;  $\delta$  8.00  $\leftrightarrow$   $\delta$  7.47;  $\delta$  7.94  $\leftrightarrow$   $\delta$  7.40;  $\delta$  7.79  $\leftrightarrow$   $\delta$  7.01;  $\delta$  7.47  $\leftrightarrow$   $\delta$  7.40.

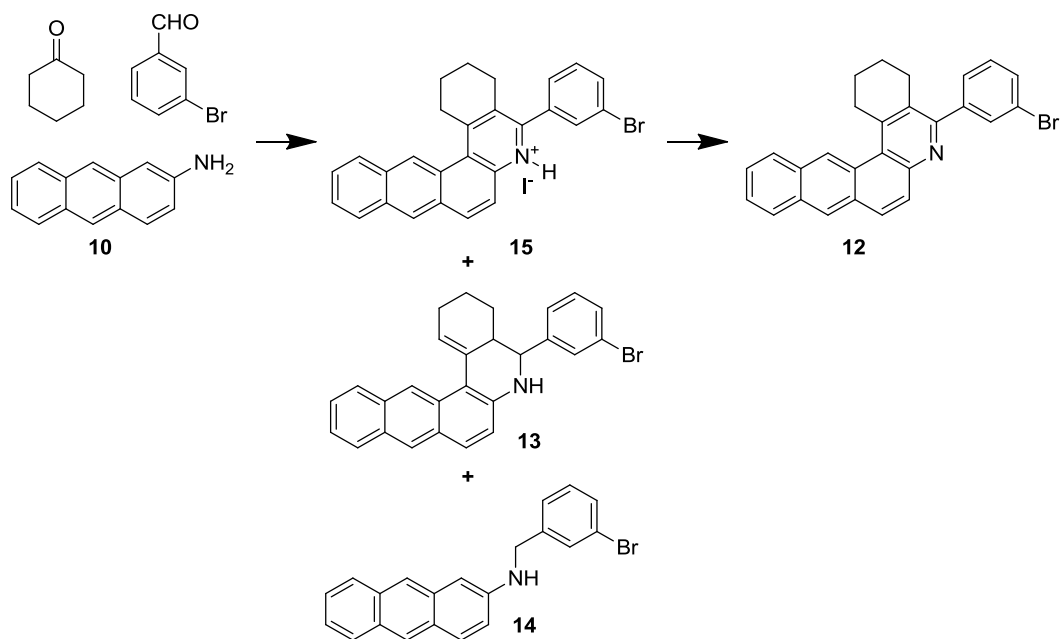
### 6.2.6 - 1,10-Dibromo-2-aminoanthracene (**24**)



2-Aminoanthracene (**10**) (39.0 mg, 0.20 mmol) was added to a round bottom flask equipped with a magnetic stir bar followed by 4mL of dry 1,2-dichloromethane. The round bottom flask was then cooled in an ice bath. Bromine (0.053 mL, 1.01 mmol) was added dropwise via syringe while stirring over the course of 2 h. The mixture was filtered, rinsed with water, aqueous Na<sub>2</sub>CO<sub>3</sub>, filtered under vacuum, and allowed to dry under vacuum. Purification via flash chromatography (10:1, hexanes – EtOAc) afforded the title compound (4.91 mg, 7 %).

Dark orange powder: IR (cast film, cm<sup>-1</sup>): <sup>1</sup>H NMR (400 MHz, CDCl<sub>3</sub>): δ 8.58 (s, 1H, H<sub>9</sub>), 8.44 (dd, *J* = 9.6 1.2 Hz, 1H, H<sub>8</sub>), 8.39 (dd, *J* = 9.2, 0.8 Hz, 1H, H<sub>5</sub>), 7.99 (dd, *J* = 7.6, 1.6 Hz, 1H, H<sub>4</sub>), 7.55 – 7.47 (m, 2H, H<sub>6</sub> H<sub>7</sub>), 7.15 (d, *J* = 9.2 Hz, 1H, H<sub>3</sub>), 4.56 (br s, 2H, -NH); COSY (400 MHz, CHCl<sub>3</sub>): δ 8.44 ↔ δ 7.55-7.47; δ 8.39 ↔ δ 7.15; δ 7.99 ↔ δ 7.55 – 7.47. No more data was obtained due to the low yield obtained.

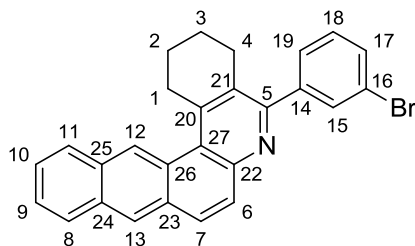
### 6.2.7 - 5-(3-Bromophenyl)-1,2,3,4-tetrahydrobenzo[b]anthraquinoline (**12**)



2-Aminoanthracene (**10**) (1.257 g, 6.5 mmol) was added to a dry round bottom flask equipped with a Teflon stirrer, fitted with a condenser, and connected to argon. After evacuating and purging the system three times, m-bromobenzaldehyde (0.77 mL, 6.5 mmol) was added by syringe. The mixture was stirred at room temperature and 32.5 mL of a 0.010 M solution of iodine in anhydrous THF was added by syringe. After several minutes, the mixture became cloudy green. At this point cyclohexanone (0.67 mL, 6.5 mmol) was added into the mixture by syringe. The mixture was then heated to reflux, eventually becoming a homogeneous and brownish-yellow solution. After several hours at reflux, a yellow precipitate began to form and the reaction was monitored by TLC. After 24 h, the system was opened to the atmosphere and allowed to reflux for an additional 24 h. Filtration of the crude mixture afforded a yellow-green solid (0.645 g, 17 %, HI adduct **15**) which was air-dried and pure by  $^1\text{H}$  NMR spectroscopy. This solid was washed with aqueous  $\text{NaCO}_3$  (100 mL) and extracted with DCM. Evaporation of

the mother liquor and recrystallization from THF/hexanes afforded dark, apparently black, crystals of the free base **15**, which were combined with the DCM extract to give a total yield of 67 % (1.914 g, 4.4 mmol). Sequential recrystallizations also afforded an impure orange powder **13** (0.430 g, 15 %) and a pure green powder **14** (0.165g, 7 %).

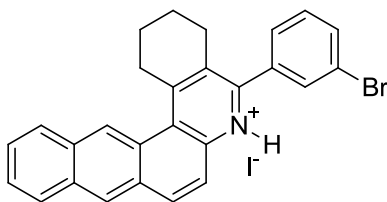
### 5-(3-Bromophenyl)-1,2,3,4-tetrahydrobenzo[b]anthraquinoline (**12**)



Dark yellow powder or black crystals; **IR** (cast film,  $\text{cm}^{-1}$ ): 3049 (w) , 2932 (m), 2894 (w), 2864 (w), 1594 (w), 1559 (w), 1533 (w), 1472 (w), 1368 (w), 1263 (w), 889 (s), 788 (w), 762 (w), 747 (s), 700 (m);  **$^1\text{H NMR}$**  (300 MHz,  $\text{CDCl}_3$ )  $\delta$  9.17 (s, 1H  $\text{H}_{12}$ ), 8.37 (s, 1H,  $\text{H}_{13}$ ), 8.11-8.03 (m, 2H,  $\text{H}_{11}$   $\text{H}_8$ ), 7.92 7.82 (AB quartet,  $J = 9.3$  Hz, 2H,  $\text{H}_7$   $\text{H}_6$ ), 7.73 (s, 1H,  $\text{H}_{15}$ ), 7.62-7.57 (m, 3H,  $\text{H}_{10}$   $\text{H}_9$   $\text{H}_{17}$ ), 7.49 (d,  $J = 7.8$  Hz, 1H,  $\text{H}_{19}$ ), 7.36 (t,  $J = 7.8$  Hz, 1H,  $\text{H}_{18}$ ), 3.70 (t,  $J = 5.7$  Hz, 2H,  $\text{H}_1$ ), 2.87 (t,  $J = 5.7$  Hz, 1H,  $\text{H}_4$ ), 1.93-1.86 (m, 4H,  $\text{H}_3$   $\text{H}_2$ );  **$^{13}\text{C APT NMR}$**  (125 MHz,  $\text{CDCl}_3$ )  $\delta$  157.0 (+,  $\text{C}_5$ ), 147.1 (+,  $\text{C}_{22}$ ), 145.8 (+,  $\text{C}_{21}$ ), 143.2 (+,  $\text{C}_{14}$ ), 132.0 (-,  $\text{C}_{15}$ ), 131.7 (+,  $\text{C}_{23}$ ), 131.3 (+,  $\text{C}_{25}$  or  $\text{C}_{24}$ ), 131.2 (+,  $\text{C}_{25}$  or  $\text{C}_{24}$ ), 131.0 (-,  $\text{C}_{17}$ ), 130.8 (-,  $\text{C}_7$ ), 129.9 (-,  $\text{C}_{19}$ ), 129.1 (-,  $\text{C}_6$ ), 128.9 (+,  $\text{C}_{20}$ ), 128.8 (-,  $\text{C}_{11}$ ), 128.5 (-,  $\text{C}_{12}$ ), 128.3 (+,  $\text{C}_{26}$ ), 127.6 (-,  $\text{C}_{18}$ ), 127.5 (-,  $\text{C}_8$ ), 126.9 (-,  $\text{C}_{13}$ ), 126.4 (-,  $\text{C}_{10}$  or  $\text{C}_9$ ), 125.9 (-,  $\text{C}_{10}$  or  $\text{C}_9$ ), 125.2 (+,  $\text{C}_{27}$ ), 122.6 (+,  $\text{C}_{16}$ ), 33.3 (+,  $\text{C}_1$ ), 28.3 (+,  $\text{C}_4$ ), 23.2 (+,  $\text{C}_2$ ), 22.2 (+,  $\text{C}_3$ ); **COSY** (500 MHz,  $\text{CHCl}_3$ ):  $\delta$  9.17  $\leftrightarrow$   $\delta$  8.37, 7.92, 7.82, 8.11-8.03;  $\delta$  8.37  $\leftrightarrow$   $\delta$  8.11-8.03, 7.92, 7.82;  $\delta$  8.11-8.03 ( $\text{H}_{11}$ )  $\leftrightarrow$   $\delta$  8.11-8.03 ( $\text{H}_8$ ), 7.62-7.57;  $\delta$  7.92  $\leftrightarrow$   $\delta$  7.82;  $\delta$  7.73  $\leftrightarrow$   $\delta$  7.62-7.57, 7.49, 7.36;  $\delta$  7.62-7.57  $\leftrightarrow$   $\delta$  7.49, 7.36;  $\delta$  7.49  $\leftrightarrow$   $\delta$  7.36;  $\delta$  3.70  $\leftrightarrow$   $\delta$  1.93-1.86;  $\delta$  2.87  $\leftrightarrow$   $\delta$  1.93-1.86; **HMQC** (500 MHz,  $\text{CDCl}_3$ ):  $\delta$  9.17  $\leftrightarrow$   $\delta$  128.5;  $\delta$  8.37  $\leftrightarrow$   $\delta$  126.9,  $\delta$  8.11-8.03 ( $\text{H}_{11}$ )  $\leftrightarrow$   $\delta$  128.8,  $\delta$  8.11-

8.02 (H<sub>8</sub>) ↔ δ 127.5, δ 7.92 ↔ δ 130.8; δ 7.82 ↔ δ 129.1; δ 7.73 ↔ δ 132.0; δ 7.62-7.57 ↔ δ 131.0, 126.4, 125.9; δ 7.49 ↔ δ 129.9; δ 7.36 ↔ δ 127.6; δ 3.70 ↔ δ 33.3; δ 2.87 ↔ δ 28.3; δ 1.93-1.86 (H<sub>2</sub>) ↔ δ 22.2; δ 1.93-1.86 (H<sub>3</sub>) ↔ δ 23.2; **HMBC** (500 MHz, CDCl<sub>3</sub>): δ 9.17 ↔ δ 128.9, 125.2; δ 8.37 ↔ δ 130.8, 128.3, δ 8.11-8.03 (H<sub>11</sub>) ↔ δ 126.4, 131.3, δ 8.11-8.02 (H<sub>8</sub>) ↔ δ 125.9, 131.3; δ 7.92 ↔ δ 147.1, 131.7, 128.3, 126.9; δ 7.82 ↔ δ 131.7, 125.2; δ 7.73 ↔ δ 157.0, 131.0, 127.6, 122.6; δ 7.62-7.57 ↔ δ 127.6; δ 7.49 ↔ δ 157.0, 122.6; δ 7.36 ↔ δ 143.2, 122.6; δ 3.70 ↔ δ 125.2, 128.9, 145.8; δ 2.87 ↔ δ 157.0, 145.8, 128.9; δ 1.93-1.86 (H<sub>2</sub>) ↔ δ 128.9, 33.3, 23.2; δ 1.93-1.86 (H<sub>3</sub>) ↔ δ 145.8, 22.2; **TROESY** (500 MHz, CDCl<sub>3</sub>): δ 9.17 ↔ δ 33.3; δ 1.93-1.86 ↔ δ 33.3; **UV VIS** (λ nm, abs): 285, 0.716; 307, 0.689; 261, 0.626; **EI-HRMS** *m/z* calcd for C<sub>27</sub>H<sub>20</sub>N<sup>79</sup>Br (M<sup>+</sup>) 437.0777; Found C<sub>27</sub>H<sub>20</sub>N<sup>79</sup>Br (M<sup>+</sup>), 437.0779; **Elemental Analysis** calculated for C<sub>27</sub>H<sub>20</sub>NBr: C, 73.89 %; H, 4.97 %; N, 3.37 %; Found: C, 73.96 %; H, 4.60 %; N, 3.20.

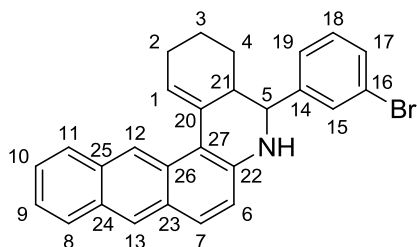
### 6.2.8 - 5-(3-Bromophenyl)-1,2,3,4-tetrahydrobenzo[b]anthraquinoline hydroiodide (15)



Bright yellow crystals; **IR** (microscope, cm<sup>-1</sup>): 3045 (w), 2935 (s), 2871 (s), 2841 (s), 2778 (w), 1606 (m), 1558 (m), 1545 (m), 1493 (m), 1339 (s), 1354 (s), 1261 (s), 1073 (m), 891 (s), 801 (s), 790 (s), 755 (m), 745 (m), 701 (m); **<sup>1</sup>H NMR** (300 MHz, CDCl<sub>3</sub>): δ 9.24 (s, 1H, H<sub>12</sub>), 8.46 (s, 1H, H<sub>13</sub>), 8.46 (chemical shift may vary, br d, *J* = 8.41 Hz, 1H, H<sub>6</sub>), 8.21-8.19 (m, 1H, H<sub>11</sub> or H<sub>8</sub>), 8.15-8.10 (m, 1H, H<sub>11</sub> or H<sub>8</sub>), 8.12 (d, 1H, *J* = 15.5 Hz, H<sub>7</sub>), 7.77 (t, 1H, *J* = 1.6 Hz, H<sub>15</sub>), 7.73-7.68 (m, 2H,

H<sub>10</sub> H<sub>9</sub>), 7.67 (br d, 1H, *J* = 8.07 Hz, H<sub>17</sub>), 7.63 (br d, 1H, *J* = 7.7 Hz, H<sub>19</sub>), 7.46 (t, 1H, *J* = 7.9 Hz, H<sub>18</sub>), 3.81 (t, *J* = 6.0 Hz, 2H, H<sub>1</sub>), 2.91 (t, *J* = 5.7 Hz, 1H, H<sub>4</sub>), 1.87-1.83 (m, 2H, H<sub>3</sub> H<sub>2</sub>); <sup>13</sup>C NMR (125 MHz, CDCl<sub>3</sub>): δ 152.4, 152.2, 152.1, 143.1, 136.2, 134.7, 133.1, 132.3, 131.9, 131.7, 130.9, 130.4, 129.1, 129.0, 128.5, 128.4, 127.7, 127.5, 127.0, 126.54, 126.53, 122.8, 122.5, 34.1, 27.9, 22.6, 21.5; **COSY** (500 MHz, CDCl<sub>3</sub>): δ 9.24 ↔ δ 8.50; δ 8.62 ↔ δ 8.12; δ 8.50 ↔ δ 8.20, 8.12; δ 8.20 ↔ δ 7.72-7.66; δ 8.13 ↔ δ 7.72-7.66; δ 7.77 ↔ δ 7.67, 7.63 ;δ 7.67 ↔ δ 7.64; δ 3.81 ↔ 2.91, 1.87-183; δ 2.91 ↔ 1.87-183; **HSQC** (500 MHz, CDCl<sub>3</sub>): δ 9.28 ↔ δ 129.1; δ 8.62 ↔ δ 122.5, δ 8.50 ↔ δ 128.4, δ 8.21-8.19 ↔ δ 129.0, δ 8.15-8.10 ↔ δ 127.7; δ 8.12 ↔ δ 134.7; δ 7.77 ↔ δ 132.3; δ 7.73-7.68 ↔ δ 127.5, 127.0; δ 7.67 ↔ δ 127.0; δ 7.63 ↔ δ 128.5; δ 7.46 ↔ δ 130.4, δ 3.81 ↔ 34.1; δ 2.91 ↔ 27.9; δ 1.87-1.83 (H<sub>3</sub>) ↔ δ 21.5, δ 187-183 (H<sub>2</sub>) ↔ 22.6; **HMBC** (500 MHz, CDCl<sub>3</sub>): δ 9.28 ↔ δ 131.9, 131.0, 129.0, 126.5, 34.1; δ 8.50 ↔ δ 134.7, 131.7, 127.7, 126.5, 129.0, 34.1; δ 8.21-8.19 ↔ δ 131.7, 127.5; δ 8.12 ↔ δ 143.1, 128.4; δ 7.77 ↔ δ 152.1, 133.0, 128.5, 122.7; δ 7.73-7.68 ↔ δ 131.7, 129.0, 127.7; δ 7.67 ↔ δ 132.2, 128.5, 122.7; δ 7.63 ↔ δ 152.1, 133.0, 132.3; δ 7.46 ↔ δ 132.3, 128.5, 122.7; δ 3.81 ↔ 126.5, 152.1; δ 2.91 ↔ 152.4, 1.52.1, 22.6, 21.5; δ 1.87-1.83 (H<sub>3</sub>) ↔ δ 22.6, δ 187-183 (H<sub>2</sub>) ↔ 21.5; **EI-HRMS** *m/z* calcd for C<sub>27</sub>H<sub>20</sub>N<sup>79</sup>Br (M-HI)<sup>+</sup> 437.0777; Found C<sub>27</sub>H<sub>20</sub>N<sup>79</sup>Br (M-HI<sup>+</sup>), 437.0782; **Elemental Analysis** calculated for C<sub>27</sub>H<sub>21</sub>NBrI: C, 57.25 %; H, 3.74 %; N, 2.47 %; Found: C, 56.67 %; H, 3.93 %; N, 2.36.

### 6.2.9 - 5-(3-Bromophenyl)-2,3,4,5,21,N-hexahydrobenzo[b]anthraquinoline (13)

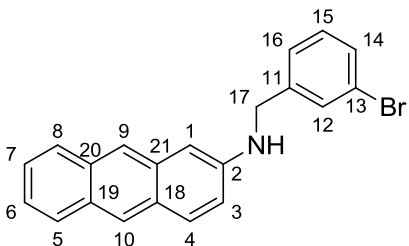


Impure orange powder; **IR** (microscope,  $\text{cm}^{-1}$ ) 3393 (w), 3049 (w), 2932, 2862 (m), 2830 (w), 1726 (w), 1635 (m), 1615 (m), 1491 (s), 1462 (s), 1408 (s), 1312 (m), 1242 (m), 1069 (w), 879 (s), 739 (s), 692 (m);  **$^1\text{H NMR}$**  (500 MHz,  $\text{CDCl}_3$ )  $\delta$  8.84 (s, 1H, H<sub>12</sub>), 8.22 (s, 1H, H<sub>13</sub>), 7.92, (d,  $J$  = 5.5 Hz, 1H, H<sub>11</sub>), 7.90 (d,  $J$  = 8.0 Hz, 1H, H<sub>8</sub>), 7.66 (d,  $J$  = 8.5 Hz, 1H, H<sub>7</sub>), 7.59 (s, 1H, H<sub>15</sub>), 7.48 (d,  $J$  = 8.0 Hz, 1H, H<sub>17</sub>), 7.41 (t,  $J$  = 7.5 Hz, 1H, H<sub>10</sub>), 7.35 (t,  $J$  = 7.5 Hz, 1H, H<sub>9</sub>), 7.31 (d,  $J$  = 7.5 Hz, 1H, H<sub>19</sub>), 7.23 (app t,  $J$  = 7.5 Hz, 1H, H<sub>18</sub>), 6.68 (d,  $J$  = 8.5 Hz, 1H, H<sub>6</sub>), 6.61 (br s, 1H, H<sub>1</sub>), 4.26 (br d,  $J$  = 11 Hz, 1H, H<sub>5</sub>), 2.68 (br d,  $J$  = 8.0 Hz, 1H, H<sub>21</sub>), 2.57 (dd,  $J$  = 19.5 5.0 Hz, 1H, H<sub>2</sub>), 2.31-2.28 (m, 1H, H<sub>2</sub>), 1.79-1.76 (m, 1H, H<sub>3</sub> or H<sub>4</sub>), 1.71-1.66 (m, 2H, H<sub>3</sub>, H<sub>4</sub>), 1.23-1.21 (m, 1H, H<sub>4</sub>);  **$^{13}\text{C APT NMR}$**  (125 MHz,  $\text{CDCl}_3$ )  $\delta$  145.1 (+, C<sub>20</sub>), 139.7 (+, C<sub>22</sub>), 132.5 (+, C<sub>24</sub>), 132.0 (+, C<sub>19</sub>), 131.2 (-, C<sub>17</sub>), 130.9 (-, C<sub>15</sub>), 130.2 (-, C<sub>18</sub>), 130.1 (+, C<sub>26</sub>), 129.0 (+, C<sub>25</sub>), 128.9 (-, C<sub>7</sub>), 128.6 (+, C<sub>23</sub>), 128.1 (-, C<sub>11</sub>), 127.9 (-, C<sub>8</sub>), 126.9 (-, C<sub>13</sub>), 126.7 (-, C<sub>19</sub>), 126.0 (-, C<sub>1</sub>), 125.2 (-, C<sub>10</sub>), 123.9 (-, C<sub>9</sub>), 122.8 (+, C<sub>16</sub>), 121.4 (-, C<sub>12</sub>), 119.0 (C<sub>6</sub>), 110.3 (+, C<sub>27</sub>), 64.1 (-, C<sub>5</sub>), 38.0 (-, C<sub>21</sub>), 26.9 (+, C<sub>4</sub>), 26.6 (+, C<sub>2</sub>), 20.3 (+, C<sub>3</sub>); **COSY** (500 MHz,  $\text{CDCl}_3$ )  $\delta$  7.92  $\leftrightarrow$   $\delta$  7.41;  $\delta$  7.66  $\leftrightarrow$   $\delta$  6.68;  $\delta$  7.59  $\leftrightarrow$   $\delta$  7.48, 7.31;  $\delta$  7.48  $\leftrightarrow$   $\delta$  7.23;  $\delta$  7.41  $\leftrightarrow$   $\delta$  7.92;  $\delta$  7.35  $\leftrightarrow$   $\delta$  7.90;  $\delta$  6.61  $\leftrightarrow$   $\delta$  2.68, 2.56, 2.31-2.58;  $\delta$  4.26  $\leftrightarrow$   $\delta$  2.68;  $\delta$  2.68  $\leftrightarrow$   $\delta$  1.79-1.72, 1.23-1.21;  $\delta$  2.57  $\leftrightarrow$   $\delta$  2.31-2.28, 1.79-1.76;  $\delta$  1.79-1.76  $\leftrightarrow$   $\delta$  1.71-1.66, 1.23-1.21; **HSQC** (400 MHz,  $\text{CDCl}_3$ )  $\delta$  8.84  $\leftrightarrow$   $\delta$  121.4;  $\delta$  8.22  $\leftrightarrow$   $\delta$  126.9 or 126.7;  $\delta$  7.92  $\leftrightarrow$   $\delta$  128.1;  $\delta$  7.90  $\leftrightarrow$   $\delta$  127.9;  $\delta$  7.66  $\leftrightarrow$   $\delta$  128.9;  $\delta$  7.59  $\leftrightarrow$   $\delta$  130.9;  $\delta$  7.48  $\leftrightarrow$   $\delta$  131.2;  $\delta$  7.41  $\leftrightarrow$   $\delta$  125.2;  $\delta$  7.35  $\leftrightarrow$   $\delta$  123.9;  $\delta$  7.31  $\leftrightarrow$   $\delta$  126.9 or 126.7;  $\delta$  7.23  $\leftrightarrow$   $\delta$  130.2;  $\delta$  6.68  $\leftrightarrow$   $\delta$  119.0;  $\delta$  6.61  $\leftrightarrow$   $\delta$  126.0;  $\delta$  4.26  $\leftrightarrow$   $\delta$  64.1;  $\delta$  2.68  $\leftrightarrow$   $\delta$  38.0;  $\delta$  2.57, 2.31-2.28  $\leftrightarrow$   $\delta$  26.2;  $\delta$  1.79-1.76, 1.71-1.66  $\leftrightarrow$   $\delta$  20.3;  $\delta$  1.71-1.66, 1.23-1.21  $\leftrightarrow$   $\delta$  20.3; **HMBC** (500 MHz,  $\text{CDCl}_3$ )  $\delta$  8.84  $\leftrightarrow$   $\delta$  129.0, 128.6;  $\delta$  8.22  $\leftrightarrow$   $\delta$  132.5, 129.0 or 128.9, 127.9;  $\delta$  7.92  $\leftrightarrow$   $\delta$  129.0, 123.9, 121.4;  $\delta$  7.90  $\leftrightarrow$   $\delta$  132.5, 125.2;  $\delta$  7.66  $\leftrightarrow$   $\delta$  139.7, 126.9;  $\delta$  7.59  $\leftrightarrow$   $\delta$  132.0, 126.7, 122.8, 64.1;  $\delta$  7.48  $\leftrightarrow$   $\delta$  130.9, 126.7,



122.8;  $\delta$  7.31  $\leftrightarrow$   $\delta$  145.1, 131.2, 122.6;  $\delta$  7.23  $\leftrightarrow$   $\delta$  131.2, 130.9, 64.1;  $\delta$  6.68  $\leftrightarrow$   $\delta$  128.6, 110.3;  $\delta$  4.26  $\leftrightarrow$   $\delta$  145.1, 130.9, 126.7, 30.0, 26.9; **UV VIS** ( $\lambda$  nm, abs): 265, 0.987; 303, 0.521; 344, 0.201; 361, 9.184; **ESI-HRMS**  $m/z$  calculated for:  $C_{27}H_{22}N^{79}Br$  (M-1)<sup>+</sup>, 438.0857; Found:  $C_{27}H_{21}NBr$  (M+1)<sup>+</sup> 438.0852; **EI-HRMS**  $m/z$  calculated for:  $C_{27}H_{24}N^{79}Br$  (M+2)<sup>+</sup>: 441.1092; Found:  $C_{27}H_{24}N^{79}Br$  (M+2)<sup>+</sup> 441.1092. **Elemental Analysis** calculated for  $C_{27}H_{22}NBr$ : C, 73.64 %; H, 5.04 %; N, 3.18 %; Found: C, 67.25 %; H, 4.76 %; N, 2.89.

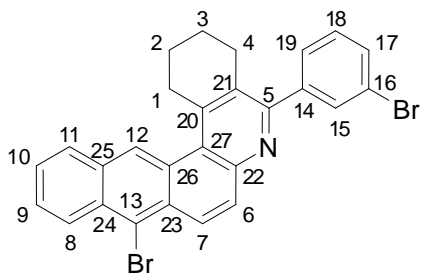
### 6.2.10 - N-(3-Bromobenzyl)anthracen-2-amine (14)



Green powder; **IR** (cast film,  $cm^{-1}$ ): 3405, 3049, 2953, 2894, 1636, 1505, 1471, 1438, 1346, 1222, 1183, 1064, 882, 739;  **$^1H$  NMR** (500 MHz,  $CDCl_3$ )  $\delta$  8.25 (s, 1H, H<sub>9</sub>), 8.09 (s, 1H, H<sub>10</sub>), 7.91 (d,  $J$  = 8.5 Hz, 1H, H<sub>5</sub>), 7.86 (d,  $J$  = 8.0 Hz, 1H, H<sub>8</sub>), 7.81 (d,  $J$  = 9.0 Hz, 1H, H<sub>4</sub>), 7.60 (br s, 1H, H<sub>12</sub>), 7.43 (dd,  $J$  = 8.0, 0.5 Hz, 1H, H<sub>14</sub>), 7.41-7.34 (m, 2H, H<sub>16</sub> H<sub>7</sub>), 7.33 (app td,  $J$  = 6.5 1.5 Hz, 1H, H<sub>6</sub>), 7.23 (t,  $J$  = 7.5 Hz, 1H, H<sub>15</sub>), 6.93 (dd,  $J$  = 9.0 2.0 Hz, 1H, H<sub>3</sub>), 6.82 (br s, 1H, H<sub>1</sub>), 4.44 (s, 2H, H<sub>17</sub>), 4.23 (br s, 1H, -NH);  **$^{13}C$  APT NMR** (125 MHz,  $CDCl_3$ )  $\delta$  144.2 (+, H<sub>2</sub>), 141.4 (+, C<sub>2</sub>), 133.4 (+, C<sub>21</sub>), 132.5 (+, C<sub>20</sub>), 130.50 (-, C<sub>16</sub> or C<sub>12</sub>), 130.48 (-, C<sub>16</sub> or C<sub>12</sub>), 130.3 (-, C<sub>15</sub>), 129.6 (+, C<sub>19</sub>), 129.5 (-, C<sub>4</sub>), 128.2 (-, C<sub>8</sub>), 127.5 (+, C<sub>18</sub>), 127.4 (-, C<sub>5</sub>), 126.2 (-, C<sub>9</sub>), 126.0 (-, C<sub>14</sub>), 125.3 (-, C<sub>6</sub> or C<sub>7</sub>), 123.7 (-, C<sub>6</sub> or C<sub>7</sub>), 122.83 (+, C<sub>13</sub>), 122.81 (-, C<sub>10</sub>), 120.0 (-, C<sub>3</sub>), 102.1 (-, C<sub>1</sub>), 47.7 (+, C<sub>17</sub>); **EI-HRMS**  $m/z$

361.0466 [M+]<sup>+</sup> (calcd for C<sub>21</sub>H<sub>16</sub>N<sup>79</sup>Br, 361.0466); **HSQC** (500 MHz, CHCl<sub>3</sub>): δ 8.25 ↔ δ 126.2; δ 8.09 ↔ δ 122.8; δ 7.91 ↔ δ 128.2; δ 7.86 ↔ δ 127.4; δ 7.81 ↔ δ 129.5; δ 7.60 ↔ δ 130.50 or 130.48; δ 7.43 ↔ δ 130.50 or 130.48; δ 7.41-7.34 ↔ δ 126.0, 125.3; δ 7.33 ↔ δ 123.7; δ 7.23 ↔ δ 130.3; δ 6.93 ↔ δ 120.0; δ 6.82 ↔ δ 102.1; δ 7.43 ↔ δ 130.50 or 130.48; **HMBC** (500 MHz, CHCl<sub>3</sub>): δ 8.25 ↔ δ 133.4, 129.6, 123.7; δ 8.09 ↔ δ 129.6, 127.5; δ 7.91 ↔ δ 132.5; δ 7.86 ↔ δ 123.7; δ 7.81 ↔ 144.4, 133.4, 126.2; δ 7.43 ↔ δ 126.0; δ 7.41-7.34 ↔ δ 132.5; δ 7.33 ↔ δ 127.4; δ 7.23 ↔ δ 141.4; δ 6.93 ↔ δ 127.4, 102.1; δ 6.82 ↔ δ 130.3, 122.8, 120.0; δ 4.44 ↔ δ 144.4, 141.4, 130.50 or 130.48, 126.2 or 126.0; **UV VIS** (λ nm, abs): 269, 0.868; 249, 0.589; 321, 0.101; **EI-MS** *m/z* calculated for: C<sub>21</sub>H<sub>16</sub>N<sup>81</sup>Br (M<sup>+</sup>), 361.0466; Found: C<sub>21</sub>H<sub>16</sub>N<sup>81</sup>Br (M<sup>+</sup>), 361.0446; **Elemental Analysis** calculated for C<sub>21</sub>H<sub>16</sub>NBr: C, 69.61 %; H, 4.45 %; N, 3.87; Found: C, 69.52 %; H, 4.50 %; N, 3.83.

### 6.2.11 - 13-Bromo-5-(3-bromophenyl)-1,2,3,4-tetrahydrobenzo[b]anthraquinoline (26)



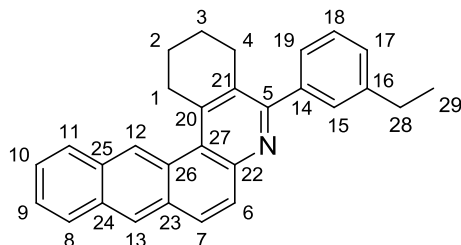
5-(3-Bromophenyl)-1,2,3,4-tetrahydrobenzo[b]anthraquinoline (**12**) (0.620 g, 1.41 mmol) was added to a round bottom flask followed by 10 mL of reagent grade DCM and equipped with a magnetic Teflon stir bar. The RBF was fitted to a condenser and the mixture was stirred until the starting material dissolved. Bromine (0.15 mL, 2.8 mmol) was added drop

wise to the solution via syringe over the course of 2 minutes. A yellow precipitate formed at the end of the bromine addition. The mixture was heated to reflux for 48 hours. Afterwards, the mixture was washed with aqueous NaOH until the precipitate dissolved. The organic layer was separated, washed with brine, dried with MgSO<sub>4</sub>, and purified by column chromatography (toluene) on silica gel to provide a dark yellow powder (0.516 g, 70.6 %).

Dark yellow solid; **IR** (cast film, cm<sup>-1</sup>) 3060 (w), 2937 (m), 2862 (w), 1549 (w), 1470 (m), 1318 (w), 1249 (w), 818 (m), 757 (s), 701 (m); **<sup>1</sup>H NMR** (500 MHz, CDCl<sub>3</sub>) δ 9.10 (s, 1H, H<sub>12</sub>), 8.57 (d, *J* = 10.0 Hz, 1H, H<sub>7</sub>), 8.54 (d, *J* = 9.0 Hz, 1H, H<sub>8</sub>), 8.05 (d, *J* = 8.0 Hz, 1H, H<sub>11</sub>), 7.90 (d, *J* = 9.5 Hz, 1H, H<sub>6</sub>), 7.73 (dd, *J* = 1.5, 1.5 Hz, 1H, H<sub>15</sub>), 7.70 (ddd, *J* = 8.5 7.0 1.0 Hz, 1H, H<sub>9</sub>), 7.61 (ddd, *J* = 9.5 8.0 1.0 Hz, 1H, H<sub>10</sub>), 7.59 (ddd, *J* = 8.0 2.0 1.5 Hz, 1H, H<sub>17</sub>), 7.49 (ddd, *J* = 7.5 1.5 1.0 Hz, 1H, H<sub>19</sub>), 7.37 (app t, *J* = 8.0 Hz, 1H, H<sub>18</sub>), 3.64 (t, *J* = 6.0 Hz, 2H, H<sub>1</sub>), 2.88 (t, *J* = 6.5 Hz, 2H, H<sub>4</sub>), 1.98-1.90 (m, 2H, H<sub>3</sub>), 1.86-1.80 (m, 2H, H<sub>2</sub>); **<sup>13</sup>C APT NMR** (125 MHz, CDCl<sub>3</sub>) δ 157.7 (+, C<sub>5</sub>), 146.5 (+, C<sub>9</sub>), 145.7 (+, C<sub>20</sub>), 143.0 (+, C<sub>14</sub>), 131.9 (-, C<sub>15</sub>), 131.2 (+, C<sub>25</sub>), 131.1 (-, C<sub>17</sub>), 131.0 (-, C<sub>6</sub>), 130.7 (+, C<sub>24</sub>), 130.3 (+, C<sub>23</sub>), 129.9 (-, C<sub>18</sub>), 129.48 (-, C<sub>7</sub>), 129.47 (+, C<sub>21</sub>), 129.0 (-, C<sub>11</sub>), 129.0 (+, C<sub>26</sub>), 128.6 (-, C<sub>12</sub>), 127.9 (-, C<sub>9</sub>), 127.56 (-, C<sub>8</sub> or C<sub>19</sub>), 127.55 (-, C<sub>8</sub> or C<sub>19</sub>), 126.3 (-, C<sub>10</sub>), 124.9 (+, C<sub>27</sub>), 123.3 (+, C<sub>13</sub>), 122.6 (+, C<sub>16</sub>), 33.2 (+, C<sub>1</sub>), 28.0 (+, C<sub>4</sub>), 23.1 (+, C<sub>2</sub>), 22.1 (+, C<sub>3</sub>); **COSY** (500 MHz, CHCl<sub>3</sub>): δ 9.10 ↔ δ 8.57, 8.54, 8.05, 3.64; δ 8.57 ↔ δ 7.90; δ 8.54 ↔ δ 7.70, 7.59; δ 8.05 ↔ δ 7.90, 7.61; δ 7.73 ↔ δ 7.49; δ 7.70 ↔ δ 7.61; δ 7.59 ↔ δ 7.37; δ 7.49 ↔ δ 7.37; δ 3.64 ↔ δ 2.88, 1.98-1.90, 1.86-1.80; δ 2.88 ↔ δ 1.98-1.90; δ 1.98-1.90 ↔ δ 1.86-1.80; **HMQC** (500 MHz, CHCl<sub>3</sub>): δ 9.10 ↔ δ 128.6; δ 8.57 ↔ δ 129.5; δ 8.54 ↔ δ 127.64 or 127.54; δ 8.05 ↔ δ 129.01; δ 7.90 ↔ δ 131.0; δ 7.73 ↔ δ 131.9; δ 7.70 ↔ δ 127.9; δ 7.61 ↔ δ 126.3; δ 7.59 ↔ δ 131.1; δ 7.49 ↔ δ 127.56 or 127.54; δ 7.37 ↔ δ 129.9; δ 3.64 ↔ δ 33.2; δ 2.88 ↔ δ 28.0; δ 1.98-1.90 ↔ δ 22.1; δ 1.86-1.80 ↔ δ 23.1; **HMBC** (500 MHz, CHCl<sub>3</sub>): δ 9.10 ↔ δ 130.7, 124.9; δ 8.57 ↔ δ

146.5, 129.0, 123.3;  $\delta$  8.54  $\leftrightarrow$   $\delta$  131.2, 126.3, 123.3;  $\delta$  8.05  $\leftrightarrow$   $\delta$  130.7, 127.9;  $\delta$  7.90;  $\leftrightarrow$   $\delta$  130.3, 124.9;  $\delta$  7.73  $\leftrightarrow$   $\delta$  157.7, 131.1, 122.6, 127.56 or 127.54;  $\delta$  7.70  $\leftrightarrow$   $\delta$  130.7;  $\delta$  7.61  $\leftrightarrow$   $\delta$  131.2, 127.56 or 127.54;  $\delta$  7.59  $\leftrightarrow$   $\delta$  131.9, 122.6;  $\delta$  7.49  $\leftrightarrow$   $\delta$  157.7, 131.9;  $\delta$  7.37  $\leftrightarrow$   $\delta$  143.0, 122.6;  $\delta$  3.64  $\leftrightarrow$   $\delta$  145.7, 129.47, 124.9, 23.1, 22.1;  $\delta$  2.88  $\leftrightarrow$   $\delta$  157.7, 145.7, 129.47, 23.1, 22.1;  $\delta$  1.98-1.90  $\leftrightarrow$   $\delta$  129.47, 33.2, 28.0, 23.1;  $\delta$  1.86-1.80  $\leftrightarrow$   $\delta$  145.7, 28.0; **UV VIS** ( $\lambda$  nm, abs): 291, 1.29; 309, 1.26; 264, 0.940; **ESI-MS**  $m/z$  calculated for:  $C_{27}H_{20}N^{79}Br^{81}Br$  (M+H)<sup>+</sup>, 518.0; Found:  $C_{27}H_{20}N^{79}Br^{81}Br$  (M+H)<sup>+</sup>, 518.0; **Elemental Analysis** calculated for  $C_{27}H_{19}NBr_2$ : C, 62.69 %; H, 3.70 %; N, 2.71 Found: C, 62.59 %; H, 3.73; N, 2.77.

#### 6.2.12 - 5-(16-Ethylphenyl)-1,2,3,4-tetrahydrobenzo[b]anthraquinoline (27)



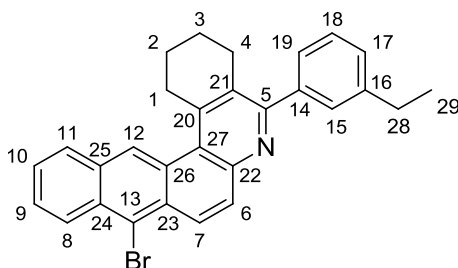
5-(3-bromophenyl)-1,2,3,4-tetrahydrobenzo[b]anthraquinoline (**12**) (4.97 g, 11.3 mmol) and  $NiCl_2(dppe)$  (0.307 g, 0.567 mmol) were added to a dry round bottom flask equipped with a magnetic Teflon stirrer. The RBF was fitted to a dry condenser and vacuum adapter and the system was then evacuated under vacuum and purged with argon three times. 10 mL of dry THF was added via syringe and the mixture was stirred until a solution formed. Upon cooling to 0 °C,  $EtMgBr$  (15.1 mL, 45.2 mmol) was added as a 3.0 M solution in  $Et_2O$  dropwise via syringe. The solution was warmed to room temperature and then heated to reflux for 18 h. THF and  $Et_2O$  solvents were removed via rotoevaporation and the crude solid was then dissolved in DCM. The

organic solution was washed with saturated NaHCO<sub>3</sub>, brine, dried over MgSO<sub>4</sub> and then filtered through a silica plug. Evaporation of the DCM afforded a dark yellow powder (4.49 g, 72 %), which was slightly impure.

Dark yellow solid; **IR** (cast film, cm<sup>-1</sup>): 3060 (w), 2937 (s), 2862 (w), 1549 (w), 1470 (w), 1318 (w), 1249 (w), 887 (m), 752 (s), 701 (w); **<sup>1</sup>H NMR** (500 MHz, CDCl<sub>3</sub>): δ 9.24 (s, 1H, H<sub>12</sub>), 8.42 (s, 1H, H<sub>13</sub>), 8.14 (m, 1H, H<sub>11</sub>), 8.08 (m, 1H, H<sub>8</sub>), 7.96-7.90 (ABq, *J* = 9.0 Hz, 2H, H<sub>7</sub> H<sub>6</sub> respectively), 7.64-7.58 (m, 2H, H<sub>9</sub> H<sub>10</sub>), 7.45 (app t, *J* = 7.5 Hz, 1H, H<sub>18</sub>), 7.43 (br d, *J* = 0.5 Hz, 1H, H<sub>15</sub>), 7.39 (app dt, *J* = 7.5 1.0 Hz, 1H, H<sub>19</sub>), 7.31 (app dt, *J* = 12.5 1.5 Hz, 1H, H<sub>17</sub>), 3.75 (t, *J* = 6.0 Hz, 1H, H<sub>1</sub>), 2.93 (t, *J* = 6.0 Hz, 1H, H<sub>26</sub>), 2.79 (q, *J* = 7.5 Hz, 2H, H<sub>28</sub>), 2.00-1.86 (m, 2H H<sub>3</sub> H<sub>2</sub>), 1.34 (t, *J* = 7.5 Hz, 3H, H<sub>29</sub>); **<sup>13</sup>C APT NMR** (125 MHz, CDCl<sub>3</sub>): 159.1 (+, C<sub>5</sub>), 147.1 (+, C<sub>22</sub>), 145.4 (+, C<sub>20</sub>), 144.3 (+, C<sub>16</sub>), 141.2 (+, C<sub>14</sub>), 131.8 (+, C<sub>23</sub>), 131.3 (+, C<sub>24</sub>), 131.4 (+, C<sub>25</sub>), 130.5 (-, C<sub>7</sub>), 129.4 (-, C<sub>6</sub>), 129.1 (+, C<sub>21</sub>), 128.8 (-, C<sub>11</sub>), 128.5 (+, C<sub>26</sub>), 128.40 (-, C<sub>12</sub> or C<sub>15</sub>), 128.36 (-, C<sub>12</sub> or C<sub>15</sub>), 128.3 (-, C<sub>18</sub>), 127.48 (-, C<sub>17</sub>), 127.44 (-, C<sub>8</sub>), 126.8 (-, C<sub>13</sub>), 126.3 (-, C<sub>9</sub>), 126.1 (-, C<sub>19</sub>), 125.8 (-, C<sub>10</sub>), 124.9 (+, C<sub>27</sub>), 33.3 (+, C<sub>1</sub>), 28.0 (+, C<sub>28</sub>), 28.4 (+, C<sub>4</sub>), 23.3 (+, C<sub>2</sub>), 22.3 (-, C<sub>3</sub>), 15.5 (-, C<sub>29</sub>); **COSY** (500 MHz, CHCl<sub>3</sub>): δ 9.24 ↔ δ 8.42, 7.96, 3.75; δ 8.42 ↔ δ 8.14, 7.96; δ 8.14 ↔ δ 7.64-7.58; δ 8.08 ↔ δ 7.64-7.58; δ 7.96 ↔ δ 7.90; δ 7.45 ↔ δ 7.39, 7.31; δ 7.43 ↔ δ 2.79, δ 3.75 ↔ δ 2.93, 2.00-1.86; δ 2.93 ↔ δ 2.00-1.86; δ 2.79 ↔ δ 1.34; **HMQC** (500 MHz, CHCl<sub>3</sub>): δ 9.24 ↔ δ 128.40 or 128.36; δ 8.42 ↔ δ 128.6; δ 8.14 ↔ δ 128.8; δ 8.08 ↔ δ 127.4; δ 7.96 ↔ δ 130.5; δ 7.90 ↔ δ 129.4; δ 7.64-7.58 ↔ δ 126.3, 125.8; δ 7.45 ↔ δ 128.3; δ 7.43 ↔ δ 128.4, 128.3; δ 7.39 ↔ δ 126.1; δ 7.30 ↔ δ 127.5; δ 3.75 ↔ δ 33.3; δ 2.93 ↔ δ 26.4; δ 2.79 ↔ δ 29.0; δ 2.00-1.86 ↔ δ 23.3, 22.3; δ 1.34 ↔ δ 15.5; **HMQC** (500 MHz, CHCl<sub>3</sub>): δ 9.24 ↔ δ 131.8, 131.3, 128.8, 124.9; δ 8.42 ↔ δ 131.1, 130.5, 128.5, 127.4; δ 8.14 ↔ δ 131.3, 126.3; δ 8.08 ↔ δ 131.4, 126.8, 125.8; δ 7.96 ↔ δ 147.1, 131.8, 128.5, 126.8; δ 7.90 ↔ δ 131.3, 127.4; δ 7.45 ↔ δ 144.3, 141.2; δ 7.43 ↔ δ

159.1, 127.5, 126.1;  $\delta$  7.39  $\leftrightarrow$   $\delta$  159.1, 128.4;  $\delta$  7.30  $\leftrightarrow$   $\delta$  126.1;  $\delta$  3.75  $\leftrightarrow$   $\delta$  145.4, 129.1, 124.9;  $\delta$  2.93  $\leftrightarrow$   $\delta$  145.4, 141.2, 129.1;  $\delta$  2.79  $\leftrightarrow$   $\delta$  144.3, 127.48 or 127.45; **UV VIS** ( $\lambda$  nm, abs): 285, 1.06; 307, 0.926, 262, 0.904; **ESI-MS**  $m/z$  calculated for:  $C_{29}H_{26}N$  (M+H)<sup>+</sup>, 388.2065; Found:  $C_{29}H_{26}N$  (M+H)<sup>+</sup>, 388.2061; **Elemental Analysis** calculated for  $C_{29}H_{25}N$ : C, 89.88 %; H, 6.50 %; N, 3.61; Found: C, 87.12 %; H, 6.77; N, 3.45.

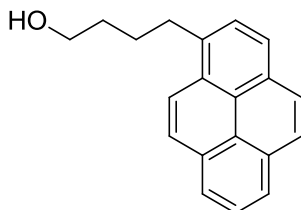
### 6.2.13 - 13-Bromo-5-(3-ethylphenyl)-1,2,3,4-tetrahydrobenzo[b]anthraquinoline (28)



Slightly impure 5-(16-ethylphenyl)-1,2,3,4-tetrahydrobenzo[b]anthraquinoline (**29**) (2.51 g, 6.5 mmol) was added to a round bottom flask equipped with a magnetic stir bar and fitted with a reflux condenser open to the atmosphere. DCM (20 mL) was added and the mixture was stirred until a solution formed. Bromine (0.67 mL, 12.9 mmol) was added slowly by syringe. The solution was stirred at room temperature for 4 h and then heated to reflux for 40 h. The mixture was then washed with aqueous NaOH until the precipitate dissolved. The organic layer was separated, washed with brine and dried with  $MgSO_4$ . Flash column chromatography (30:1, hexanes – ethyl acetate) afforded the title compound (2.11 g, 70 %) as an impure brown powder. Further purification attempts using flash column chromatography and recrystallization were unsuccessful.

Brown solid; **IR** (cast film,  $\text{cm}^{-1}$ ): 3055 (w), 3011 (w), 2963 (m), 2935 (m), 2868 (w), 1604 (w), 1551 (m), 1471 (w), 1318 (w), 1247 (w), 755 (s);  **$^1\text{H NMR}$**  (500 MHz,  $\text{CDCl}_3$ ):  $\delta$  9.06 (s, 1H,  $\text{H}_{12}$ ), 8.56 (d,  $J = 10.0$  Hz, 1H,  $\text{H}_7$ ), 8.52 (dd,  $J = 9.0$  0.5 Hz,  $\text{H}_{11}$ ), 8.04 (d,  $J = 9.5$  Hz, 1H,  $\text{H}_8$ ), 8.03 (d,  $J = 8.0$ , 1H,  $\text{H}_6$ ), 7.69 (app td,  $J = 6.7$  1.3 Hz, 1H,  $\text{H}_9$ ), 7.59 (app td,  $J = 6.8$  1.0 Hz, 1H,  $\text{H}_{10}$ ), 7.46 (t,  $J = 7.5$  Hz,  $\text{H}_{18}$ ), 7.45 (d,  $J = 0.5$  1H,  $\text{H}_{15}$ ), 7.40 (app dt,  $J = 7.7$  1.4 Hz, 1H,  $\text{H}_{19}$ ), 7.33 (app dt,  $J = 7.5$  1.4 Hz, 1H,  $\text{H}_{17}$ ), 3.63 (t,  $J = 6.1$  Hz, 1H,  $\text{H}_1$ ), 2.93 (t,  $J = 6.6$  Hz, 1H,  $\text{H}_4$ ), 2.79 (q,  $J = 7.5$  Hz, 1H,  $\text{H}_{28}$ ), 1.98-1.92 (m, 2H,  $\text{H}_3$ ), 1.88-1.81 (m, 2H,  $\text{H}_2$ ), 1.36 (t,  $J = 7.5$  Hz, 1H,  $\text{H}_{29}$ );  **$^{13}\text{C APT NMR}$**  (125 MHz,  $\text{CDCl}_3$ ): 159.1 (+,  $\text{C}_5$ ), 146.1 (+,  $\text{C}_{22}$ ), 146.0 (+,  $\text{C}_{16}$  or  $\text{C}_{14}$ ), 144.4 (+,  $\text{C}_{21}$ ), 141.2 (+,  $\text{C}_{16}$  or  $\text{C}_{14}$ ), 131.1 (+,  $\text{C}_{25}$ ), 130.7 (-,  $\text{C}_6$ ), 130.5 (+,  $\text{C}_{24}$ ), 130.2 (+,  $\text{C}_{26}$ ), 129.9 (+,  $\text{C}_{20}$ ), 129.4 (-,  $\text{C}_7$ ), 129.08 (-,  $\text{C}_{11}$ ), 129.0 (+,  $\text{C}_{23}$ ), 128.5 (-,  $\text{C}_{12}$ ), 128.4 (-,  $\text{C}_{19}$  or  $\text{C}_{15}$ ), 128.3 (-,  $\text{C}_{19}$  or  $\text{C}_{15}$ ), 127.9 (-,  $\text{C}_9$ ), 127.7 (-,  $\text{C}_{18}$ ), 127.5 (-,  $\text{C}_8$ ), 126.3 (-,  $\text{C}_{10}$ ), 126.2 (-,  $\text{C}_{18}$ ), 124.6 (+,  $\text{C}_{27}$ ), 123.3 (+,  $\text{C}_{13}$ ), 33.3 (+,  $\text{C}_1$ ), 28.9 (+,  $\text{C}_4$ ), 28.1 (+,  $\text{C}_{28}$ ), 23.1 (+,  $\text{C}_2$ ), 22.1 (+,  $\text{C}_3$ ), 15.5 (-,  $\text{C}_{29}$ ); **COSY** (500 MHz,  $\text{CHCl}_3$ ):  $\delta$  8.56  $\leftrightarrow$   $\delta$  8.03;  $\delta$  8.52  $\leftrightarrow$   $\delta$  7.69;  $\delta$  8.04  $\leftrightarrow$   $\delta$  7.59;  $\delta$  7.69  $\leftrightarrow$   $\delta$  7.59;  $\delta$  3.63  $\leftrightarrow$   $\delta$  1.88-1.81;  $\delta$  2.93  $\leftrightarrow$   $\delta$  1.98-1.92  $\delta$  2.79  $\leftrightarrow$   $\delta$  1.36; **HSQC** (500 MHz,  $\text{CHCl}_3$ ):  $\delta$  9.06  $\leftrightarrow$   $\delta$  128.5;  $\delta$  8.56  $\leftrightarrow$   $\delta$  129.4;  $\delta$  8.52  $\leftrightarrow$   $\delta$  127.5;  $\delta$  8.04  $\leftrightarrow$   $\delta$  129.0;  $\delta$  7.69  $\leftrightarrow$   $\delta$  127.9;  $\delta$  7.59  $\leftrightarrow$   $\delta$  126.3;  $\delta$  7.46, 7.45  $\leftrightarrow$   $\delta$  128.38, 128.35;  $\delta$  7.40  $\leftrightarrow$   $\delta$  126.2;  $\delta$  7.33  $\leftrightarrow$   $\delta$  127.7;  $\delta$  3.63  $\leftrightarrow$   $\delta$  33.3;  $\delta$  2.93  $\leftrightarrow$   $\delta$  28.9;  $\delta$  2.79  $\leftrightarrow$   $\delta$  28.1;  $\delta$  1.98-1.92  $\leftrightarrow$   $\delta$  22.1;  $\delta$  1.88-1.81  $\leftrightarrow$   $\delta$  23.1;  $\delta$  1.36  $\leftrightarrow$   $\delta$  15.5; **HMBC** (500 MHz,  $\text{CHCl}_3$ ):  $\delta$  9.06  $\leftrightarrow$   $\delta$  131.1, 129.9, 129.0;  $\delta$  8.56  $\leftrightarrow$   $\delta$  146.1, 128.98, 123.3;  $\delta$  8.52  $\leftrightarrow$   $\delta$  131.1, 128.98, 126.3, 123.3;  $\delta$  8.04  $\leftrightarrow$   $\delta$  130.5;  $\delta$  7.69  $\leftrightarrow$   $\delta$  130.5;  $\delta$  7.59  $\leftrightarrow$   $\delta$  127.5;  $\delta$  7.46  $\leftrightarrow$   $\delta$  144.4, 141.2;  $\delta$  7.45  $\leftrightarrow$  159.1, 127.5, 126.2;  $\delta$  7.40  $\leftrightarrow$   $\delta$  159.1, 127.7;  $\delta$  7.33  $\leftrightarrow$   $\delta$  128.4;  $\delta$  3.63  $\leftrightarrow$   $\delta$  146.1, 129.9, 124.6;  $\delta$  2.93  $\leftrightarrow$   $\delta$  146.0;  $\delta$  1.98-1.92  $\leftrightarrow$   $\delta$  159.1, 129.9, 33.3;  $\delta$  1.36  $\leftrightarrow$   $\delta$  144.4, 28.9; **UV VIS** ( $\lambda$  nm, abs): 289, 0.613; 309, 0.555; 264, 0.541; **ESI-MS**  $m/z$  calculated for:  $\text{C}_{29}\text{H}_{25}\text{NBr}$  ( $\text{M}+\text{H}$ ) $^+$ , 466.1170; Found:  $\text{C}_{29}\text{H}_{25}\text{NBr}$  ( $\text{M}+\text{H}$ ) $^+$ , 466.1165; **Elemental Analysis** calculated for  $\text{C}_{29}\text{H}_{24}\text{BrN}$ : C, 74.68 %; H, 5.19 %; N, 3.00; Found: C, 68.28 %; H, 5.40; N, 2.76.

### 6.2.14 - 1-Pyrenebutanol (34)



A dry round bottom flask equipped with a magnetic stir bar and vacuum adapter was evacuated and purged with argon three times. The flask was charged with THF (20 mL) and then LiAlH<sub>4</sub> (0.176 g, 4.63 mmol). Commercial 1-pyrenebutanoic acid (12 mL, 3.1 mmol) was added dropwise by syringe as a 0.15 M solution in THF over 20 min at room temperature. The mixture was stirred for an additional 20 min and then cooled in an ice bath. 2 mL of 10% KOH was then added dropwise over 10 min. The mixture was stirred for 80 min at room temperature. The mixture was vacuum filtered and rinsed with Et<sub>2</sub>O. The filtrate was washed with 10 mL pH 7 aqueous phosphate buffer<sup>69</sup> and the aqueous layer extracted with Et<sub>2</sub>O, which was then dried over anhydrous sodium sulfate and filtered. Concentration under vacuum gave the crude title compound (0.74 g, 87 %) as an impure brown oil, which was used without further purification.

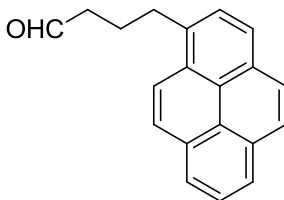
Brown oil; **IR** (cast film, cm<sup>-1</sup>): 3341 (br, m), 3040 (m), 2934 (s), 2862 (m), 1603 (w), 1182 (w), 1060 (m), 843 (s), 756 (m); **<sup>1</sup>H NMR** (500 MHz, CDCl<sub>3</sub>): δ 8.30 (d, *J* = 9.4 Hz, 1H), 8.20 (dd, *J* = 3.7 0.9 Hz, 1H), 8.18 (br d, *J* = 2.8 Hz, 1H), 8.14, (d, *J* = 2.7 Hz, 1H), 8.12 (d, *J* = 4.13, 1H), 8.05 8.04 (ABq, *J* = 8.8 Hz, 2H), 8.02 (app t, *J* = 7.6 Hz, 1H), 7.89 (d, *J* = 7.8 Hz, 1H), 3.72 (t, *J* = 6.5 Hz, 1H), 3.39 (t, *J* = 7.7 Hz, 1H), 1.96 (tt, *J* = 9.0 9.0 Hz, 2H), 1.76 (tt, *J* = 8.8 6.5 Hz, 2H); **<sup>13</sup>C APT NMR** (125 MHz, CDCl<sub>3</sub>): δ 136.7 (+), 131.5 (+), 131.0 (+), 129.9 (+), 128.7 (+), 127.6 (-) 127.3 (-, 2C), 126.6 (-), 125.9 (-), 125.14 (+), 125.11 (+), 124.92 (-), 124.85(-), 124.8 (-), 133.4 (-), 62.7 (+), 33.2 (+), 32.7



(+), 28.0 (+); **EI-MS**  $m/z$  calculated for:  $C_{20}H_{18}O$  ( $M^+$ ), 272.1201; Found:  $C_{20}H_{18}O$  ( $M^+$ ), 272.1201;

**Elemental Analysis** calculated for  $C_{20}H_{18}O$ : C, 87.56 %; H, 6.61 %; Found: C, 80.50 %; H, 6.25.

### 6.2.15 - 1-Pyrenebutanal (**32**)

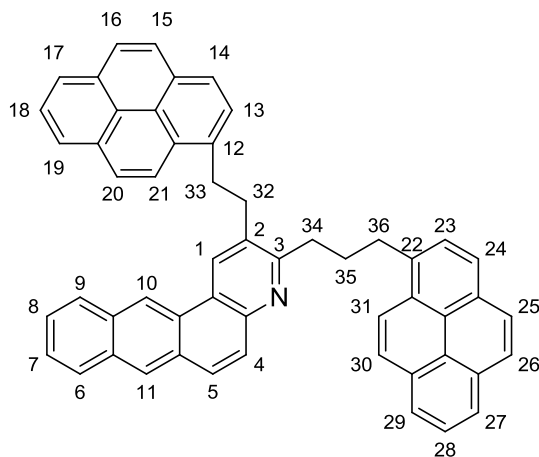


A three-neck flask equipped with a magnetic stir bar, low-temperature thermometer, glass stopper, and a vacuum adapter. The flask was charged with 1 mL of DCM followed by 0.105 mL of oxalyl chloride (1.2 mmol). The reaction flask was then cooled to  $-78\text{ }^{\circ}\text{C}$  and 0.174 mL of DMSO (2.4 mmol) was added dropwise by syringe over 25 min. The flask was then warmed to  $-60\text{ }^{\circ}\text{C}$  over 20 min. 1-Pyrenebutanol (**36**) (0.224 g, 0.82 mmol) was then added as a solution in DCM (1 mL) dropwise by syringe over 50 min. The reaction flask was then warmed to  $-45\text{ }^{\circ}\text{C}$  over 30 min and then charged with 0.825 mL of *N,N*-diisopropylethylamine (4.7 mmol) dropwise by syringe. The solution was warmed to  $0\text{ }^{\circ}\text{C}$ , transferred to a separatory funnel containing 10 mL of 1 M ice-cooled HCl, and then extracted with DCM. The organic phase washed with pH 7 aqueous phosphate buffer, dried with anhydrous sodium sulfate and filtered. The solvent was removed under vacuum to afford the title compound (0.201 g, 90 %) as a crude brown oil, which was not further purified.

Brown oil; **IR** (cast film,  $\text{cm}^{-1}$ ): 3040 (w), 2939 (w), 2874 (w), 2822 (w), 2721 (w), 1720 (s), 1602 (w), 1102 (w) 1071 (w), 845 (s);  **$^1\text{H NMR}$**  (500 MHz,  $\text{CDCl}_3$ ):  $\delta$  9.80 (d,  $J = 1.4\text{ Hz}$ , 1H), 8.29

(d,  $J = 9.1$  Hz, 1H, H<sub>12</sub>), 8.21 (br d,  $J = 3.4$  Hz, 1H, H<sub>11</sub> or H<sub>9</sub>), 8.19 (br d,  $J = 3.4$  Hz, 1H, H<sub>11</sub> or H<sub>9</sub>), 8.14, (d,  $J = 9.1$  Hz, 1H, H<sub>13</sub>), 8.13 (d,  $J = 8.0$ , 1H, H<sub>5</sub>), 8.06 (app s, 2H, H<sub>13</sub>, H<sub>12</sub>), 8.03 (app t,  $J = 8.0$  Hz, 1H, H<sub>10</sub>), 7.84 (br d,  $J = 8.0$  Hz, 1H, H<sub>6</sub>), 3.37 (td,  $J = 6.7$  1.3 Hz, 2H), 2.55 (td,  $J = 7.1$  1.5 Hz, 1H), 2.2 (tt,  $J = 7.4$  7.4 Hz, 2H); <sup>13</sup>C APT NMR (125 MHz, CDCl<sub>3</sub>): δ 202.2 (-), 135.5 (+), 131.5 (+), 130.9 (+), 130.1 (+), 128.8 (+), 127.5 (-, 2C), 127.3 (-), 126.8 (-), 125.9 (-), 125.1 (+), 125.0 (-), 124.9 (-, 2C), 123.2 (-), 43.3 (+), 32.6 (+), 24.0 (+); EI-MS  $m/z$  calculated for: C<sub>20</sub>H<sub>16</sub>O (M<sup>+</sup>), 274.1358; Found: C<sub>20</sub>H<sub>16</sub>O (M<sup>+</sup>), 274.1358; Elemental Analysis calculated for C<sub>20</sub>H<sub>16</sub>N: C, 88.20 %; H, 5.92 %; Found: C, 86.69 %; H, 6.67.

#### 6.2.16 - 2-(1-Ethylpyrene)-3-(1-propylpyrene)-benzo[*b*]anthraquinoline (30):



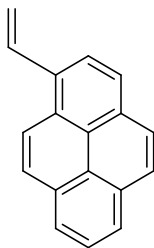
2-Aminoanthracene (**10**) (33.8 mg, 0.17 mmol) was added to a dry round bottom flask equipped with a Teflon stirrer, fitted with a condenser, and connected to argon. After evacuating and purging the system three times, 1-pyrenebutanal (**32**) (47.6 mg, 0.17 mmol) was added as a solution in 2 mL of dry THF by syringe. The mixture was stirred at room temperature

and 1.75 mL of a 0.010 M solution of iodine in THF was added by syringed. 5.0 mL of a 2.22 M solution of water in THF was then added by syringe, forming a yellow precipitate. 0.0181 mL of cyclohexanone (0.17 mmol) was added by syringe and the mixture was heated to reflux for 24 h. Afterwards, the system was opened to the atmosphere and allowed to reflux for an additional 24 h. 10% aqueous KOH (20 mL) was added and the mixture was shaken in a separatory funnel until a solution formed. The organic layer was extracted, washed with water, dried with MgSO<sub>4</sub>, filtered and the solvent evaporated until reduced pressure to afford the crude title compound (0.0278 g, 45 %) as a light beige powder.

Beige solid; **IR** (cast film, cm<sup>-1</sup>): 3043 (m), 2933 (m), 2860(w), 1624 (m), 1602 (m), 1264 (m), 845 (s), 737 (s); **<sup>1</sup>H NMR** (600 MHz, CDCl<sub>3</sub>): δ 8.74 (br s, 1H), 8.59 (br s, 1H), 8.38 (s, 1H, H<sub>1</sub>), 8.32 (d, *J* = 9.0 Hz), 8.26 (br d, *J* = 9.0 Hz, 1H), 8.18 (d, *J* = 7.8 Hz, 1H), 8.15 (d, *J* = 7.8 Hz, 1H), 8.12 (d, *J* = 7.2 Hz, 1H), 8.08 (d, *J* = 7.8 Hz, 1H), 8.06 (d, *J* = 9.6 Hz, 1H), 8.05 (dd, *J* = 7.2 2.4Hz, 1H), 8.03-8.01 (m, ?H), 8.01 (app t, *J* = 7.2 Hz, 1H), 8.00 (d, *J* = 9.6 Hz, 1H), 7.99 (d, *J* = 9.0 Hz, 1H), 7.97 (app s, 3H), 7.96 (d, *J* = 8.4 Hz, 1H), 7.95 (app t, *J* = 7.2 Hz, 1H), 7.94-7.90 (br s, ?H), 7.85 (d, *J* = 7.8 Hz, 1H), 7.84 (d, *J* = 6.6 Hz, 1H), 7.58-7.53 (m, 2H), 7.51 (br d, *J* = 7.8 Hz), 3.68 (t, *J* = 8.4 Hz, 1H), 3.49 (t, *J* = 7.2 Hz, 1H), 3.31 (t, *J* = 8.4 Hz, 1H), 3.21 (t, *J* = 7.0 Hz, 1H), 2.47 (app p, *J* = 7.8 Hz, 1H); **<sup>13</sup>C APT NMR** (125 MHz, CDCl<sub>3</sub>): 136.5 (+, 2C), 134.95 (+), 134.93 (+), 133.1(+), 132.0 (+), 131.9 (+), 131.5 (+), 131.4 (+), 130.9 (+), 130.9 (+), 130.1 (+), 129.9 (+), 129.8 (+), 128.8 (+), 128.6 (+), 128.3 (-), 127.9 (-), 127.7 (-), 127.5 (-), 127.5 (-), 127.4 (-), 127.3 (-), 127.2 (-), 127.1 (-, 2C), 126.9 (-), 126.5 (-), 126.0 (-), 125.9 (-), 125.7 (-), 125.1 (-), 125.1 (+), 125.03 (+), 125.02 (+), 124.9 (-), 124.8 (-), 124.8 (-, 2C), 124.7 (-), 124.1 (+), 123.6 (-), 122.8 (-), 121.4 (-), 34.7 (+), 34.4 (+), 33.4 (+, 2C), 31.3 (+); **COSY** (500 MHz, CHCl<sub>3</sub>): δ 8.32 ↔ δ 8.01; δ 8.26 ↔ δ 8.05; δ 8.18 ↔ δ 8.01; δ 8.15 ↔ δ 8.01; δ 8.12 ↔ δ 7.95; δ 8.08 ↔ δ 7.95; δ 8.05 ↔ δ 7.56; δ 8.03 ↔ δ 7.85; δ

7.92 ↔ δ 7.56; δ 7.84 ↔ δ 7.56, 7.51; δ 3.67 ↔ δ 3.32; δ 3.49 ↔ δ 3.21, 2.46; **HSQC** (500 MHz, CHCl<sub>3</sub>): δ 8.74 ↔ δ 121.4; δ 8.38 ↔ δ 127.1; δ 8.32 ↔ δ 123.6; δ 8.26 ↔ δ 122.8; δ 8.18 ↔ δ 125.1; δ 8.15, 8.12 ↔ δ 124.9, 124.8; δ 8.08 ↔ δ 124.7; δ 8.06, 8.05 ↔ δ 127.9, 127.7; δ 8.00 ↔ δ 127.2; δ 7.95 ↔ δ 127.5; δ 7.92 ↔ δ 128.3; δ 3.68 ↔ δ 34.4; δ 3.49 ↔ δ 33.4; δ 3.31 ↔ δ 34.4; δ 3.21 ↔ δ 34.7; δ 2.47 ↔ δ 31.3; **HMBC** (500 MHz, CHCl<sub>3</sub>): δ 3.68 ↔ δ 134.9, 130.1, 127.2, 34.4; δ 3.49 ↔ δ 136.5, 130.9 or 130.8, 127.4 or 127.3 or 127.2, 31.3; δ 3.31 ↔ δ 133.1, 34.7; δ 2.47 ↔ δ 136.5, 33.4; **TROSEY** (600 MHz, CDCl<sub>3</sub>) 8.59 ↔ 3.68, 3.31; 8.38 ↔ 8.05, 8.00, 7.92; 8.32 ↔ 7.99, 3.49, 2.47; 8.26 ↔ 8.06, 3.68, 3.31; 8.18 ↔ 8.01; 8.23 ↔ 7.94; 8.09 ↔ 7.99, 7.94; 8.05 ↔ 7.56; 8.02 ↔ 7.84; 7.96 ↔ 7.84; 7.92 ↔ 7.55; 7.84 ↔ 7.52, 3.49, 2.47; 7.56 ↔ 3.68, 3.31; 3.68 ↔ δ 3.31, 3.21, 2.47; 3.49 ↔ 3.21; 3.21 ↔ 2.47; **ESI-MS** *m/z* calculated for: C<sub>54</sub>H<sub>38</sub>N (M+H)<sup>+</sup>, 700.3004; Found: C<sub>54</sub>H<sub>38</sub>N (M+H)<sup>+</sup>, 700.2986. No EA was performed.

### 6.2.17 - 1-Vinylpyrene (36):

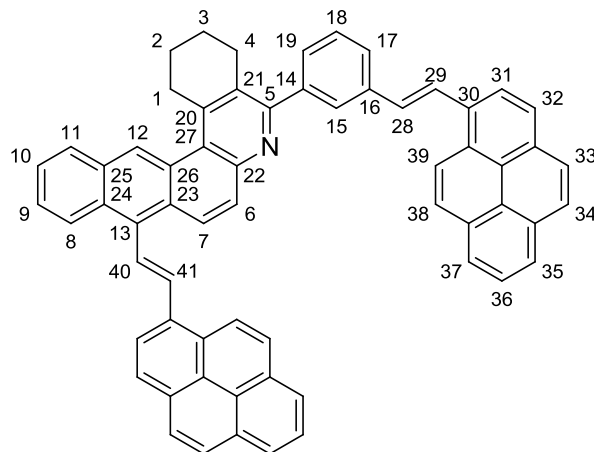


A modified literature procedure from Silversmith et al.<sup>70</sup> was followed. 1-Formylpyrene (0.58 g, 2.5 mmol) and MePh<sub>3</sub>PBr (5.0 g, 25mmol) was added to a round bottom flask equipped with a large magnetic stir bar, followed by 5 mL of DCM and 20 mL of 50% NaOH. The mixture was connected to a condenser and stirred vigorously, open to the atmosphere, at room temperature overnight. The mixture was then heated to reflux for 24 hours. The reaction was

monitored by TLC and stopped when the conversion was complete. The solution was extracted with DCM and then evaporated under pressure to give a brown gel. The gel was transferred to a silica plug via pipette first by heating to liquefy. The remaining gel was transferred by adding a minimal amount of DCM. Washing the plug with hexanes followed by rotoevaporation gave the title compound as a light yellow powder (0.40 g, 70%). Following the elution of 1-vinylpyrene, the starting material, 1-formylpyrene, was flushed from the silica plug and can be re-subjected to the reaction conditions to obtain a total yield of 93%. 1-Vinylpyrene was stored in cool place away from light to prevent polymerization.

Nearly pure yellow powder; **IR** (cast film,  $\text{cm}^{-1}$ ): 3040 (w), 3021 (w), 2857 (w), 2718 (w), 1679 (s), 1596 (m), 1508 (m), 1227 (m), 1202 (m), 848 (s), 755 (s), 712 (m);  **$^1\text{H NMR}$**  (500 MHz,  $\text{CDCl}_3$ ):  $\delta$  8.38 (d,  $J = 9.2$  Hz, 1H), 8.20 (app ddd,  $J = 8.1$  8.0 7.9 7.7 Hz, 4H), 9.24 (d,  $J = 9.2$  Hz, 1H), 8.20 (app s, 2H), 8.00 (app t,  $J = 7.6$  Hz, 1H), 7.79 (dd,  $J = 17.3$  11.0, 1H), 6.06 (dd,  $J = 17.5$  1.0 Hz, 1H), 5.66 (dd,  $J = 11.0$  1.0 Hz, 1H);  **$^{13}\text{C APT NMR}$**  (125 MHz,  $\text{CDCl}_3$ ):  $\delta$  134.2 (+), 132.4 (-), 131.5 (-), 131.0 (-), 130.9 (-), 128.1 (-), 127.6 (+), 127.4 (+), 127.4 (+), 127.3 (+), 125.9 (+), 125.2, 125.02 (+), 125.01 (+), 124.97 (+), 124.95 (-), 123.7 (+), 123.1 (+); **EI-MS**  $m/z$  calculated for:  $\text{C}_{18}\text{H}_{12}$  ( $\text{M}^+$ ), 228.0939; Found:  $\text{C}_{18}\text{H}_{12}\text{O}$  ( $\text{M}^+$ ), 228.0939; **Elemental Analysis** calculated for  $\text{C}_{29}\text{H}_{26}\text{N}$ : C, 94.70 %; H, 5.30 %; Found: C, 93.67 %; H, 5.31.

#### **6.2.18 - 13-(1-Vinylpyrene)-5-(3-(1-vinylpyrene)phenyl)-1,2,3,4-tetrahydrobenzo[b]anthraquinoline (31)**



In a glove box, dibromo compound **26** (61.4 mg, 0.12 mmol), Pd(OAc)<sub>2</sub> (5.4 mg, 0.024 mmol), (o-tolyl)<sub>3</sub>P (14.6 mg, 0.048 mmol), and 1-vinylpyrene (**36**) (0.148 g, 0.649 mmol) were added to a glass reaction vessel equipped with a magnetic stir bar, side arm and Teflon screw cap. The reaction vessel was then connected to a Schlenk flask under argon in a fume hood and triethylamine (0.083 mL, 0.60 mmol) and 1 mL of dry DMF was added by syringe. The reaction vessel was then sealed and heated at 120°C for 3 h while stirring. Afterwards, the contents were added to a separatory funnel via glass pipette. The reaction vessel was rinsed with toluene, the contents of which were added to the separatory funnel. 5 mL of toluene was added to the separatory funnel and the organic layer was washed with 50 mL of water three times. Evaporation of the solvent followed by flash column chromatography (toluene) gave the title compound (83.5 mg, 86 %), which was obtained as a brown powder, clean by <sup>1</sup>H NMR accompanied by trace residual solvents.

Light brown solid; IR (cast film, cm<sup>-1</sup>): 3044 (w), 2935 (737 (w), 714 (w); <sup>1</sup>H NMR (500 MHz, CDCl<sub>3</sub>): δ 9.20(s, 1H, H<sub>12</sub>), 8.66 (d, *J* = 8.0 Hz, 1H), 8.60 (d, *H* = 9.5 Hz, H<sub>11</sub>), 8.58 (m, 1H), 8.51 (d, *J* = 9.0 Hz, 1H), 8.44 (d, *J* = 8.5 Hz, 1H), 8.55-8.10 (m, 2H), 8.28 (d, *J* = 16.0 Hz, H<sub>29</sub>), 8.24-7.93 (m, ?H), 7.78 (d, *J* = 7.4 Hz, 1H, H<sub>17</sub>), 7.69-7.67 (m, 2H), 7.61 (t, *J* = 7.5 Hz, 1H, H<sub>18</sub>), 7.58 (d, *J*

= 7.5 Hz, 1H, H<sub>19</sub>), 7.46 (d, *J* = 16.0 Hz, 1H, H<sub>28</sub>), 3.81 (t, *J* = 1.5 Hz, 1H, H<sub>1</sub>), 3.04 (t, *J* = 6.5 Hz, 1H, H<sub>4</sub>), 2.08-2.00 (m, 2H, H<sub>3</sub>), 1.98-1.89 (m, 1H, H<sub>2</sub>); **<sup>13</sup>C APT NMR** (500 MHz, CDCl<sub>3</sub>): δ 158.9 (+, C<sub>5</sub>), 146.9 (+, C<sub>2</sub>), 145.7 (+, C<sub>21</sub>), 141.9 (+), 138.1 (+, C<sub>16</sub>), 135.5 (-, C<sub>31</sub>), 133.7 (+), 131.9 (+), 131.8 (-), 131.7 (+), 131.5 (+, 2C), 131.3 (+), 130.98 (+), 130.96 (+), 130.92 (+), 130.8 (+), 130.1 (+), 129.6 (+), 129.3 (-), 129.2 (-), 128.9 (-), 128.9 (-), 128.6 (+), 128.5 (+, 2C), 128.5 (-), 128.41 (-, 2C), 128.35 (-), 128.32 (-), 128.2 (-), 127.9 (-), 126.61 (-), 127.57 (-), 127.52 (-), 127.48 (-), 127.42 (-), 127.3 (-), 127.1 (-), 126.6 (-), 126.52 (-), 126.47 (-), 126.18 (-), 126.1 (-), 126.0 (-), 125.9 (-), 125.8 (-), 125.4 (-), 125.33 (+), 125.28 (-, 2C), 125.19 (-), 125.16 (-), 125.09 (+), 125.05 (-), 124.98 (+), 123.8 (-), 123.7(-), 123.1 (-), 123.0 (-), 33.3 (+), 28.2 (+), 23.3 (+), 22.3 (+); **COSY** (500 MHz, CHCl<sub>3</sub>): δ 9.20 ↔ δ 9.60, 8.22, 8.19; δ 8.66 ↔ δ 8.32; δ 8.60 ↔ δ 7.97; δ 8.58 ↔ δ 8.21, 7.69-7.67; δ 8.51 ↔ δ 8.13; δ 8.44 ↔ δ 8.11; δ 8.37 ↔ δ 8.20; δ 8.28 ↔ δ 7.46; δ 7.95 ↔ δ 7.79, 7.58, 7.61; δ 7.61 ↔ δ 7.79, 7.58; δ 7.69-7.67 ↔ δ 8.21; δ 3.81 ↔ δ 3.04, 1.98-1.89; δ 3.04 ↔ δ 2.08-2.00; **HMBC** (500 MHz, CDCl<sub>3</sub>): δ 9.20 ↔ δ 129.6; δ 8.66 ↔ δ 135.5; δ 8.28 ↔ δ 138.1, 135.5; δ 7.98 ↔ δ 135.5; δ 7.78 ↔ δ 158.9; δ 7.69-7.67 ↔ δ 138.1; δ 7.61 ↔ δ 141.9, 138.1; δ 7.58 ↔ δ 158.9; **HSQC** (500 MHz, CHCl<sub>3</sub>): δ 8.66 ↔ δ 123.8; δ 8.51 ↔ δ 123.1; δ 8.44 ↔ δ 123.0; δ 8.28 ↔ δ 123.7; δ 7.69-7.67 ↔ δ 128.9; δ 7.61 ↔ δ 128.41, δ 3.81 ↔ δ 33.2; δ 3.04 ↔ δ 28.2; δ 3.04 ↔ δ 2.08-2.00; δ 2.08-2.00 ↔ δ 22.4; δ 1.98-1.89 ↔ δ 23.3; **UV VIS** (λ nm, abs): 236, 0.917; 280, 0.668; 375, 0.519; 486, 0.011; 656, 0.0073; 808, 0.0053; **ESI-MS** *m/z* calculated for: C<sub>29</sub>H<sub>42</sub>N (M+H)<sup>+</sup>, 812.3317; Found: C<sub>63</sub>H<sub>42</sub>N (M+H)<sup>+</sup>, 812.3312.

### 6.3 - References for Experimentals

65. Yamato, T.; Fujimoto, M.; Nagano, Y.; Miyazawa, A.; Tashiro, M. Electrophilic Substitution of t-tert-Butyl-1-Substituted Pyrenes. A New Route for the Preparation of 1,2-Disubstituted Pyrenes. *Org. Prep. Proced. Int.* **1997**, *29*, 321-330.
66. Koelsch, F. C.. 6-Bromo-2-naphthol. *Org. Synth.* **1955**, *3*, 132.

- 
67. Rasowsky, A.; Battaglia, J.; Chen, K. K. N.; Papathanasopoulos, N.; Modest, E. J. Synthesis of Some Heteronuclear Mono- and Di-Chloro-2-Naphthylamines. *J. Chem. Soc. C* **1969**, *10*, 1376-1378.
68. Zhang, C. Z.; Yang, H.; Wu, D.L.; Lu, G.Y. A Convenient and Environmentally Benign Method of Reducing Aryl Ketones or Aldehydes by Zinc Powder in an Aqueous Alkaline Solution. *Chin. J. Chem.* **2007**, *25*, 653-660.
69. Dondoni, A.; Perrone, D. Synthesis of 1,1-Dimethylethyl (S)-4-Formyl-2,2-Dimethyl-3-Oxazolidine Carboxylate by Oxidation of the Alcohol. *Org. Synth* **2000**, *77*, 64-71.
70. Silversmith, E. D. A Wittig Reaction that gives only One Stereoisomer. *J. Chem. Ed.* **1986**, *63*, 645-646.



## Appendix

### 1 – Selected spectra for 6-bromo-2-naphthol (20)

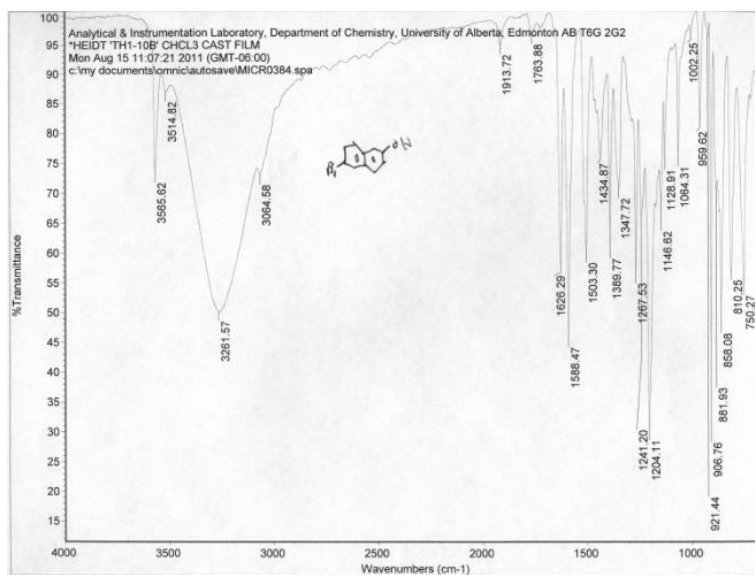
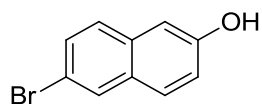


Figure A1 – IR (cast film, cm<sup>-1</sup>) of 6-bromo-2-naphthol **20**

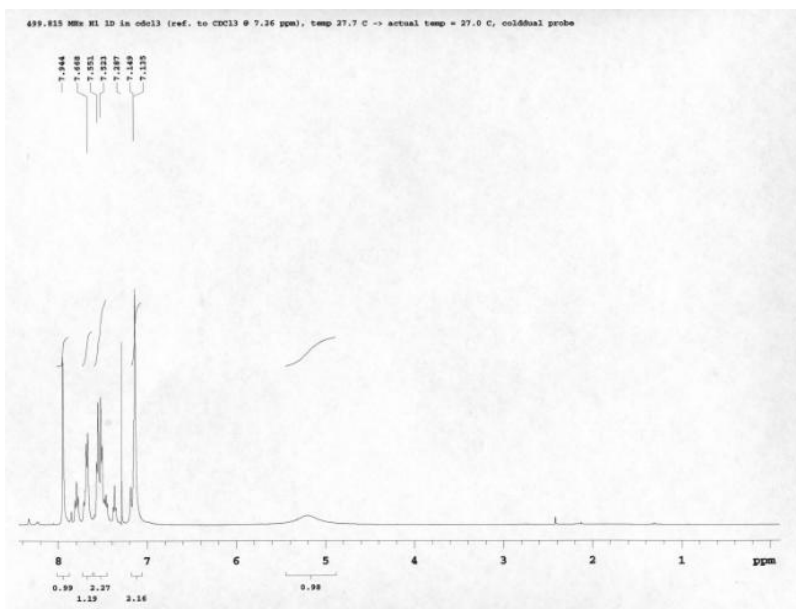


Figure A2 - <sup>1</sup>H NMR (500 MHz, CDCl<sub>3</sub>) of 6-bromo-2-naphthol **20**

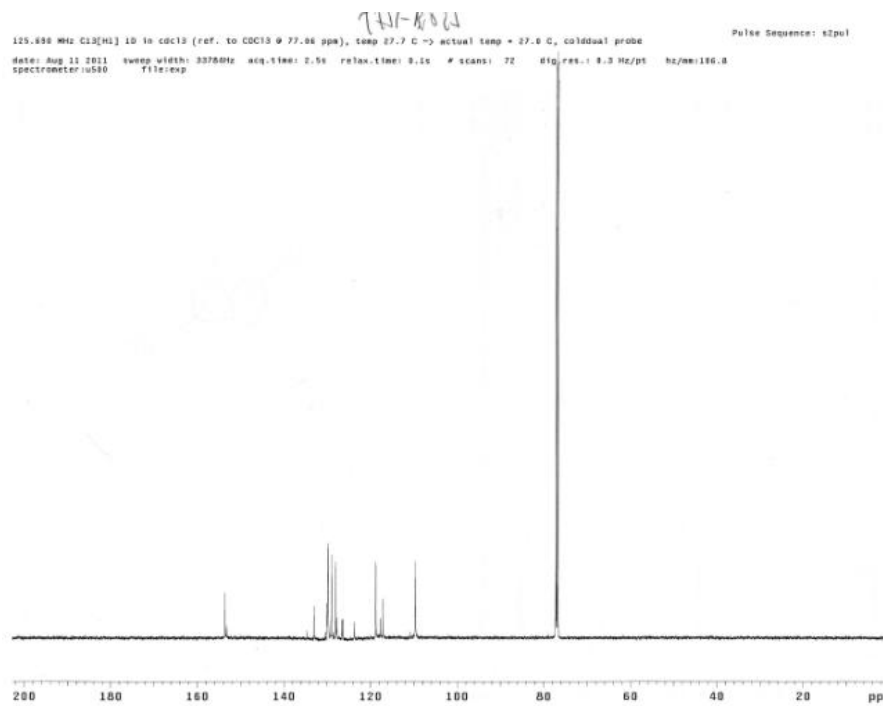


Figure A3 - <sup>13</sup>C NMR (500 MHz, CDCl<sub>3</sub>) of 6-bromo-2-naphthol **20**

2 – Selected spectra for 2-aminonaphthalene (1)

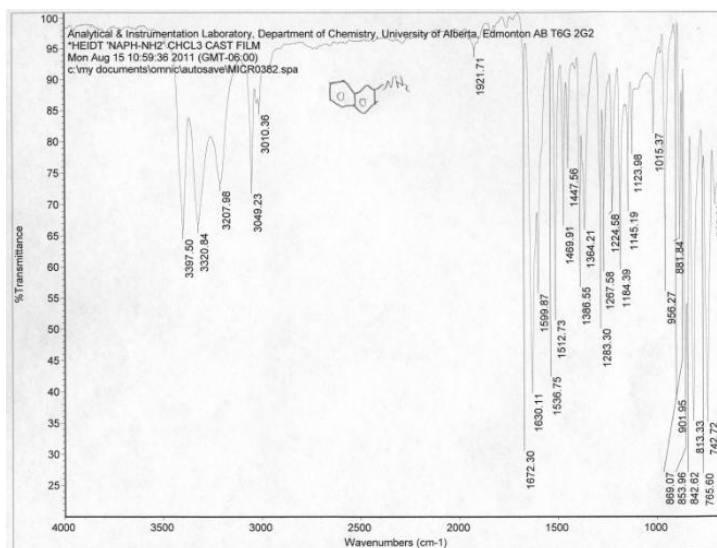
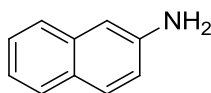


Figure A4 - IR (cast film, cm-1) of 2-aminonaphthalene 1

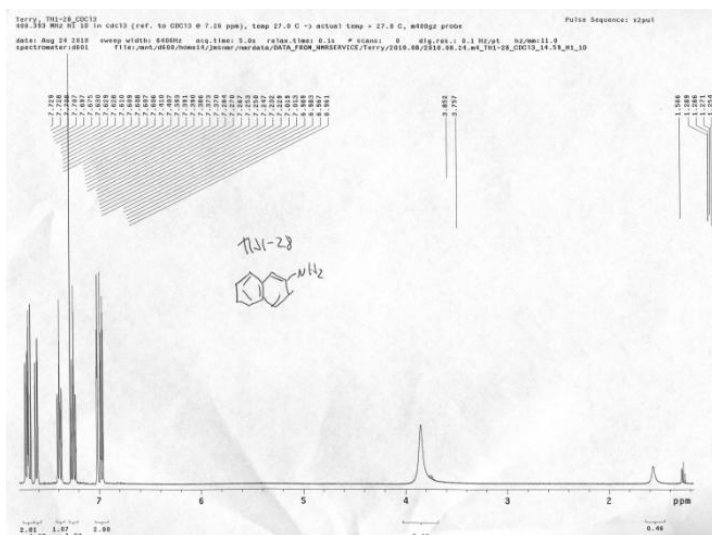


Figure A5 - <sup>1</sup>H NMR (500 MHz, CDCl<sub>3</sub>) of 2-aminonaphthalene 1

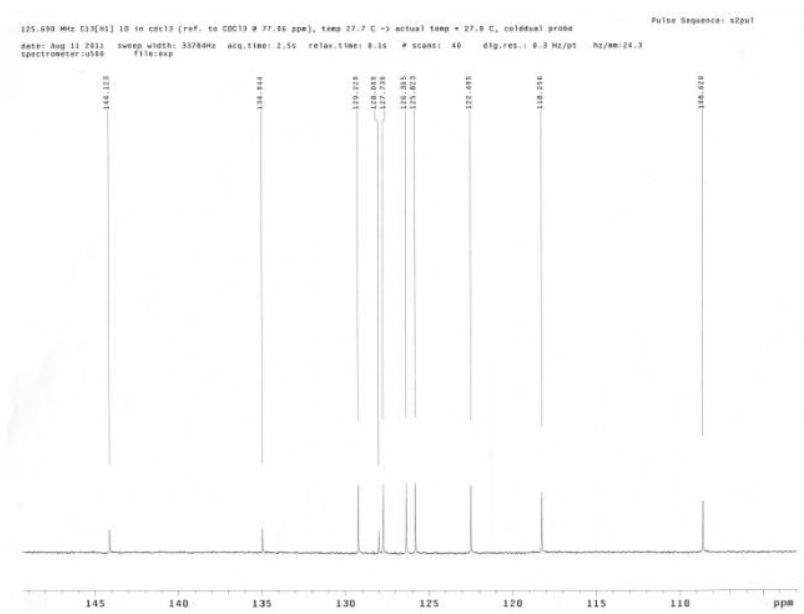
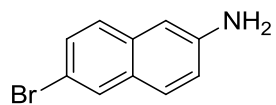


Figure A6 -  $^{13}\text{C}$  NMR (125 MHz,  $\text{CDCl}_3$ ) of 2-aminonaphthalene **1**

### 3 – Selected spectra for 6-Bromo-2-aminonaphthalene (**21**)



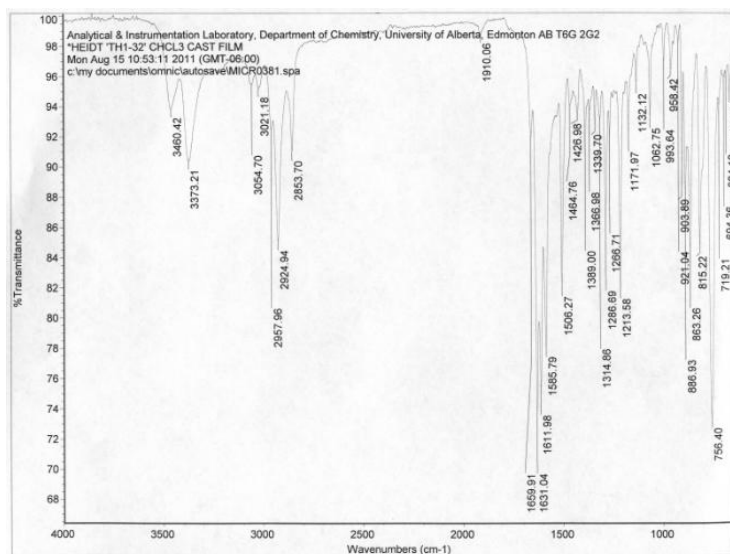


Figure A7 - IR (neat film,  $\text{cm}^{-1}$ ) of 6-Bromo-2-aminonaphthalene **21**

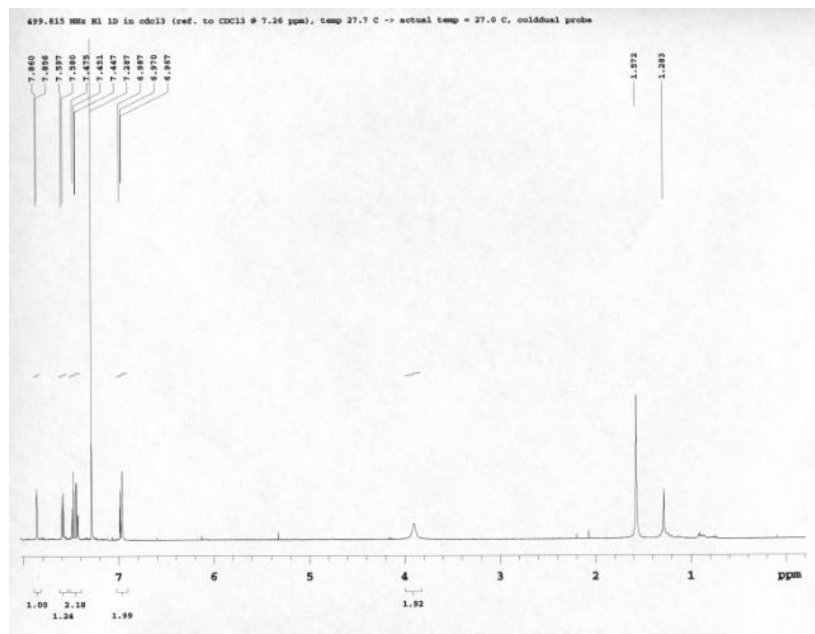


Figure A8 -  $^1\text{H}$  NMR (500 MHz,  $\text{CDCl}_3$ ) of 6-Bromo-2-aminonaphthalene **21**

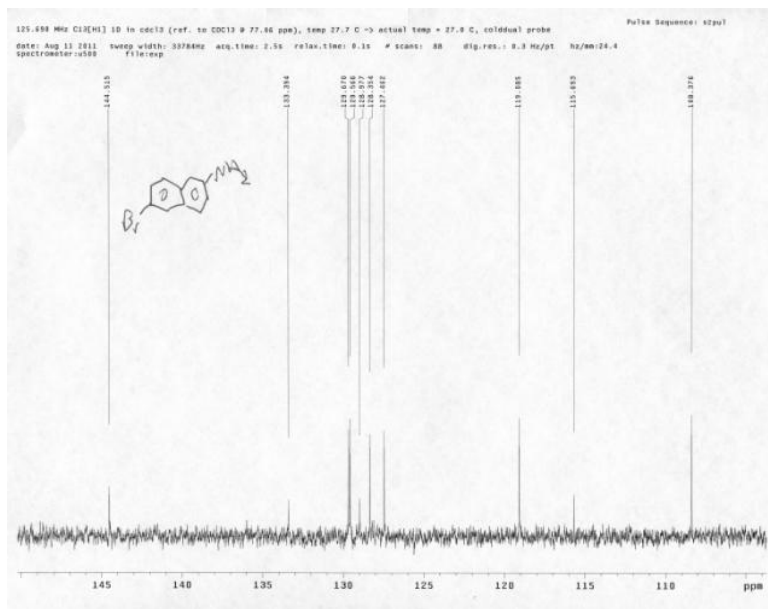


Figure A9 -  $^{13}\text{C}$  NMR (125 MHz,  $\text{CDCl}_3$ ) of 6-Bromo-2-aminonaphthalene **21**

#### 4 – Selected spectra for 2-aminoanthracene (**10**)

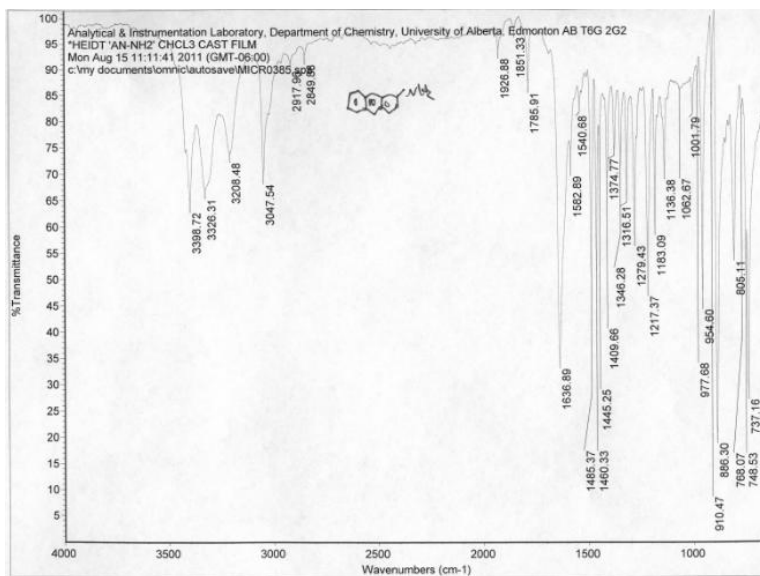
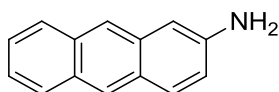


Figure 10 - IR (cast film,  $\text{cm}^{-1}$ ) of 2-aminoanthracene **10**

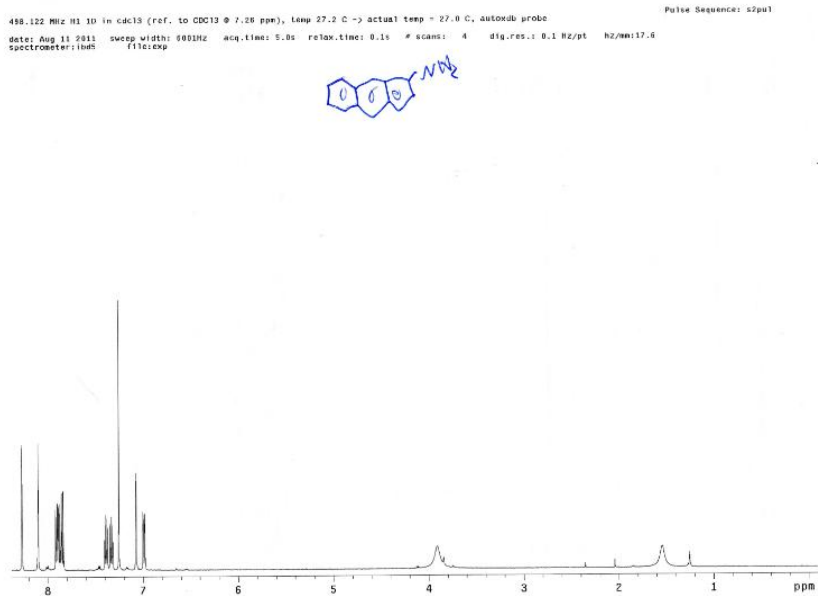


Figure 11 - <sup>1</sup>H NMR (500 MHz, CDCl<sub>3</sub>) of 2-aminoanthracene **10**

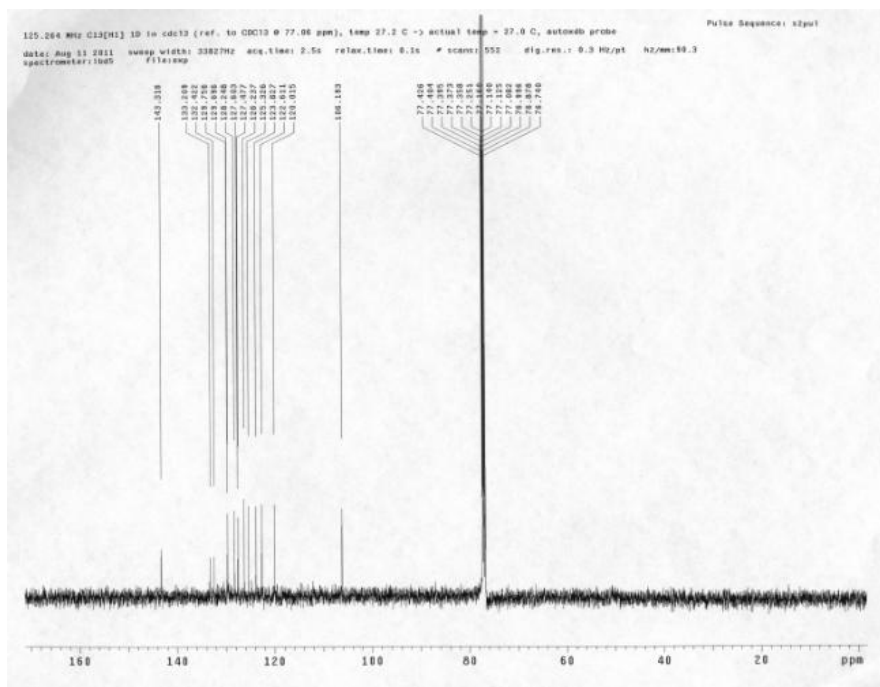


Figure 12 - <sup>13</sup>C NMR (125 MHz, CDCl<sub>3</sub>) of 2-aminoanthracene **10**

5 – Selected spectra for 1-bromo-2-aminoanthracene (**23**)

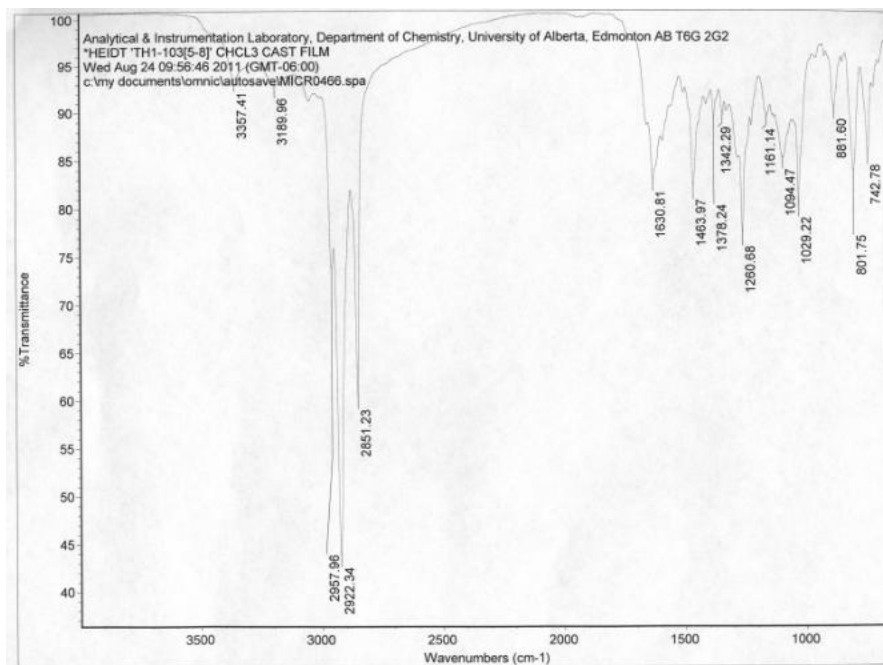
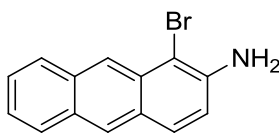


Figure 13 - IR (cast film, cm<sup>-1</sup>) of 1-bromo-2-aminoanthracene **23**



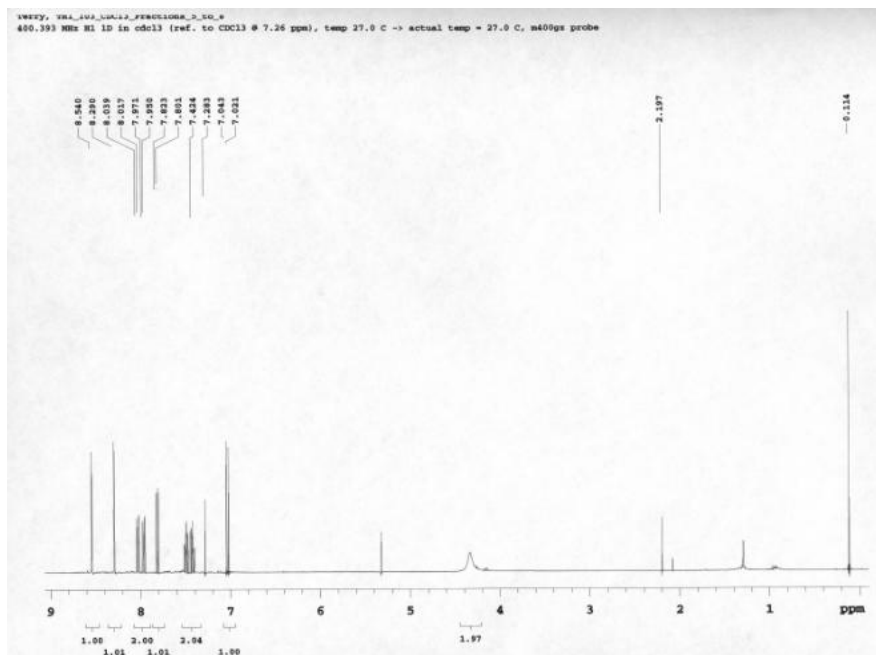


Figure 14 -  $^1\text{H}$  NMR (300 MHz,  $\text{CDCl}_3$ ) of 1-bromo-2-aminoanthracene **23**

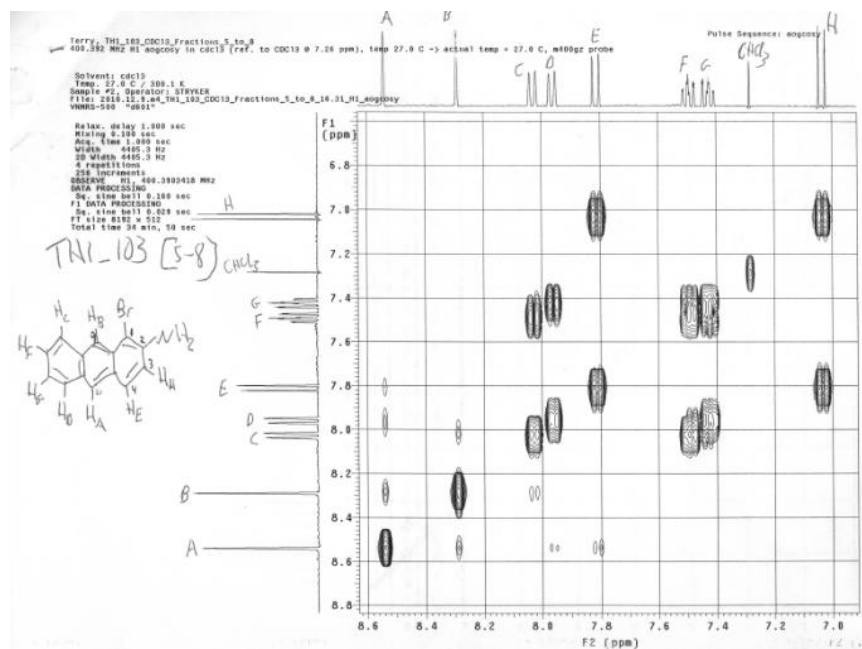


Figure 15 - COSY (400 MHz,  $\text{CHCl}_3$ ) of 1-bromo-2-aminoanthracene **23**

5 – Selected spectra for 1,10-dibromo-2-aminoanthracene (**24**)

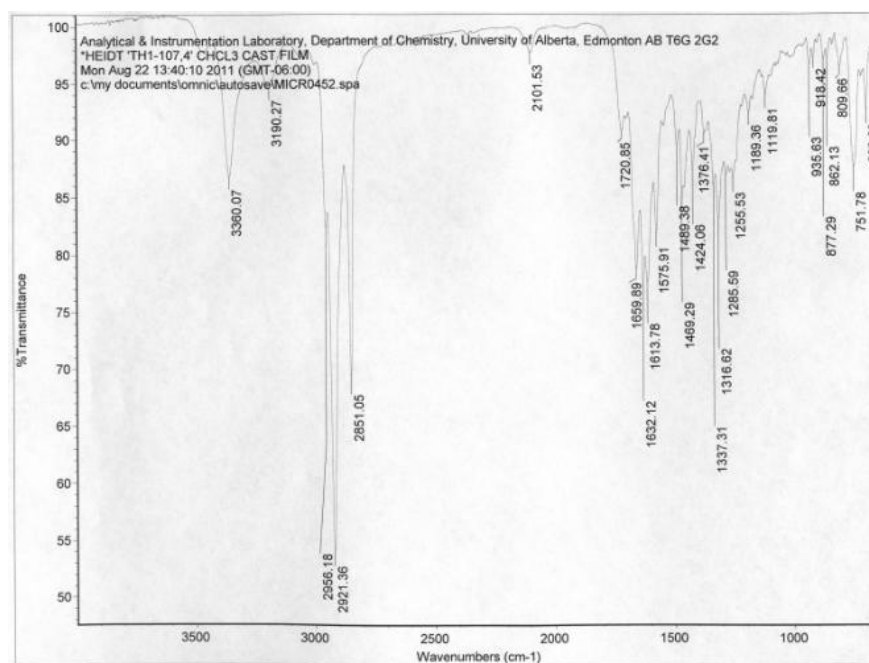
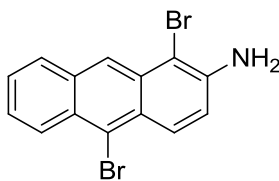


Figure 16 - IR (cast film, cm<sup>-1</sup>) of 1,10-dibromo-2-aminoanthracene **24**

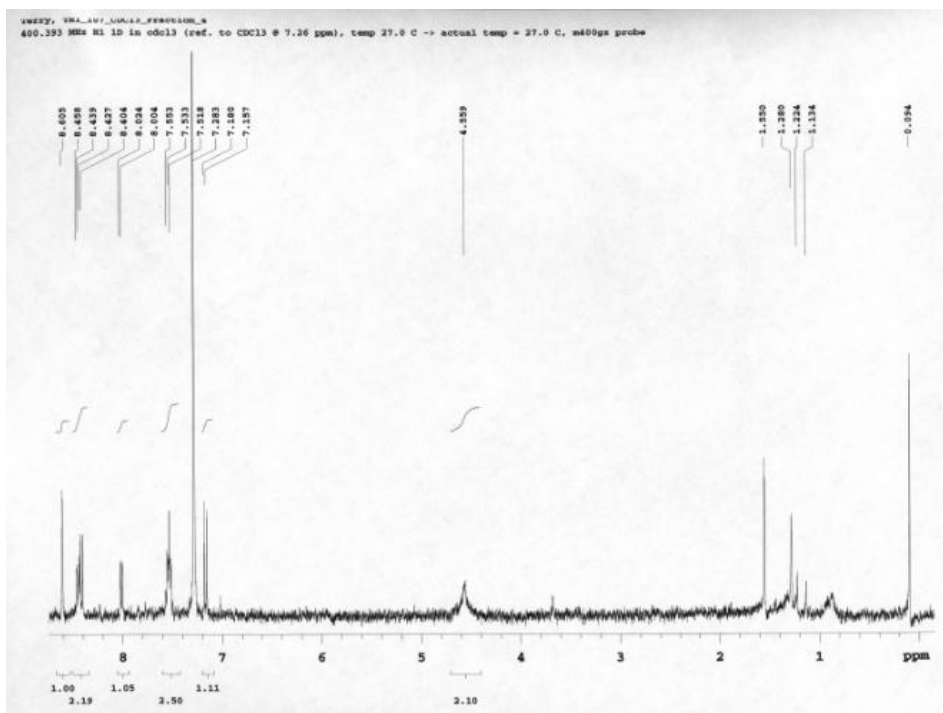


Figure 17 -  $^1\text{H}$  NMR (400 MHz,  $\text{CDCl}_3$ ) of 1,10-dibromo-2-aminoanthracene **24**

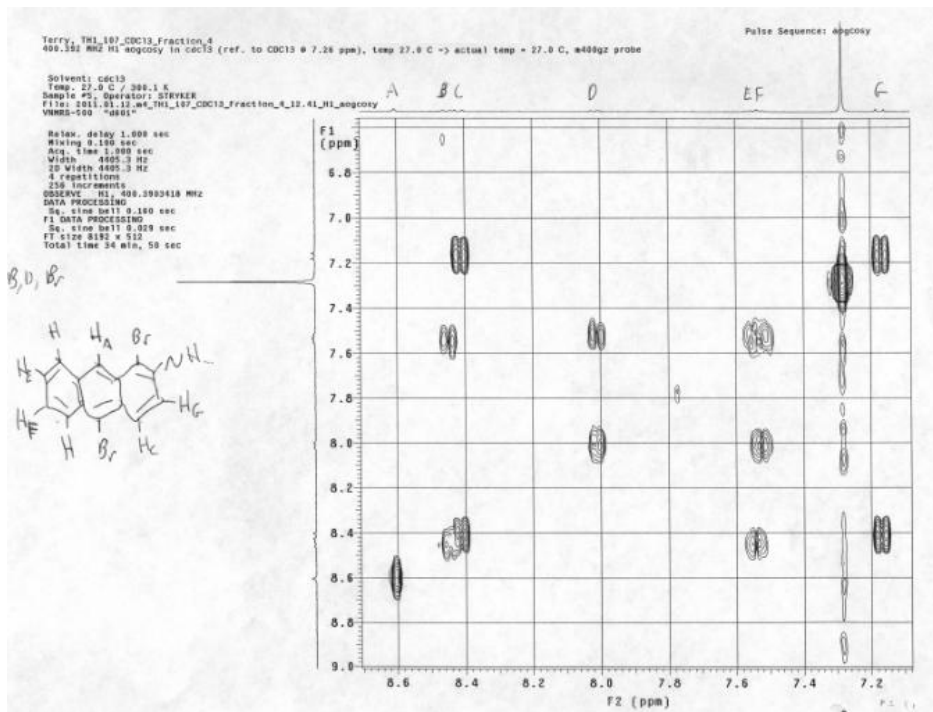


Figure 18 - COSY (400 MHz,  $\text{CHCl}_3$ ) of 1,10-dibromo-2-aminoanthracene **24**

6 – Selected spectra for 5-(3-bromophenyl)-1,2,3,4-tetrahydrobenzo[b]anthraquinoline(12)

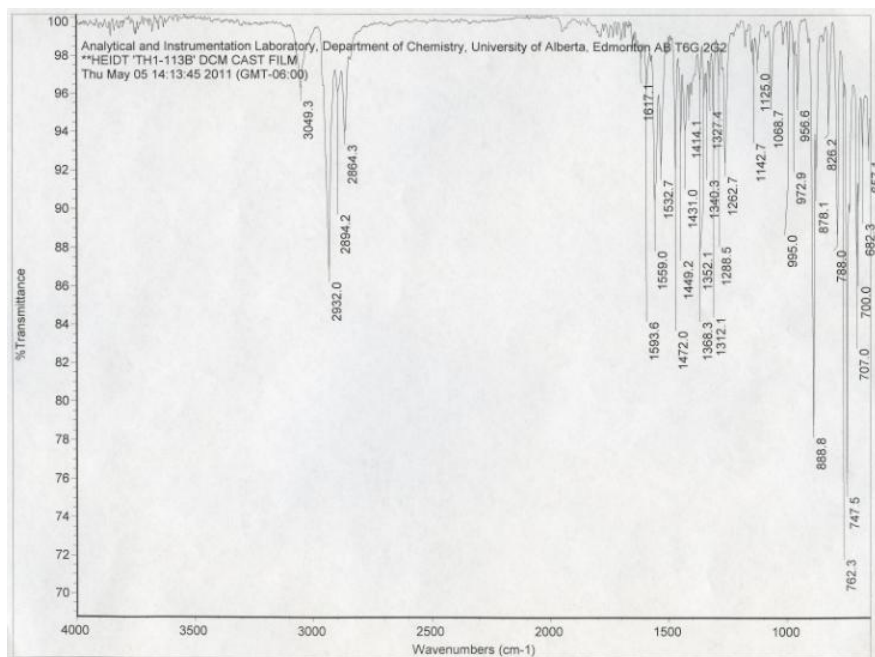
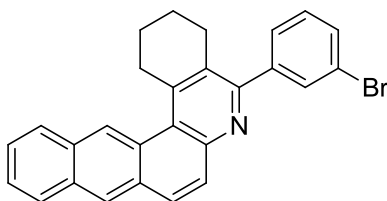


Figure 19 - IR (cast film, cm<sup>-1</sup>) of 5-(3-bromophenyl)-1,2,3,4-tetrahydrobenzo[b]anthraquinoline

12

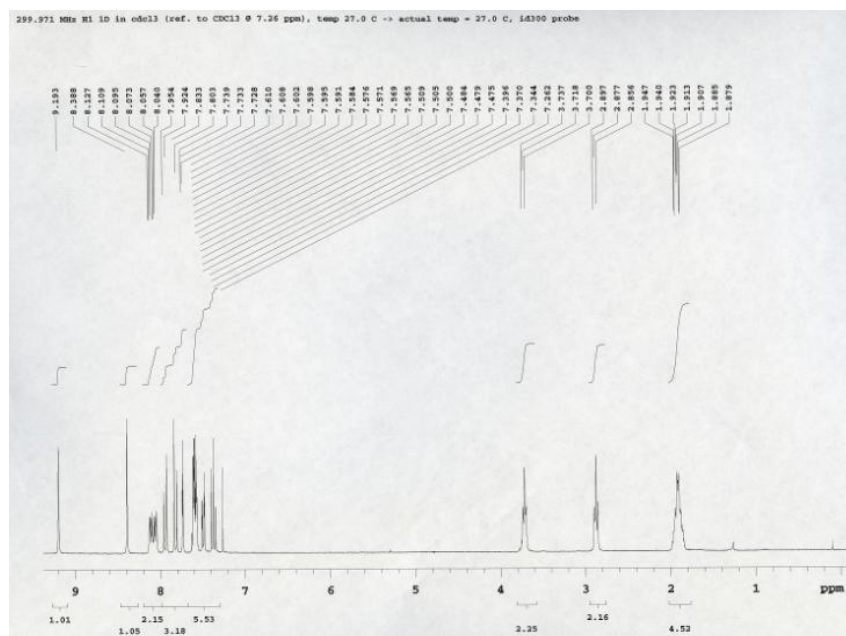


Figure 20 -  $^1\text{H}$  NMR (300 MHz,  $\text{CDCl}_3$ ) of 5-(3-bromophenyl)-1,2,3,4-tetrahydrobenzo[b]anthraquinoline **12**

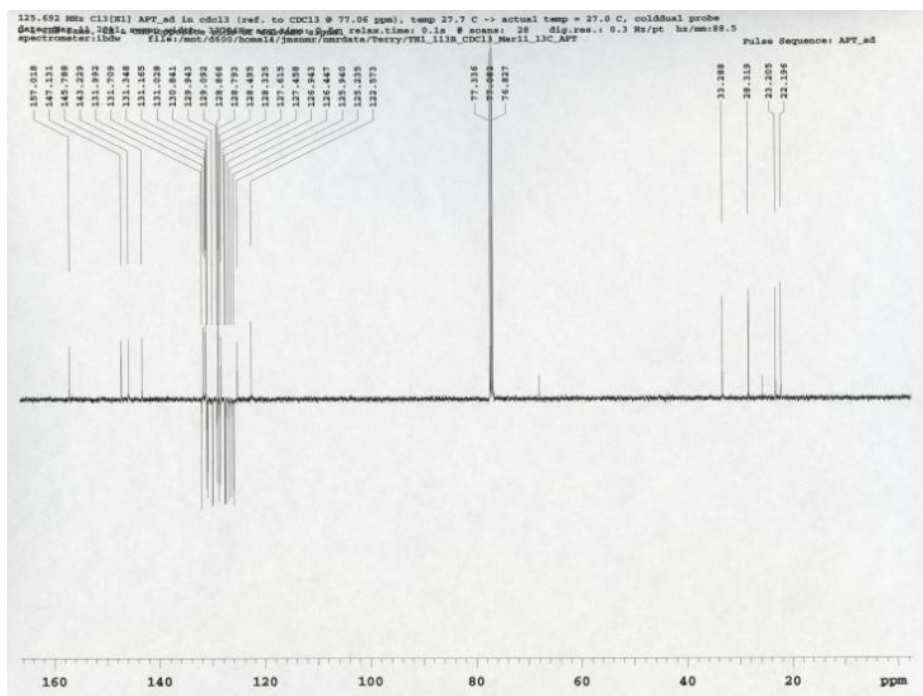


Figure 20 -  $^{13}\text{C}$  APT NMR of 5-(3-bromophenyl)-1,2,3,4-tetrahydrobenzo[b]anthraquinoline **12**

Table A1 - Crystal Structure Report of 5-(3-bromophenyl)-1,2,3,4-tetrahydrobenzo[b]anthraquinoline **12**

**XCL Code:** JMS1135 **Date:** 6 April 2011  
**Compound:** 5-(3-bromophenyl)-1,2,3,4-tetrahydronaphtho[2,3-*a*]phenanthridine  
**Formula:** C<sub>27</sub>H<sub>20</sub>BrN  
**Supervisor:** J. M. Stryker **Crystallographer:** M. J. Ferguson

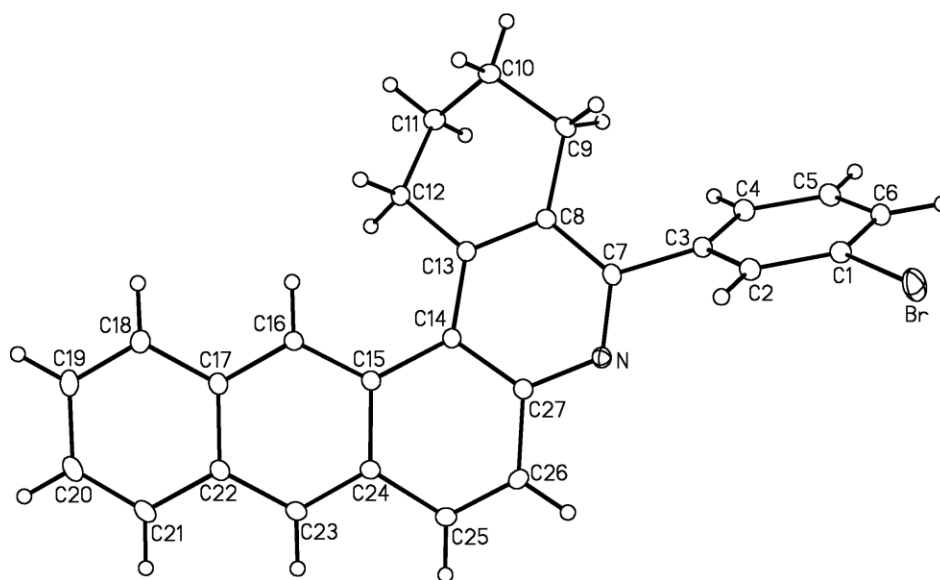


Figure 21 - Perspective view of the 5-(3-bromophenyl)-1,2,3,4-tetrahydronaphtho[2,3-*a*]phenanthridine molecule showing the atom labelling scheme. Non hydrogen atoms are represented by Gaussian ellipsoids at the 20% probability level. Hydrogen atoms are shown with arbitrarily small thermal parameters.

Table A2. Crystallographic Experimental Details for **12**

*A. Crystal Data*

|                |                                     |
|----------------|-------------------------------------|
| formula        | C <sub>27</sub> H <sub>20</sub> BrN |
| formula weight | 438.35                              |

|   |   |
|---|---|
| crystal dimensions (mm)                                 | 0.44 × 0.35 × 0.34  |
| crystal system  | monoclinic  |
| space group   | <i>Ia</i> (an alternate setting of <i>Cc</i> [No. 9])                       |
| unit cell parameters <sup>a</sup>                       |   |
| <i>a</i> (Å)  | 9.5665 (4)  |
| <i>b</i> (Å)  | 16.3080 (6)   |
| <i>c</i> (Å)  | 12.6051 (5)   |
| β (deg)   | 96.9439 (4)   |
| <i>V</i> (Å <sup>3</sup> )                              | 1952.10 (13)  |
| <i>Z</i>  | 4   |
| $\rho_{\text{calcd}}$ (g cm <sup>-3</sup> )             | 1.492   |
| $\mu$ (mm <sup>-1</sup> )                               | 2.119   |
| <br><i>B. Data Collection and Refinement Conditions</i> |   |
| diffractometer  | Bruker D8/APEX II CCD <sup>b</sup>  |
| radiation ( $\lambda$ [Å])                              | graphite-monochromated Mo K $\alpha$ (0.71073)                              |
| temperature (°C)  | −100  |
| scan type   | $\omega$ scans (0.3°) (20 s exposures)                                      |
| data collection $2\theta$ limit (deg)                   | 55.32   |
| total data collected                                    | 8349 ( $-12 \leq h \leq 12$ , $-21 \leq k \leq 21$ , $-16 \leq l \leq 16$ ) |
| independent reflections                                 | 4397 ( $R_{\text{int}} = 0.0108$ )  |
| number of observed reflections ( <i>NO</i> )            | 4282 [ $F_o^2 \geq 2\sigma(F_o^2)$ ]  |
| structure solution method                               | direct methods ( <i>SHELXD</i> <sup>c</sup> )                               |
| refinement method                                       | full-matrix least-squares on $F^2$ ( <i>SHELXL-97</i> <sup>d</sup> )        |
| absorption correction method                            | Gaussian integration (face-indexed)   |
| range of transmission factors                           | 0.5344–0.4578   |

|  |                                    |
|--|------------------------------------|
| data/restraints/parameters   | 4397 / 0 / 262                     |
| Flack absolute structure parameter <sup>e</sup>  | 0.015(5)                           |
| goodness-of-fit ( <i>S</i> ) <sup>f</sup> [all data]   | 1.037                              |
| final <i>R</i> indices <sup>g</sup>  |                                    |
| <i>R</i> <sub>1</sub> [ <i>F</i> <sub>o</sub> <sup>2</sup> ≥ 2σ( <i>F</i> <sub>o</sub> <sup>2</sup> )] | 0.0208                             |
| <i>wR</i> <sub>2</sub> [all data]  | 0.0568                             |
| largest difference peak and hole   | 0.259 and –0.277 e Å <sup>–3</sup> |

<sup>a</sup>Obtained from least-squares refinement of 9897 reflections with 4.96° < 2θ < 55.26°.

<sup>b</sup>Programs for diffractometer operation, data collection, data reduction and absorption correction were those supplied by Bruker.

<sup>c</sup>Schneider, T. R.; Sheldrick, G. M. *Acta Crystallogr.* **2002**, *D58*, 1772-1779.

<sup>d</sup>Sheldrick, G. M. *Acta Crystallogr.* **2008**, *A64*, 112–122.

<sup>e</sup>Flack, H. D. *Acta Crystallogr.* **1983**, *A39*, 876–881; Flack, H. D.; Bernardinelli, G. *Acta Crystallogr.* **1999**, *A55*, 908–915; Flack, H. D.; Bernardinelli, G. *J. Appl. Cryst.* **2000**, *33*, 1143–1148. The Flack parameter will refine to a value near zero if the structure is in the correct configuration and will refine to a value near one for the inverted configuration.

<sup>f</sup> $S = [\sum w(F_o^2 - F_c^2)^2 / (n - p)]^{1/2}$  (*n* = number of data; *p* = number of parameters varied;  $w = [\sigma^2(F_o^2) + (0.0226P)^2 + 0.5107P]^{-1}$  where  $P = [\text{Max}(F_o^2, 0) + 2F_c^2]/3$ ).

<sup>g</sup> $R_1 = \sum ||F_o| - |F_c|| / \sum |F_o|$ ;  $wR_2 = [\sum w(F_o^2 - F_c^2)^2 / \sum w(F_o^4)]^{1/2}$ .

## 7 – Selected spectra for 5-(3-bromophenyl)-1,2,3,4-tetrahydrobenzo[b]anthraquinoline hydroiodide (15)



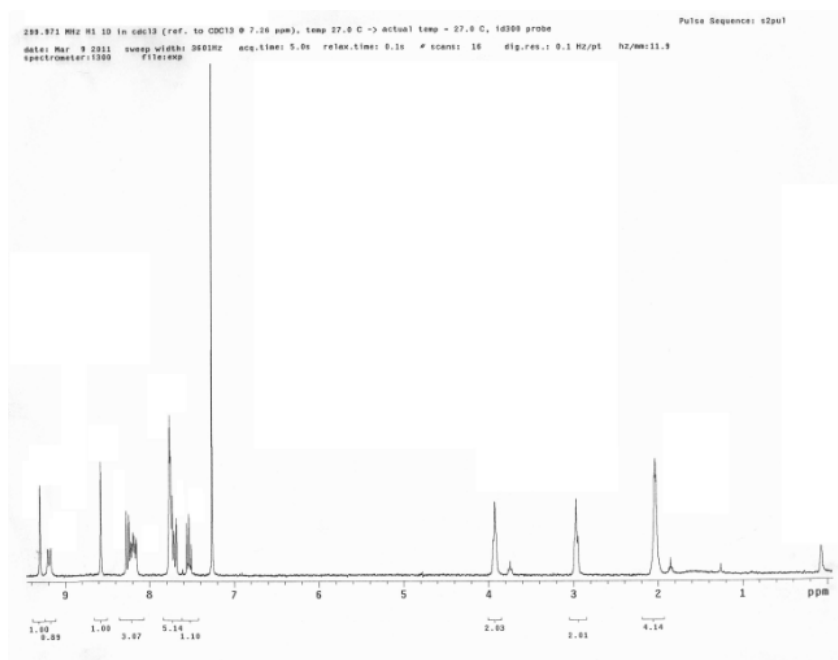
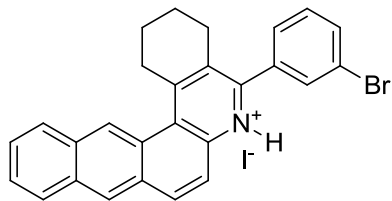


Figure 22 –  $^1\text{H}$  NMR (300 MHz,  $\text{CDCl}_3$ ) of 5-(3-bromophenyl)-1,2,3,4-tetrahydrobenzo[b] anthraquinoline hydroiodide **15**

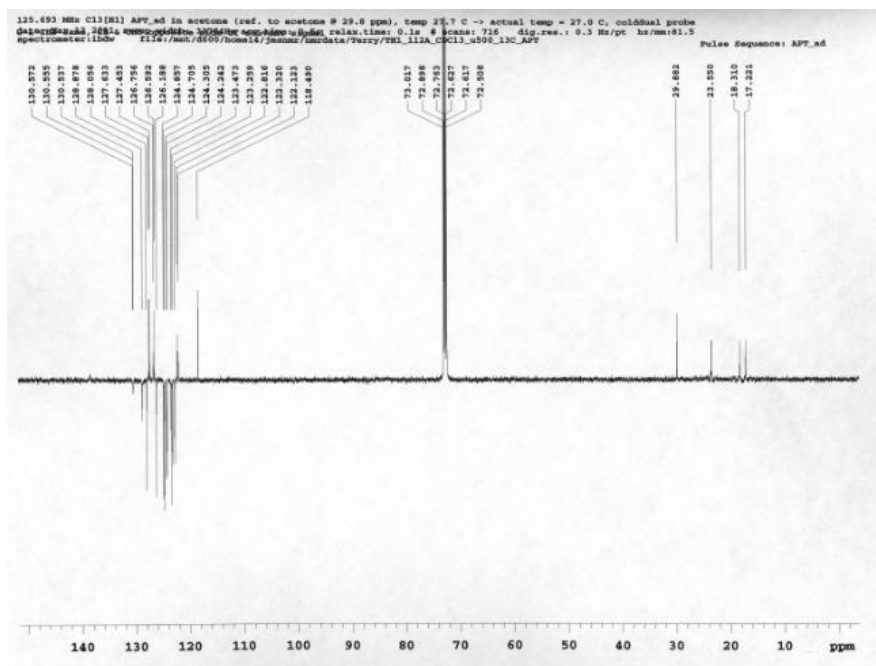
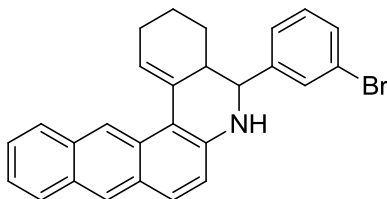


Figure 23 –  $^{13}\text{C}$  APT NMR (125 MHz,  $\text{CDCl}_3$ ): of 5-(3-bromophenyl)-1,2,3,4-tetrahydrobenzo[b]anthraquinoline hydroiodide **15**

8 – Selected spectra for 5-(3-bromophenyl)-2,3,4,5,21,N-hexahydrobenzo[b]anthraquinoline (13)



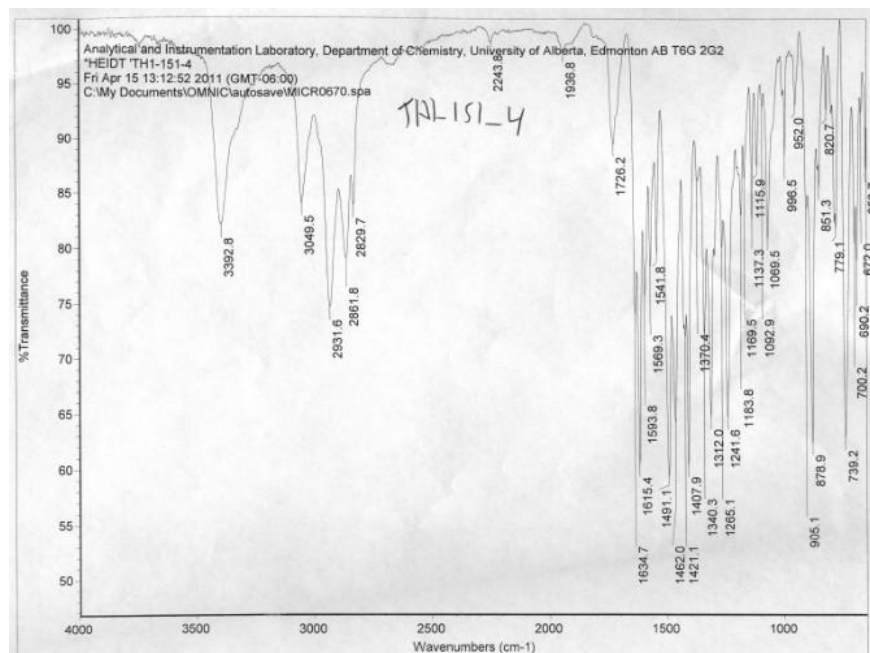


Figure 24 - IR (microscope,  $\text{cm}^{-1}$ ) of -(3-Bromophenyl)-2,3,4,5,21,N-hexahydrobenzo[b]anthraquinoline **13**

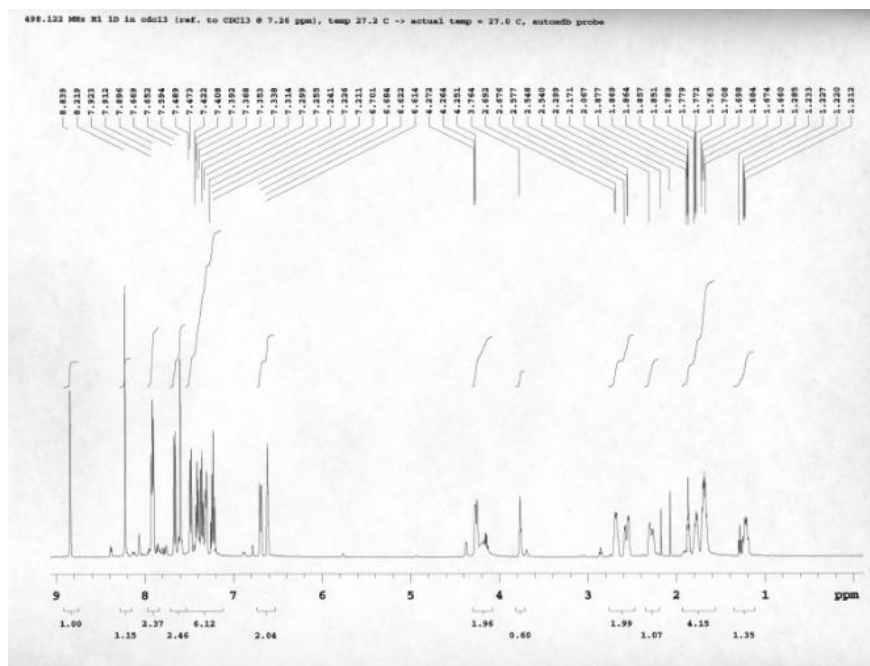


Figure 25 -  $^1\text{H}$  NMR (500 MHz,  $\text{CDCl}_3$ ) of -(3-Bromophenyl)-2,3,4,5,21,N-hexahydrobenzo[b]anthraquinoline **13**

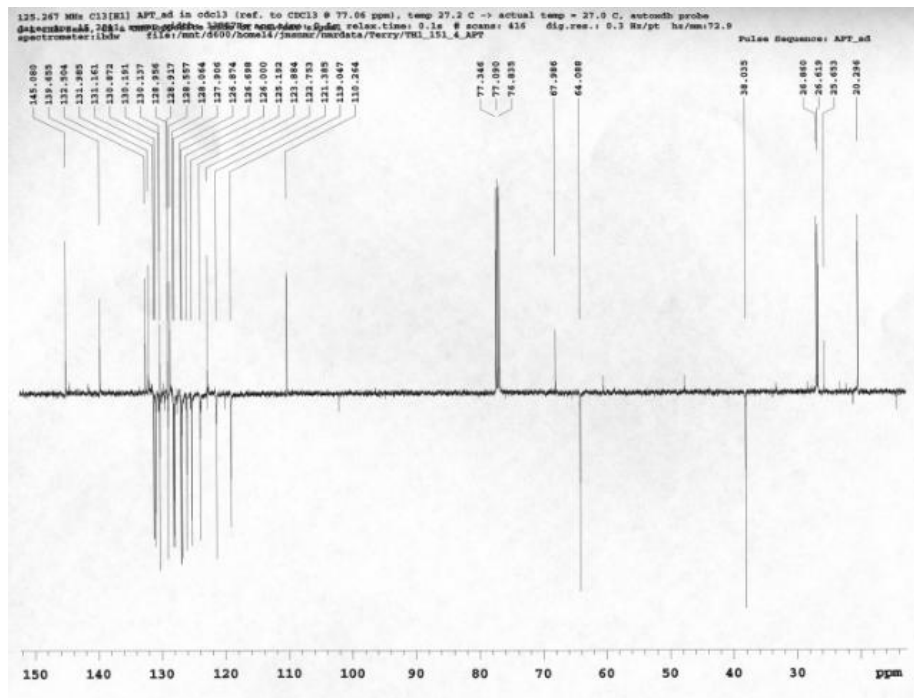
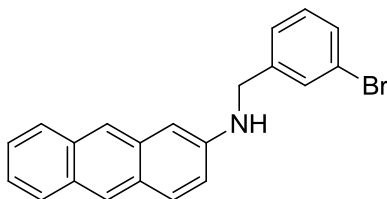


Figure 26 -  $^1\text{H}$  NMR (500 MHz,  $\text{CDCl}_3$ ) of -(3-Bromophenyl)-2,3,4,5,21,N-hexahydrobenzo[b]anthraquinoline **13**

9 – Selected spectra for N-(3-bromobenzyl)anthracen-2-amine (**14**)



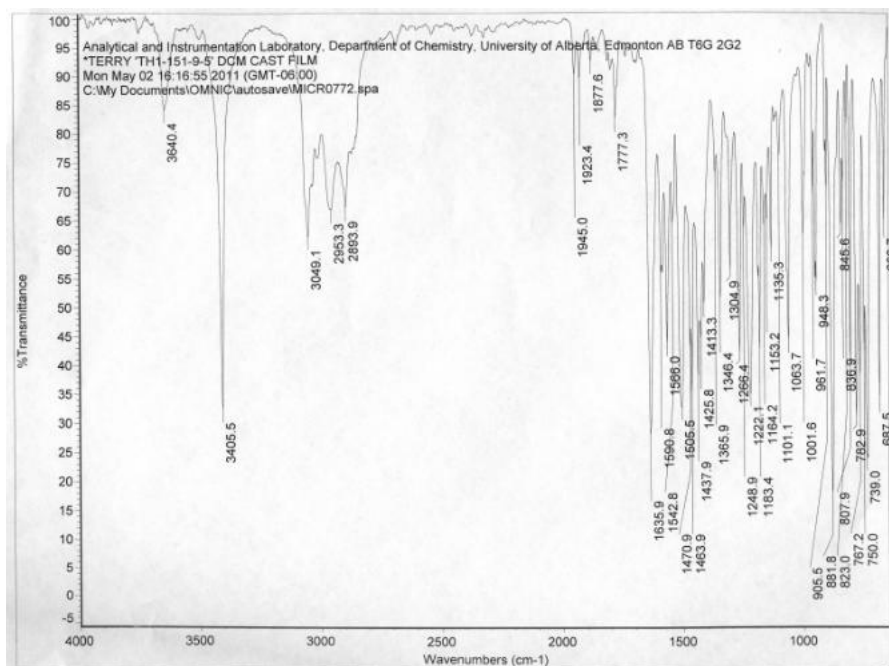


Figure 27 - IR (cast film,  $\text{cm}^{-1}$ ) of N-(3-bromobenzyl)anthracen-2-amine **14**

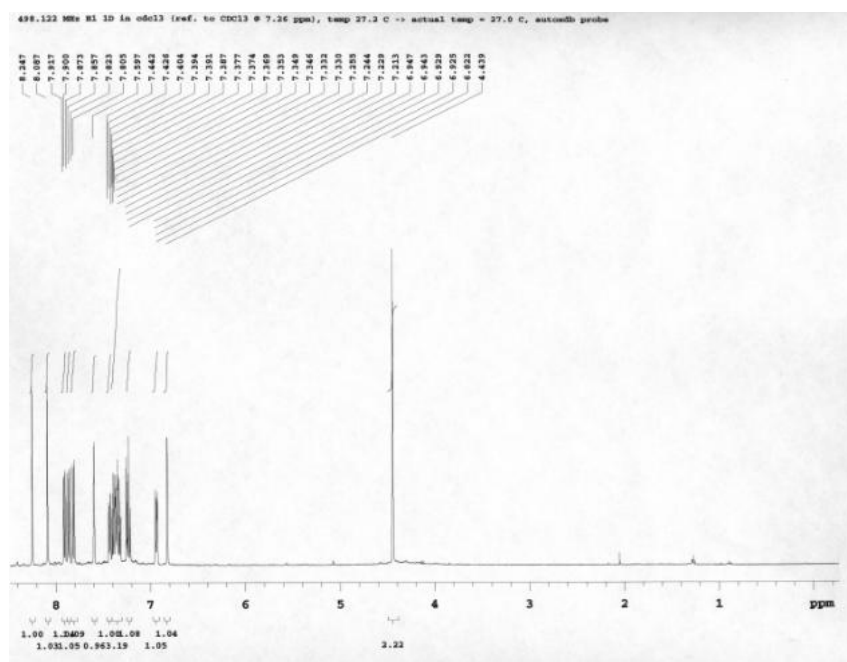


Figure 28 -  $^1\text{H}$  NMR (500 MHz,  $\text{CDCl}_3$ ) of N-(3-bromobenzyl)anthracen-2-amine **14**

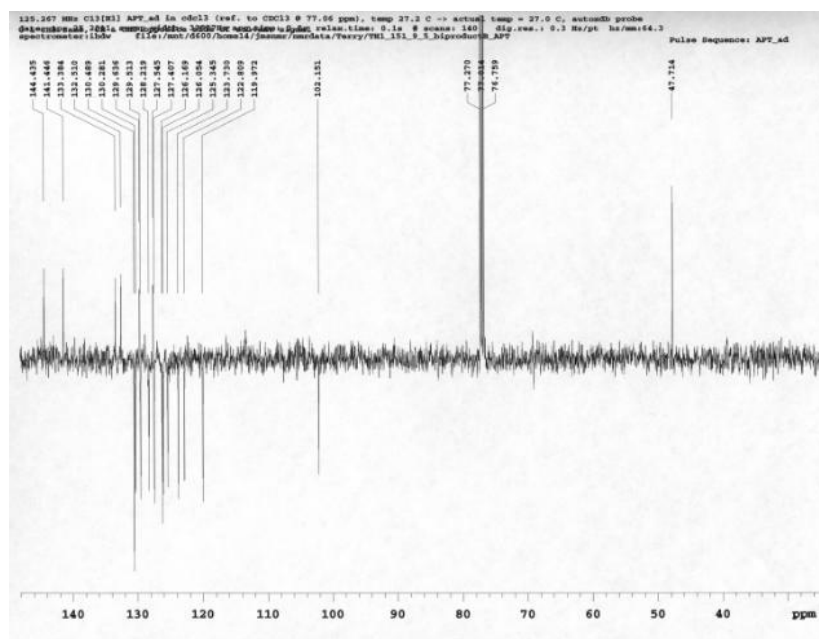
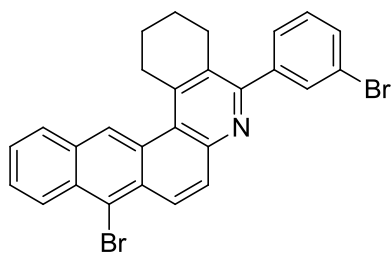


Figure 29 -  $^{13}\text{C}$  APT NMR (125 MHz,  $\text{CDCl}_3$ ) of N-(3-bromobenzyl)anthracen-2-amine **14**

**10 – Selected spectra for 13-bromo-5-(3-bromophenyl)-1,2,3,4-tetrahydrobenzo[b]anthraquinoline (26)**



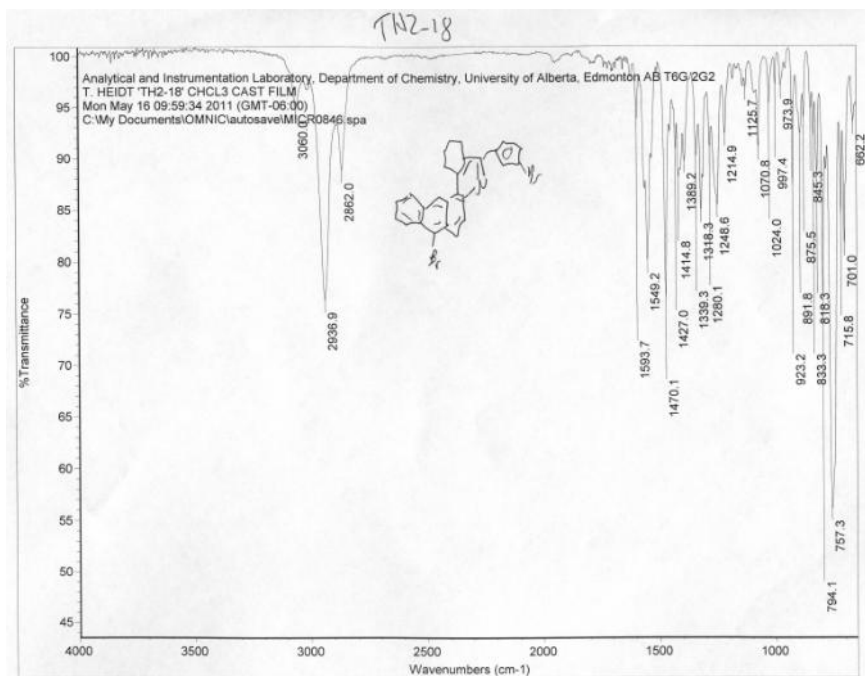


Figure 30 - IR (cast film,  $\text{cm}^{-1}$ ) of 13-bromo-5-(3-bromophenyl)-1,2,3,4-tetrahydrobenzo[b]anthraquinoline **26**

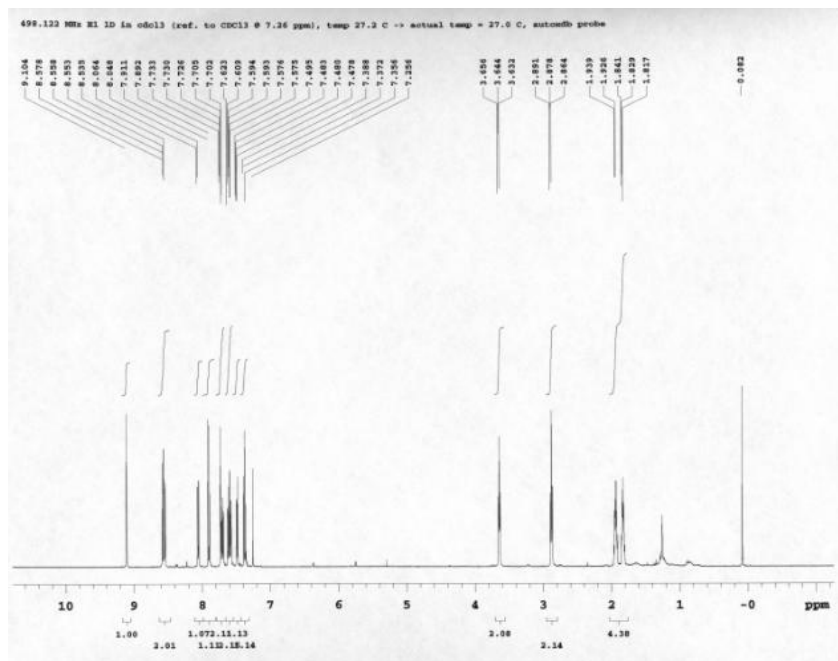


Figure 31 -  $^1\text{H}$  NMR (500 MHz,  $\text{CDCl}_3$ ) of 13-bromo-5-(3-bromophenyl)-1,2,3,4-tetrahydrobenzo[b]anthraquinoline **26**

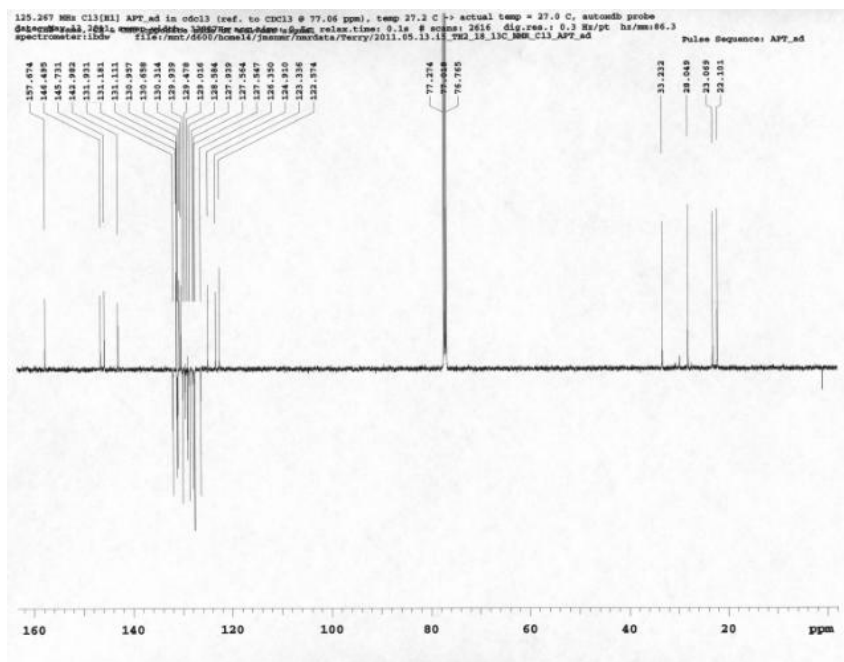
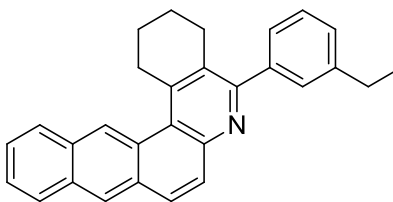


Figure 32 –  $^{13}\text{C}$  APT NMR (125 MHz,  $\text{CDCl}_3$ ) of 13-bromo-5-(3-bromophenyl)-1,2,3,4-tetrahydrobenzo[b]anthraquinoline **26**

**11 –Selected spectra for 5-(16-Ethylphenyl)-1,2,3,4-tetrahydrobenzo[b]anthraquinoline (27)**





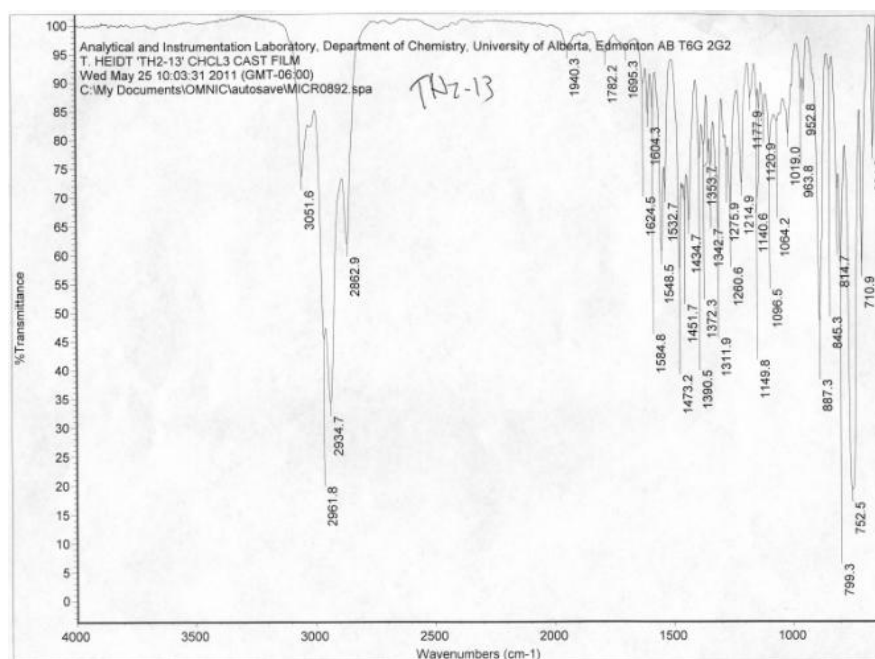


Figure 33 - IR (cast film,  $\text{cm}^{-1}$ ) of 5-(16-Ethylphenyl)-1,2,3,4-tetrahydrobenzo[b] anthraquinoline **27**

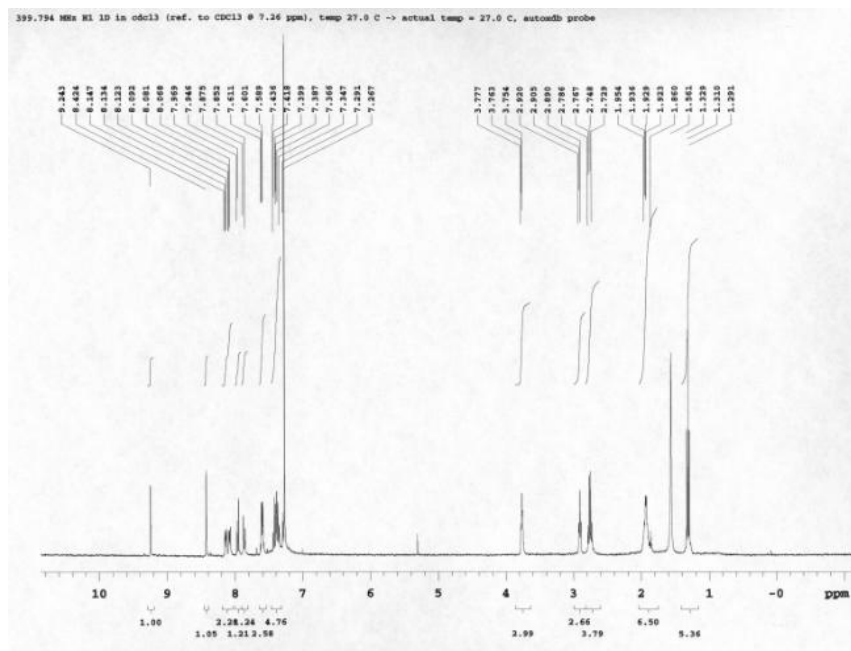


Figure 34 -  $^1\text{H}$  NMR (400 MHz,  $\text{CDCl}_3$ ) of 5-(16-Ethylphenyl)-1,2,3,4-tetrahydrobenzo[b] anthraquinoline **27**

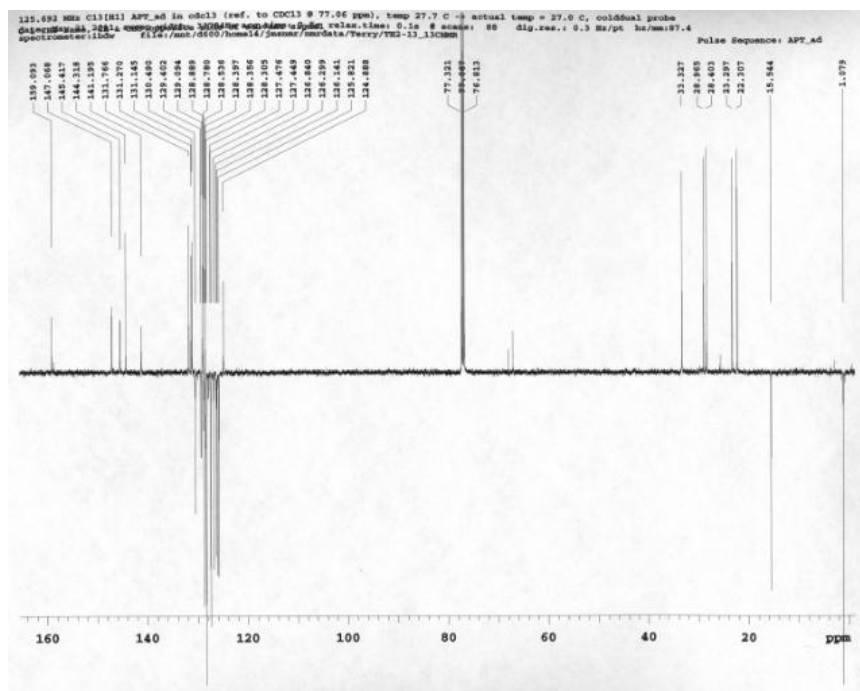
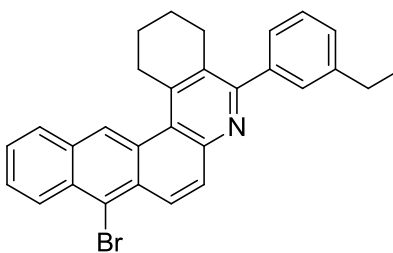


Figure 35 –  $^{13}\text{C}$  APT NMR (125 MHz,  $\text{CDCl}_3$ ) of 5-(16-Ethylphenyl)-1,2,3,4-tetrahydrobenzo[b]anthraquinoline **27**

**11 –Selected spectra for 13-Bromo-5-(3-ethylphenyl)-1,2,3,4-tetrahydrobenzo[b]anthraquinoline (28)**



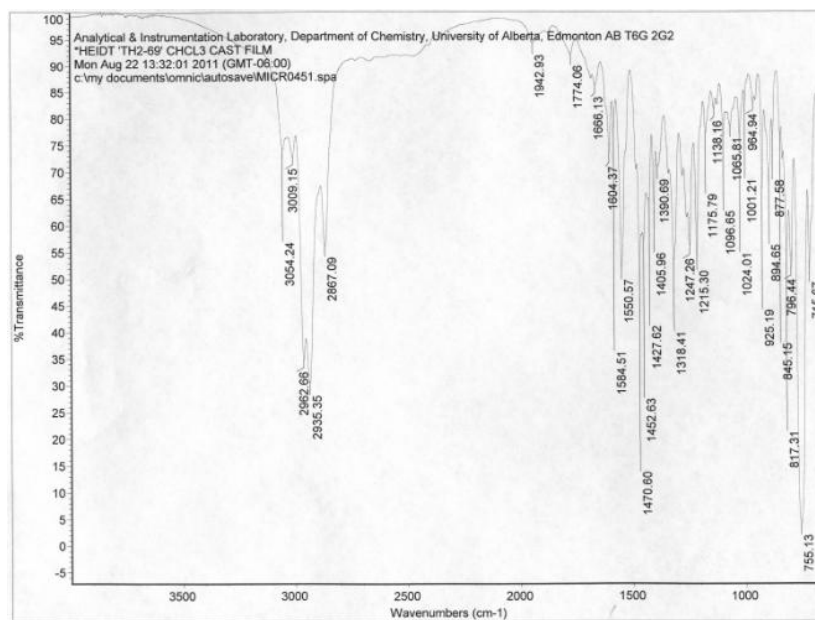


Figure 36 - IR (cast film,  $\text{cm}^{-1}$ ) of 13-Bromo-5-(3-ethylphenyl)-1,2,3,4-tetrahydrobenzo[b]anthraquinoline **28**

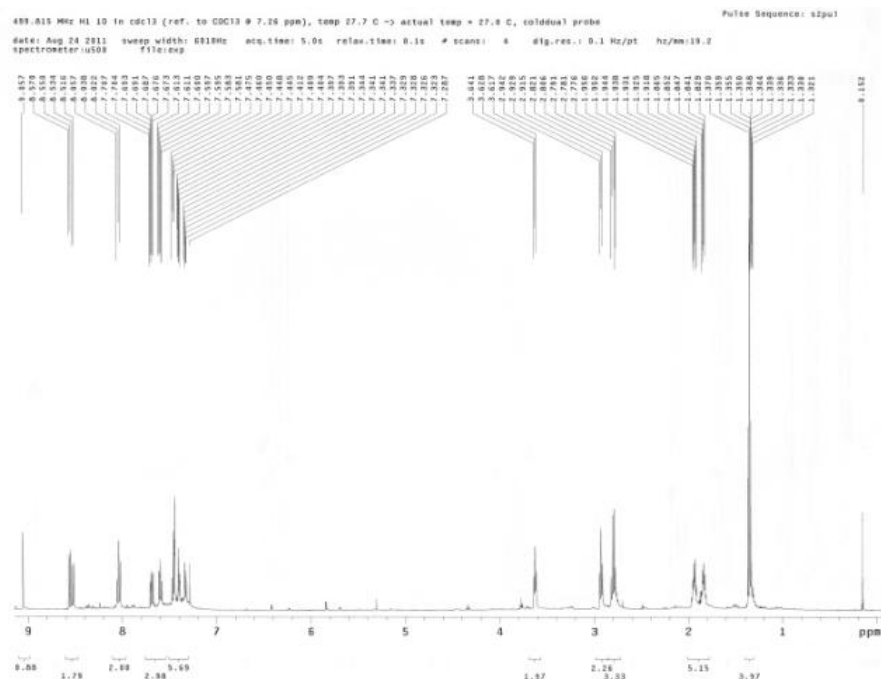


Figure 37 -  $^1\text{H}$  NMR (500 MHz,  $\text{CDCl}_3$ ) of 13-Bromo-5-(3-ethylphenyl)-1,2,3,4-tetrahydrobenzo[b]anthraquinoline **28**

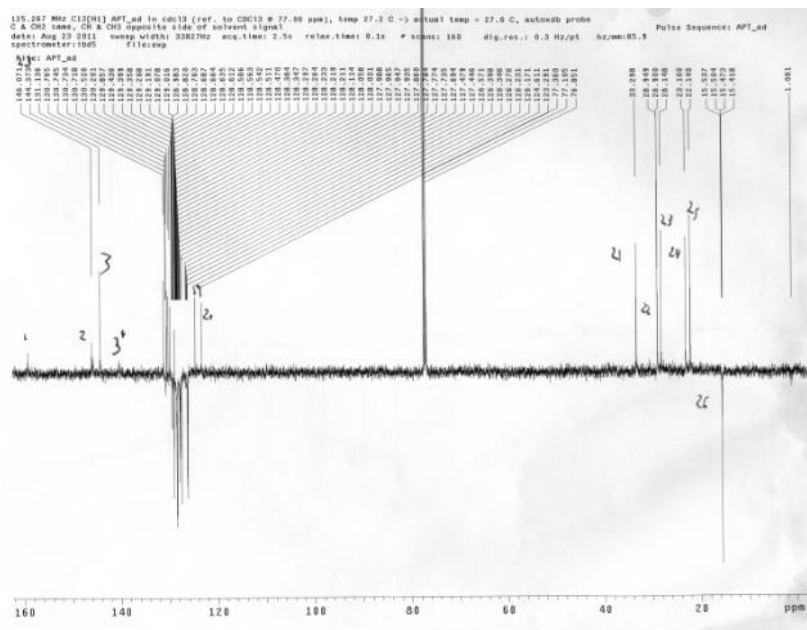
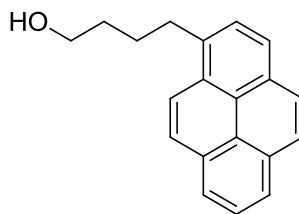


Figure 38 –  $^{13}\text{C}$  APT NMR (125 MHz,  $\text{CDCl}_3$ ) of 13-Bromo-5-(3-ethylphenyl)-1,2,3,4-tetrahydrobenzo[b]anthraquinoline **28**

12 –Selected spectra for 1-pyrenebutanol (**34**)



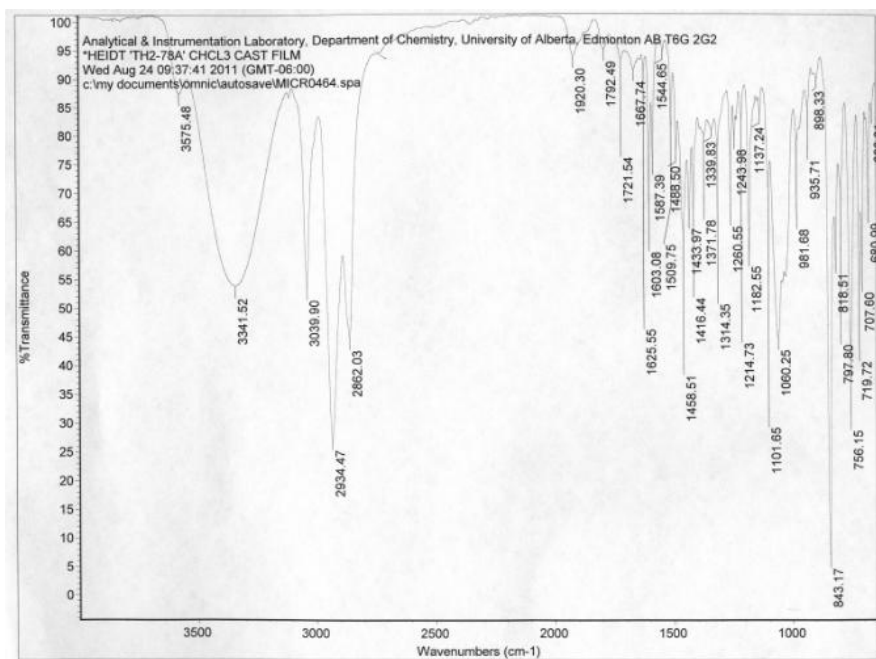


Figure 39 - IR (cast film,  $\text{cm}^{-1}$ ) of 1-pyrenebutanol **34**

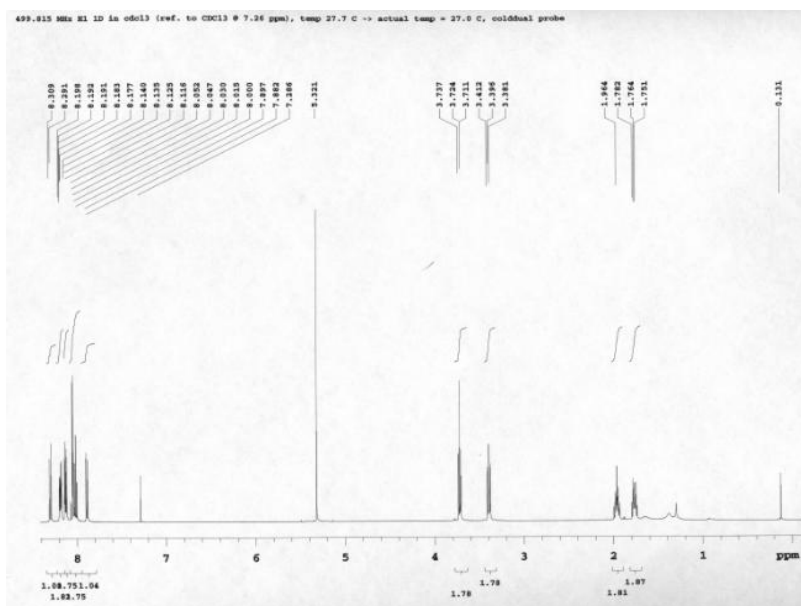


Figure 40 -  $^1\text{H}$  NMR (500 MHz,  $\text{CDCl}_3$ ) of 1-pyrenebutanol **34**

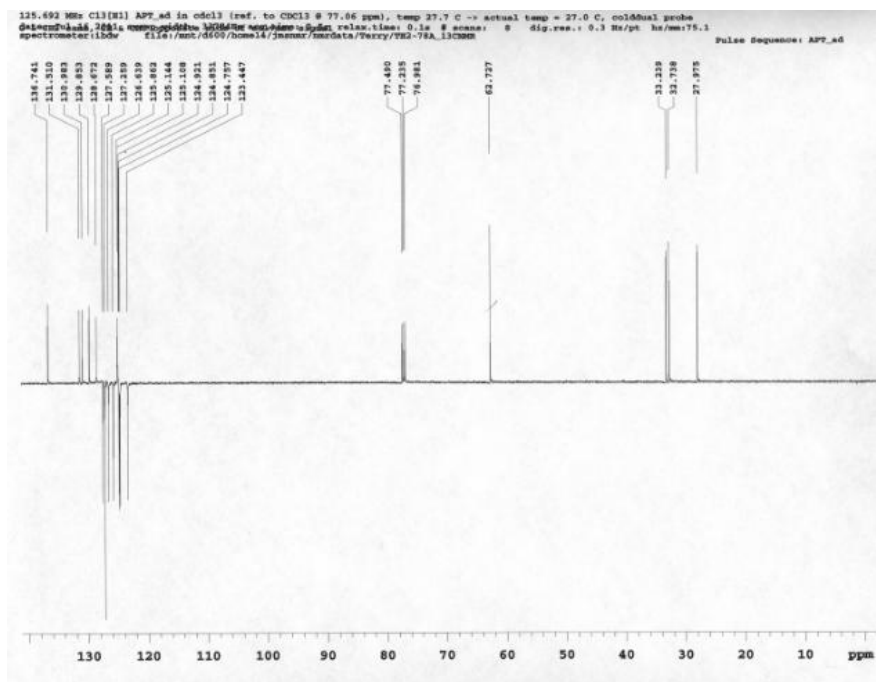
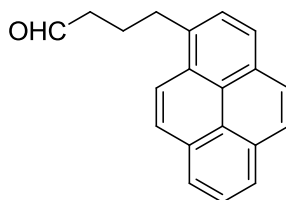


Figure 41 –  $^{13}\text{C}$  APT NMR (125 MHz,  $\text{CDCl}_3$ ) of 1-pyrenebutanol **34**

13 –Selected spectra for 1-pyrenebutanal (**32**)



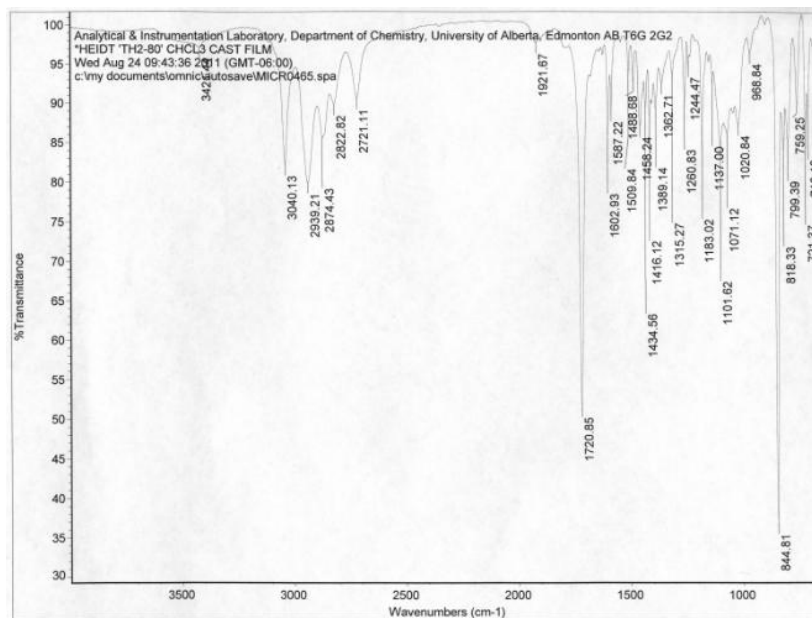


Figure 42 - IR (cast film, cm<sup>-1</sup>) of 1-pyrenebutanal **32**

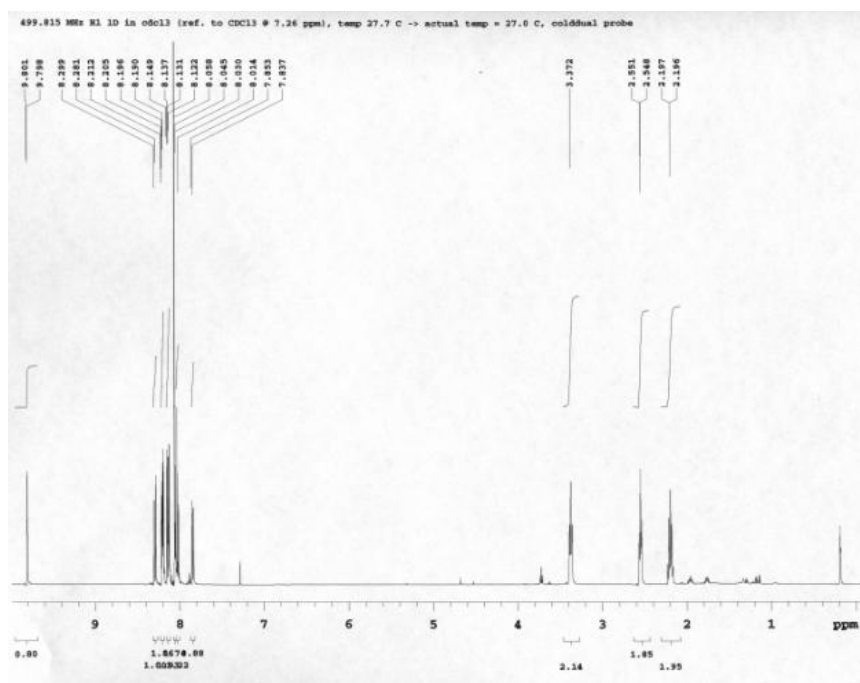


Figure 43 - <sup>1</sup>H NMR (500 MHz, CDCl<sub>3</sub>) of 1-pyrenebutanal **32**

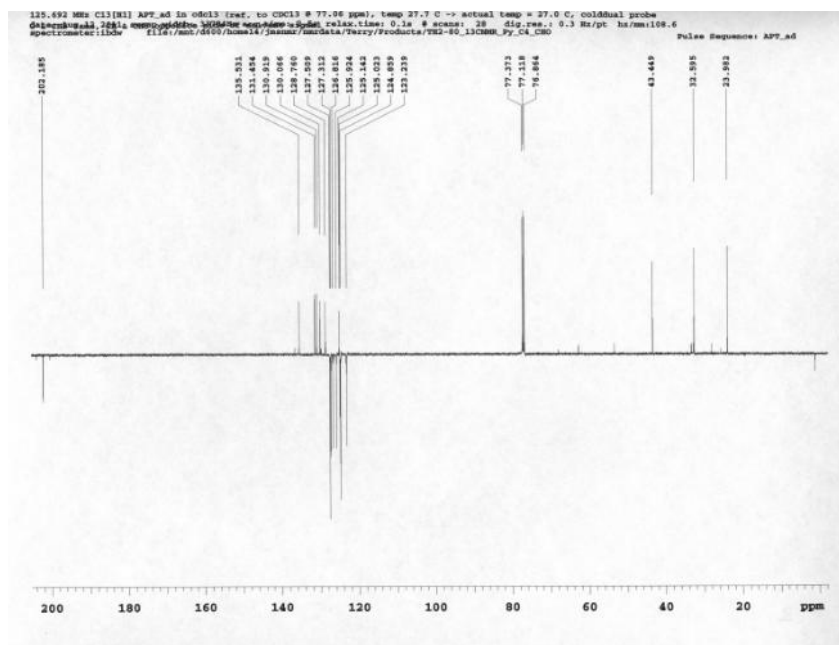
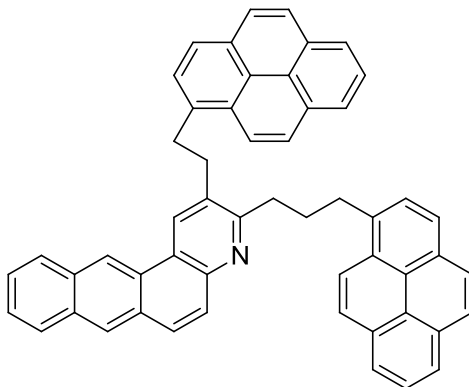


Figure 44 –  $^{13}\text{C}$  APT NMR (125 MHz,  $\text{CDCl}_3$ ) of 1-pyrenebutanal **32**

**14 –Selected spectra for 2-(1-Ethylpyrene)-3-(1-propylpyrene)-benzo[b] anthraquinoline (32)**







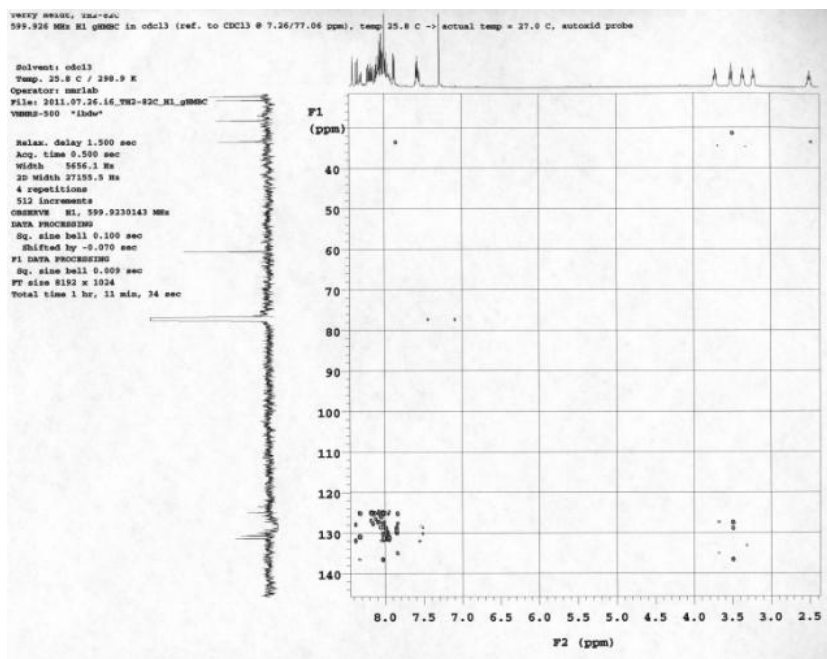


Figure 47 – HMBC of 2-(1-Ethylpyrene)-3-(1-propylpyrene)-benzo[b]anthraquinoline **30**

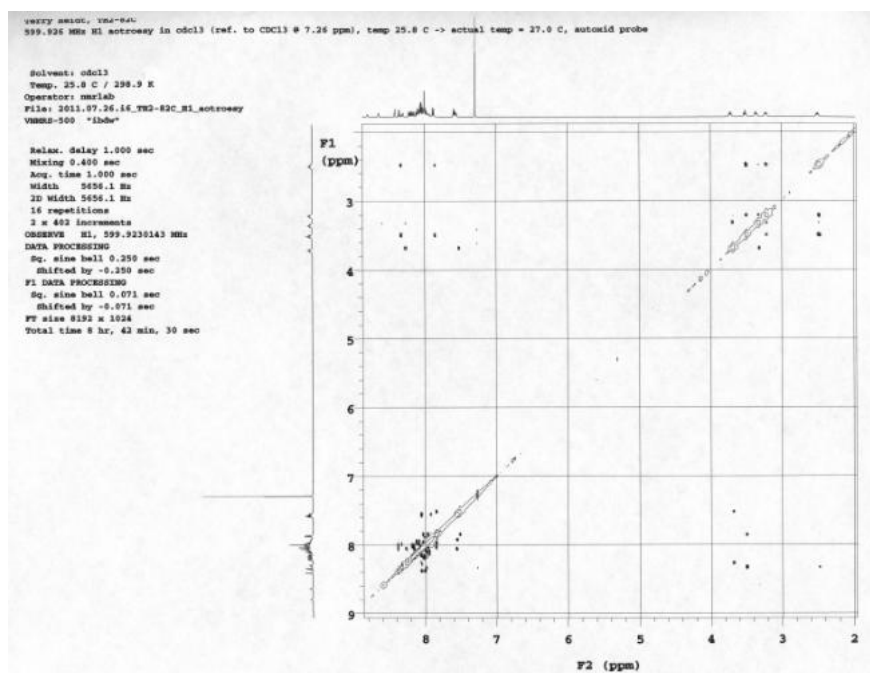


Figure 48 – TROSEY of 2-(1-Ethylpyrene)-3-(1-propylpyrene)-benzo[b]anthraquinoline **30**

15 –Selected spectra for 1-vinylpyrene (36)

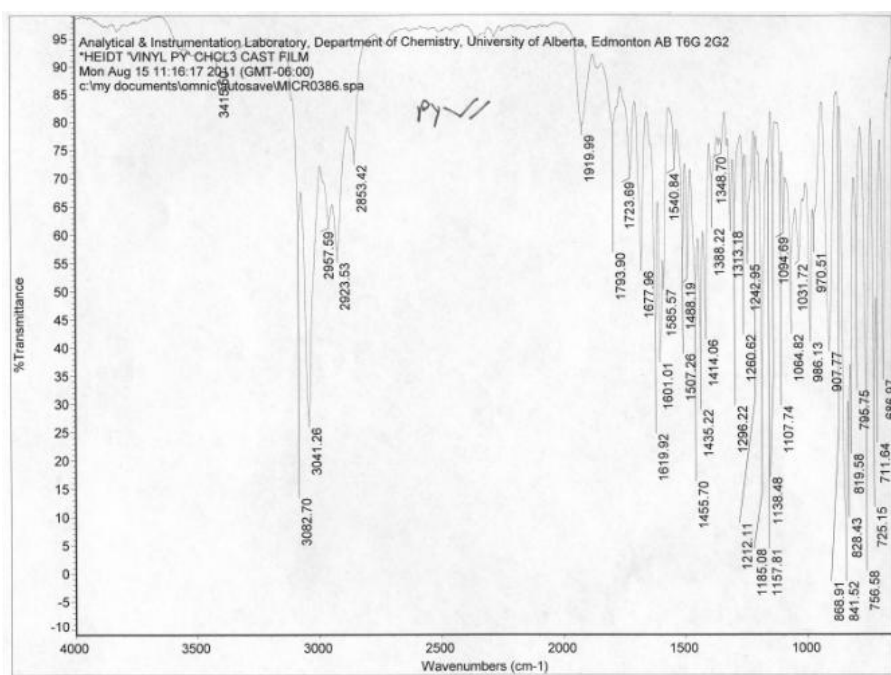
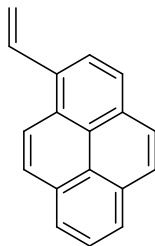


Figure 49 - IR (cast film, cm<sup>-1</sup>) of 1-vinylpyrene **36**

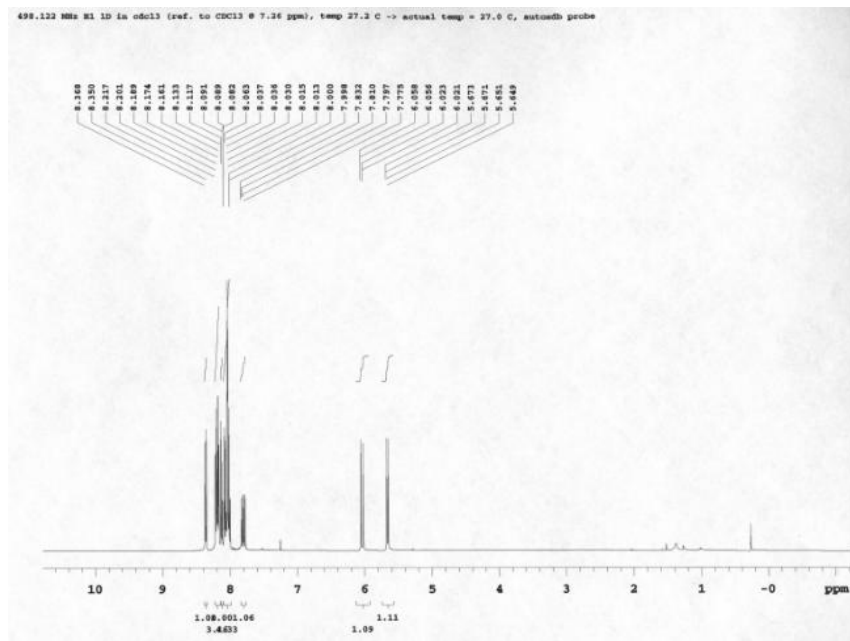


Figure 50 - <sup>1</sup>H NMR (500 MHz, CDCl<sub>3</sub>) of 1-vinylpyrene **36**

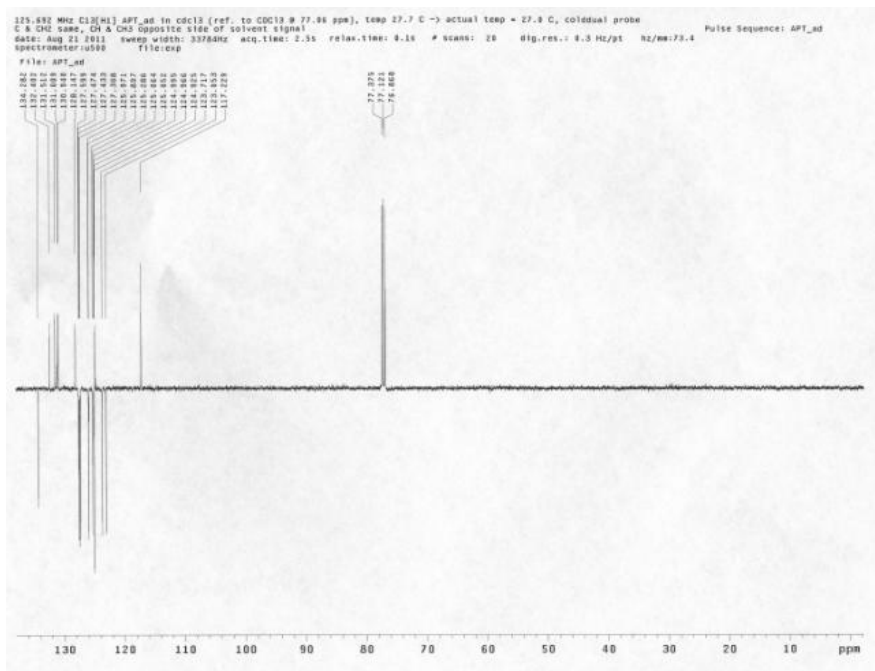


Figure 51 - <sup>13</sup>C NMR (125 MHz, CDCl<sub>3</sub>) of 1-vinylpyrene **36**

15 –Selected spectra for 13-(1-vinylpyrene)-5-(3-(1-vinylpyrene)phenyl)-1,2,3,4-tetrahydrobenzo[b]anthraquinoline (**31**)

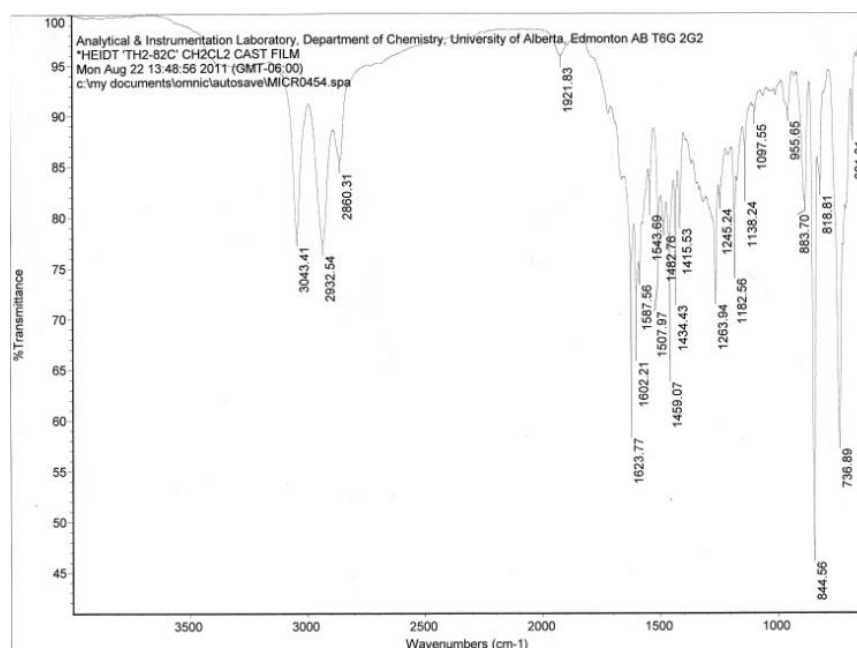
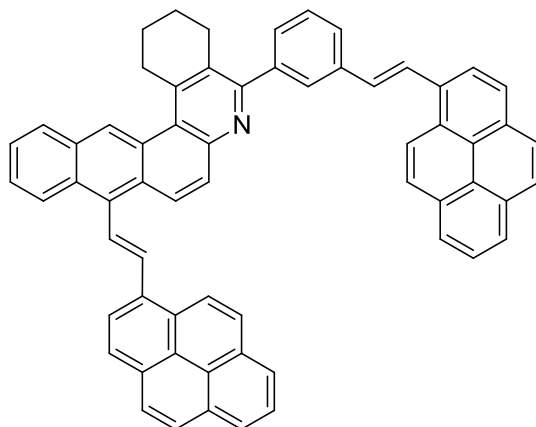


Figure 52 – IR (cast film,  $\text{cm}^{-1}$ ) of 13-(1-vinylpyrene)-5-(3-(1-vinylpyrene)phenyl)-1,2,3,4-tetrahydrobenzo[b]anthraquinoline **31**

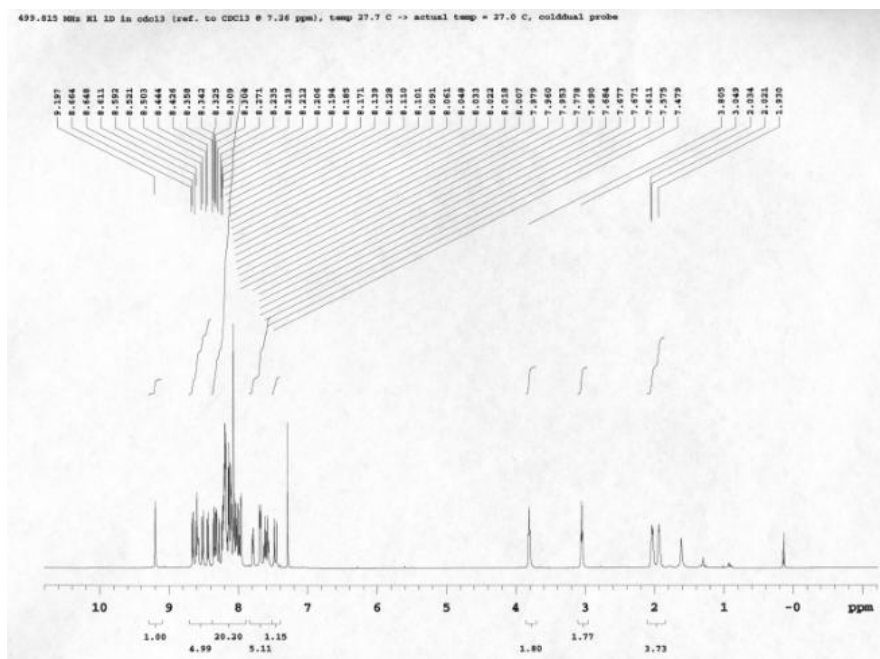


Figure 53 –  $^1\text{H}$  NMR (500 MHz,  $\text{CDCl}_3$ ) of 13-(1-vinylpyrene)-5-(3-(1-vinylpyrene)phenyl)-1,2,3,4-tetrahydrobenzo[b]anthraquinoline **31**

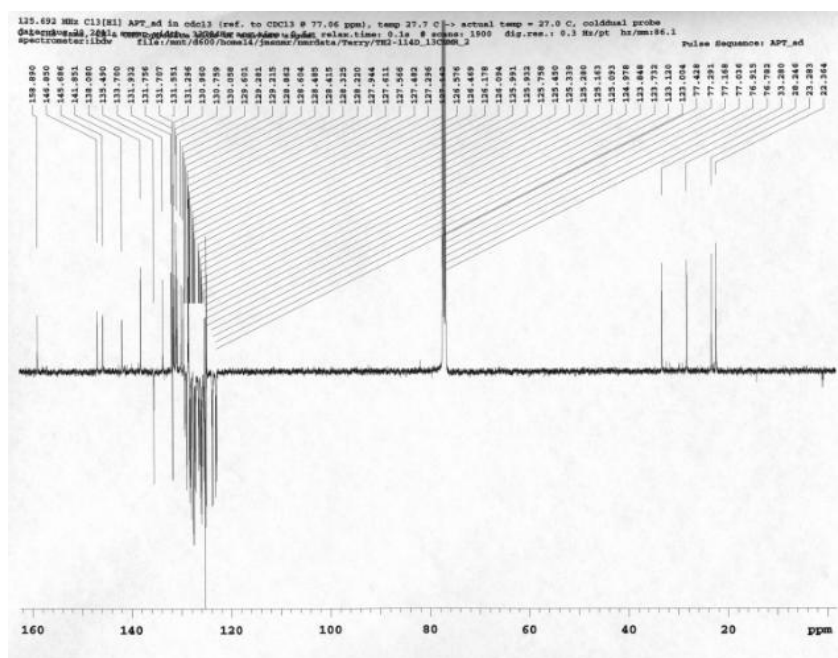


Figure 54 –  $^{13}\text{C}$  APT NMR (500 MHz,  $\text{CDCl}_3$ ) of 13-(1-vinylpyrene)-5-(3-(1-vinylpyrene)phenyl)-1,2,3,4-tetrahydrobenzo[b]anthraquinoline **31**

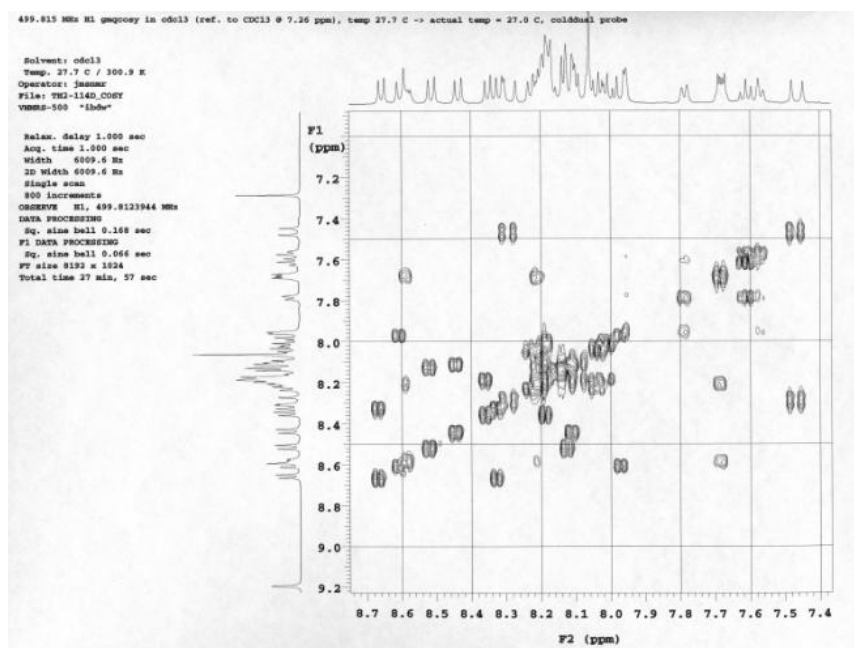


Figure 55 – COSY (aromatic region) of 13-(1-vinylpyrene)-5-(3-(1-vinylpyrene)phenyl)-1,2,3,4-tetrahydrobenzo[b]anthraquinoline **31**

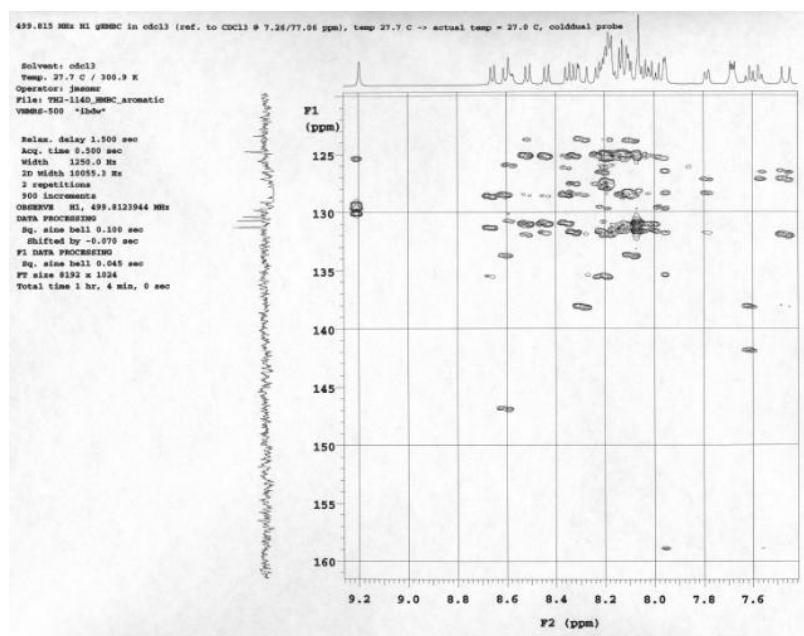


Figure 56 – HMBC (aromatic region) of 13-(1-vinylpyrene)-5-(3-(1-vinylpyrene)phenyl)-1,2,3,4-tetrahydrobenzo[b]anthraquinoline **31**